Bulletin 227

Rut Depth Prediction on Flexible Pavements

Calibration and Validation of Incremental-Recursive Models

Sven Agardh

2005

Lunds Tekniska Högskola
Institutionen för Teknik och samhälle
Avdelning Vägbyggnad

Rut Depth Prediction on Flexible Pavements

Calibration and Validation of Incremental-Recursive Models

Sven Agardh

CODEN:LUTVDG/(TVTT-1034) 1-152/2005
ISSN 1404-272X
ISBN 91-628-6555-2

Bulletin 227

Department of Technology and Society
Lund Institute of Technology
Box 118
S-221 00 Lund
Sweden

Rut Depth Prediction on Flexible Pavements

Calibration and Validation of Incremental-Recursive Models

Doctoral Thesis

Sven Agardh

ACKNOWLEDGEMENTS

On this page I would like to say thank you to my supervisors during the work: Per Ullidtz and Christian Busch, and also to everyone else who deserves it.

This project has been financed by Kommunikationsforskningberedningen (KFB) and Vägverket.

SUMMARY

Large amounts of money are spent on pavement maintenance every year. A helpful tool in planning how to spend the money for constructing and maintaining roads in the best way possible is a Pavement Management System (PMS). To get a normal PM System to work fine it is important to have an accurate deterioration model. Unfortunately the deterioration of a pavement is a complex process and is therefore not easy to predict.

Deterioration models are not only used in PM systems, but also for design purpose. Since the development of the AASHTO Design Guides from the AASHO Road Trials most design methods have been empirical and often based on either in-service roads or more controlled tests, such as AASHO Road Trials.

Parallel to the purely empirical design methods, more analytically based methods have also been developed. About 25 years ago Shell Petroleum International (Claessen et al., 1977) and Asphalt Institute (Shook et al., 1982) released pavement design methods based on calculations of stresses and strains in the pavement.

In later years the development has gone towards more and more analytically based design methods. The EU research project COST 333 (1999) (Development of New Bituminous Pavement Design Method) recommends that an incremental calculation procedure should be used for calculating the future performance in a new design method. This means that the model should be able to describe the increment of damage for each layer under each loading cycle. This design method consists of two different models: A response model and a performance model. A similar concept is used in the 2002 Design Guide (NCHRP, 2004)

Based on knowledge about pavement material behaviour the response in the pavement can probably be calculated with analytical models. Even though a normal pavement structure has a simple geometry, the deterioration of a pavement is a very complicated process and therefore the pavement performance has to be calculated with empirically obtained relationships. Improvements from the current situation have to be done on both response models and performance models for such a design method. (Hildebrand, 2002)

Objective

The objective of this study is to evaluate different types of pavement deterioration models that can be used in an incremental design process. The

research is limited to flexible pavements and the focus is on rut depth development. The evaluation will lead to recommendations on which types of models that should be further developed to be used for real pavements with reasonable accurate results.

Deterioration factors and response models

A pavement is geometrically a very simple engineering structure. Unfortunately the materials in a normal pavement and their behaviour are not simple. Therefore it is not easy to analyze the deterioration of a pavement. The deterioration consists of different elements and depends on different factors.

There are many ways to calculate the pavement response. The most common method is to assume that the materials are homogenous, isotropic and linear-elastic. These assumptions are not true for most pavement materials. The unbound materials are obviously not homogenous since they consist of particles. It is however possible that despite the fact that the basic assumptions are false, the theories can still be used with reasonable accurate results. At least for granular materials it has been known for a long time that the linear elastic theory does not agree very well with measured values (Frölich, 1934). In the last century many models have been developed to make the calculated stresses and strains fit better with the measured values.

Elastic material models have been evaluated in a licentiate thesis by Agardh (2002). The results showed that a model with stress dependant subgrade resulted in calculated responses that were closest to the measured responses. This has also been shown in other studies (e.g. Hildebrand, 2002). Such a model is used for all response calculations in this thesis.

Deterioration Models

Pavements deteriorate in several different ways and the condition of the pavement can be described in many ways. According to the EU-project COST 324 (1997) there are seven indicators for pavement condition:

- Longitudinal profile
- Transverse profile
- Surface cracking
- Structural cracking
- Structural adequacy
- Surface defects
- Skid resistance

Deterioration models should be developed for each of the seven indicators (COST 324, 1997). Two models for calculating rut depth were chosen for further studies.

1. Rut depth development based on energy

   Rutting occurs because of permanent deformation in some part of the pavement. It is often assumed that most of the rutting occurs in the subgrade. It is therefore reasonable to believe that the critical response for rutting should be at the top of the subgrade. Based on tests at the Danish Road Testing Machine, an evaluation of deterioration models with stress, strain and strain energy as the critical response was conducted (Zhang et al., 1998). The result showed the energy model as the best at predicting the pavement performance. It also sounds reasonable to believe that the damage (rutting) is due to the internal energy and not only the resilient strain.

2. Rut depth development based on plastic strain

   This way of calculating rutting is used in the 2002 Design Guide (NCHRP, 2004). Instead of using a certain location for the critical strain, the plastic strain through the whole pavement is calculated. Since rutting occurs in all pavement layers, and not only in the subgrade, this method is one more step towards analytical design. The models used are based on the assumption that the plastic strain depends on the resilient strain.

The two models used in the study can be seen as representatives for two different approaches to rut depth development. The model from the 2002 Design Guide is used as a representative of the plastic strain through the whole pavement approach, and the strain energy model is used as a representative of the approach with critical response at a certain location.

Method

The study of deterioration model in this thesis consists of three phases:

1. Selection of models for further investigation
2. Test of potential of the models and calibration
3. Validation of the calibrated models

Two models were chosen for further studies according to the following criteria:

- Ability to fit in an incremental design process
- Simplicity of the model
- Interpretation of parameters

The potential of the model is tested by obtaining one set of model parameters (calibrating the model) for each test section. This test will show if the models are able to accurately describe the rut depth development of the pavements. The models are then calibrated to all test sections. Five sections from accelerated tests are used. At all sections responses were measured at different locations in the pavement. These measured responses were used together with FWD measurements to obtain the needed material parameters.

The purpose of the calibration is to find one set of model parameters that are common to all test sections. If such a set of parameters can be found, then the parameters are probably fairly general and can be used on different pavement sections, which is necessary if the model will be used for real pavements. The same test sections were used for this part of the evaluation. A simple sensitivity analysis of the calibrated models was also performed.

The validation was performed in two ways. First the models were validated to six theoretical roads that were designed according to Swedish standards. The purpose of this evaluation is to find out if the calculated rut depths are on a reasonable level or a large correction factor is needed.

The second part of the validation was done against two real roads. Both are located in southern Scandinavia where the frost heave likely will only have minor impact on the rutting. Except for that there is at least one significant difference between these sections and the sections for the accelerated tests where the model parameters are obtained from. Both sections are highways with relatively high traffic volume, and therefore also considerably stronger than the sections at the accelerated tests.

Results

The test of potential of the models shows that both models can reasonably accurate describe the deterioration. On most of the sections the difference between measured and calculated rut depth is definitely within the measurement error of the rut depth.

Some of the model parameters show a variation of more than a factor of 10 between the different test sections. Therefore it is probably not a good idea to just take the average value of all test sections as general parameters.

After obtaining model parameters that should fit all section a sensitivity analysis was performed. The most interesting result from this sensitivity analysis is the great impact of the β_1 parameter for the AC layer. Normally it is assumed that most of the rutting consists of permanent deformation in the subgrade, and a very small part of the rutting is from the AC layer. With these model parameters almost half of the rutting is from the AC layer. This is

definitely more than expected. To reflect reality, the β_1 parameter probably should be lower than what was obtained from the best fit to all sections.

Because of the unreasonable results with large deformations of the AC layer a new analysis was performed where the β_1 parameter was set to the value suggested in the 2002 Design Guide (0.479244).

With the new set of model parameters the energy model gives the best prediction (lowest RMS) for 4 of the 5 sections.

The model parameters have been obtained only from accelerated tests with controlled climate. Often when laboratory results will be transformed to reality a shift factor is needed. To get an indication if such a shift factor is needed for these models, a validation is performed in two different ways. First rut depth development is calculated for theoretical pavements. Six different sections were designed according to the Swedish standards, ATB Väg (SNRA, 2001). This validation can give a hint if the obtained model parameters give rut depth development of reasonable size for real pavements or if a correction factor is needed when the accelerated tests are transformed to real pavements. The material parameters for these calculations are the material parameters used in ATB Väg.

With the energy model the calculated rut depth will increase with traffic. Since all sections according to the design standard (ATB Väg) have a base and subbase of at least 500 mm, it is possible that sections with lower traffic are a bit thicker than what is necessary to avoid rutting, and therefore experiences less rutting. All calculated rut depths are of reasonable magnitudes.

With the energy model the difference in rut depth development between different seasons is not very pronounced, but with the plastic strain model the there is a significant difference with faster rut depth development in the summers. The plastic strain model seems to be more sensitive to climate variations.

For the plastic strain model the difference between the sections is quite small. Most of the rutting occurs in the first year. After that the rut depth development is considerably smaller. The rutting with the energy model is more linear with the parameters used for these calculations.

Even though the total rut depths from these calculations seem to be of reasonable size, it is not certain that calculations with these parameters will always be reasonable. The calculations with the plastic strain model show that only a small part of the rutting occurs in the subgrade.

The model parameters are then validated against two real pavement sections. Both sections are highways and are considerable stronger pavements than the accelerated test sections used to obtain the model parameters. One section is located close to Hirtshals in northern Denmark on highway M90. The other section is located in southern Sweden on highway E4, close to Eket.

Both models overestimate the rut depth on these roads. There can be several reasons for that. With the obtained model parameters for the plastic strain model probably more deformation than in real pavements occurs in the pavement than in the subgrade. This means that the calculated deformation of the base course and subbase is larger than the real deformation in these layers. Hence with thick base course and subbase the calculated deformation is likely to be too large. Since these layers are thicker in these two pavements than in the ones used to obtain the parameters, the calculated total deformation will be too large for these sections. It is possible that these parameters would work better for low volume roads.

In the validation to theoretical sections the energy model resulted in larger rut depth for the pavements with high traffic volume. In the validation against real pavements it is shown that the parameters for that model results in too big rut depth for roads with much traffic. The α parameter shows the sensitivity to traffic load. It is possible that this parameter should be lower than the suggested 0.344. It is also possible that some of the model parameters should not be constant, but vary with either traffic or bearing capacity.

Conclusions

Both models can describe the rut depth development of all test sections, and it is not obvious that one gives better description of the rut depth than the other.

The model parameters vary a lot between the sections, so an average value of the parameters is probably not a good estimation of the true parameters.

With the same model parameters for all sections the result from the energy model is closer to the measured value on four of the five sections.

The best fit of model parameters for the plastic strain model results in large deformation in the AC layer. By setting one of the AC parameters to a fixed value it is possible to get more reasonable results, even though the deformation of the subgrade is smaller than expected.

The small deformation of the subgrade with the plastic strain model indicates that the model parameters obtained from this study probably don't describe the real deformations. To obtain better model parameters probably

measurements of permanent deformations of different layers of the pavement are necessary.

The theoretical pavements designed with ATB Väg (SNRA, 2001), results in reasonable rut depths for both models. That indicates that probably no shift factor is needed to transform the laboratory results from this study to real pavements. With the model parameters used in this study the energy model results in larger rut depth for sections with a lot of traffic. That indicates either that the value of the α parameter is too high or that the model parameters should vary with either traffic or bearing capacity.

Both models over estimate the rut depth at the two real pavements used for the evaluation. Especially for the M90 section one reason can be that the traffic volume used for the calculations is not the real traffic volume. For the energy model another reason can be that the model parameters were obtained from low volume roads, and it is possible that the value of the α parameter has been overestimated.

The model parameters were obtained from accelerated tests on relatively weak pavements, and the results from these tests could not be directly transformed to strong pavements under real traffic. Since there are two differences between the sections used to obtain the parameters and the validation sections, the reason for the difference can be found in two places. Either the main difference is the strength of the pavements or the main difference is the different nature of accelerated tests and reality. The rest period between loads on real pavements can result in longer service life than in accelerated tests. Tests at the Danish Road Testing Machine show that the bearing capacity will increase during rest periods (Zhang et al, 1998).

The measurements used for this study were not enough to get a good calibration of the plastic strain model. Measurements of permanent deformations of layers or parts of the pavement should be used to get a good calibration of the model.

The energy model can probably be used for normal flexible pavements. The most important model parameter (α) has almost the same value in two different studies, which indicates that that value is probably close to the best possible value. On the other hand, the validation against real roads gave an indication that perhaps the α parameter should be lower than the suggested value. For the other two parameters, this study differs from the other, and calibration to more test sections can probably improve the parameter values.

SAMMANFATTNING

Varje år spenderas stora summor pengar på vägunderhåll. Ett värdefullt verktyg för att planera underhållet på bästa sätt är ett så kallat PM-system (Pavement Management System). För att ett normalt PM-system ska fungera optimalt är det viktigt att det innehåller en nedbrytningsmodell som stämmer väl överens med verkligheten. Tyvärr är nedbrytningen av en väg en komplicerad process och därför svår att bestämma i förväg.

Nedbrytningsmodeller används inte bara i PM-system, utan också vid dimensionering. Sedan AASHTO Design Guide utvecklades från AASHO-försöken på 50-talet, har de flesta dimensioneringsmetoder varit empiriska och baserade antingen på verkliga vägar eller mer kontrollerade fullskaleförsök som AASHO-försöken.

Parallellt med de rent empiriska dimensioneringsmetoderna har även mer analytiskt baserade metoder utvecklats. För ungefär 25 år sedan gav Shell Petroleum International (Claessen et al., 1977) och Asphalt Institute (Shook et al., 1982) ut dimensioneringsmetoder som baserades på beräkning av spänningar och töjningar i vägkroppen.

På senare år har utvecklingen gått mot mer och mer analytiskt baserade dimensioneringsmetoder. Det EU-finansierade forskningsprojektet COST 333 (1999) (Development of New Bituminous Pavement Design Method) rekommenderar att nedbrytningen i framtida dimensioneringsmetoder ska beräknas inkrementellt. Det betyder att modellen ska kunna beskriva ökningen av skadorna på vägen för varje belastningscykel. En sådan dimensioneringsmetod består av två olika modeller: en modell för beräkning av momentana påkänningar (spänningar, töjningar och deformationer) under belastning och en modell för beräkning av de bestående skadorna. Ett exempel på en sådan dimensioneringsmetod är 2002 Design Guide.

Baserat på kunskaper om hur vägens material beter sig under belastning kan de momentana påkänningarna troligen beräknas med analytiska metoder. Även om en väg geometriskt sett är en enkel konstruktion, är nedbrytningen av en väg en komplicerad process. Därför måste nedbrytningen troligen beräknas med empiriskt framtagna samband. Förbättringar av dagens situation måste göras av båda modellerna för att de ska fungera tillfredsställande (Hildebrand, 2002).

Syfte

Syftet med denna studie är att utvärdera olika typer av nedbrytningsmodeller som kan användas för inkrementella beräkningar av skador på vägar.

Studierna är begränsade till flexibla överbyggnader och särskilt fokus är lagt på beräkning av spårdjupsutveckling. Utvärdering leder fram till rekommendationer om vilka typer av modeller som bör utvecklas vidare.

Faktorer som påverkar nedbrytning samt responsmodeller

Geometriskt är en väg en enkel konstruktion. Tyvärr är materialen och dess beteende i en normal vägkonstruktion inte lika enkla. Därför är det inte lätt att analysera nedbrytningen av en väg. Den består av flera olika delar och beror på många olika faktorer.

Det finns många sätt att beräkna respons (momentana påkänningar under belastning) i en väg. Den mest använda metoden basers på antagandena att materialen är homogena, isotropa och linjärelastiska. Dessa antaganden är inkorrekta för de flesta vägbyggnadsmaterial. Obundna material är inte homogena eftersom de består av partiklar. Det är dock möjligt att även om teorierna baseras på felaktiga antaganden kan de ge någorlunda korrekta resultat. Åtminstone för obundna material har det länge varit känt att linjärelastisk teori inte stämmer överens med uppmätt spänningar och töjningar (Frölich, 1934). Under de senaste 100 åren har flera modeller utvecklats för att få teorierna att stämma bättre överens med verkligheten.

Elastiska materialmodeller har utvärderats i en licentiatuppsats av Agardh (2002). Resultaten från den studien visar att en modell med spänningsberoende elasticitetsmodul för undergrunden stämde bäst överens med uppmätt respons. Detta har också visats i andra studier (t.ex. Hildebrand, 2002). En sådan modell har använts till alla responsberäkningar i denna avhandling.

Nedbrytningsmodeller

Vägar bryts ner på många olika sätt och vägens tillstånd kan därför också beskrivas på olika sätt. Enligt det EU-finansierade forskningsprojektet COST 324 (1997) finns det sju indikatorer på vägens tillstånd:

- Längsgående profil
- Tvärgående profil
- Ytsprickor
- Strukturella sprickor
- bärighet
- Ytskador
- Friktion

Nedbrytningsmodeller bör utvecklas för var och en av de sju tillståndsindikatorerna (COST 324, 1997). Två modeller för beräkning av spårdjup (tvärgående profil) valdes ut för vidare studier.

1. Spårutveckling baserat på energi

   Spår uppkommer på grund av deformation i någon del av vägkroppen. Ofta antar man att den största delen av deformationen uppstår i undergrunden. Därför kan det vara rimligt att den kritiska responsen i vägen bör vara i ovankant av undergrunden. Baserat på mätningar i den danska Vejprøvemaskinen, utvärderades modeller som baserar spårutvecklingen på spänning, töjning samt energi (Zhang et al., 1998). Det visade sig att modellen baserad på energi fungerade bäst för att förutsäga vägens spårdjup. Det är också rimligt att anta att skador (deformation) beror på tillförd energi och inte bara på momentan töjning.

2. Spårutveckling baserat på plastisk töjning

   Detta sätt att beräkna spårdjup används i 2002 Design Guide (NCHRP, 2004). I stället för att använda en speciell plats för en kritisk respons beräknas den plastiska töjningen genom hela vägkroppen. Eftersom deformation förekommer i alla lager, och inte bara i undergrunden, är denna beräkningsmetod ytterligare ett steg mot en analytisk dimensioneringsmetod. Den modell som används i denna studien baseras på antagandet att den plastiska töjningen beror på den elastiska töjningen.

De två modeller som använts kan ses som representanter för två olika synsätt på spårutveckling. Modellen från 2002 Design Guide används som representant för synsättet med plastisk töjning genom hela vägkroppen, och energimodellen används som representant för modeller med kritisk respons.

Metod

Studien av nedbrytningsmodeller i denna avhandling består av tre delar:
1. Val av modeller för vidare utredning
2. Test av modellernas potential samt kalibrering av modellerna
3. Validering av de kalibrerade modellerna

Två modeller valdes ut för vidare utredning enligt följande kriterier:

- Möjlighet att fungera i en inkrementell dimensioneringsmetod
- Modellens komplexitet
- Möjlighet att tolka modellparametrarna

Modellernas potential testades genom att ta fram en uppsättning modellparametrar (kalibrering av modellen) för var och en av teststräckorna.

Detta test kan visa om modellerna kan beskriva spårutvecklingen på vägen på ett riktigt sätt. Sedan kalibrerades modellerna mot samtliga teststräckor på en gång. Fem sträckor från accelererade test användes för kalibreringen. Samtliga teststräckor var instrumenterade med mätinstrument för responsmätningar. Dessa mätningar tillsammans med fallviktsmätningar användes för att ta fram nödvändiga materialparametrar.

Syftet med kalibreringen var att hitta en uppsättning parametrar som är generell för alla sträckor. Om en sådan uppsättning kan hittas är troligen modellparametrarna någorlunda generella och samma parametrar kan användas på olika vägar, vilket är nödvändigt om modellerna ska användas på verkliga vägar. För denna kalibrering användes samma fem teststräckor från accelererade försök. En enkel känslighetsanalys av modellparametrarna genomfördes också.

Valideringen av modellerna genomfördes på två sätt. Först validerades modellerna mot sex teoretiska vägar som dimensionerades enligt svensk standard. Syftet med den valideringen vara att se om modellerna gav rimligt stora spårdjup eller om en korrektionsfaktor är nödvändig.

Den andra delen av valideringen gjordes mot två verkliga vägar. Båda ligger i södra Skandinavien där tjälen troligen bara har marginell inverkan på spårutvecklingen. Det finns åtminstone en stor skillnad mellan dessa vägar och teststräckorna från de accelererade försöken som användes för kalibreringen. Båda vägarna är motorvägar och har därför relativt mycket trafik, och är därför betydligt starkare konstruktioner än de som användes i de accelererade försöken.

Resultat

Testet av modellernas potential visar att båda modellerna kan beskriva spårutvecklingen. För de flesta sektioner var skillnaden mellan beräknat och uppmätt spår inom felmarginalen för mätningen.

Några av modellparametrarna varierade mer än en faktor 10 mellan de olika teststräckorna. Därför är det troligen inte en bra idé att använda medelvärdet för varje parameter som ett generellt värde.

Efter att ha tagit fram en uppsättning modellparametrar som passar samtliga teststräckor utfördes en känslighetsanalys. Det mest intressanta resultatet från den analysen vara att parametern β_1 för asfaltlagret har väldigt stor inverkan på det beräknade spårdjupet. Normalt borde det mesta av spåret härröra från undergrunden, och endast en mycket liten del från asfalten. Med dessa parametrar kommer nästan hälften av spårdjupet från asfalten. Det är definitivt mer än förväntat. För att ge en bättre återspegling av verkligheten är

det troligt att värdet för parametern β_1 borde ha varit lägre än vad som kom ut från denna kalibrering.

På grund av den onaturligt stora deformationen i asfaltlagret gjordes en ny analys där värdet för β_1 fastställdes till det värde som föreslås i 2002 Design Guide (0.479244)

Med dessa nya parametervärden ger energimodellen bäst beskrivning av spårdjupsutvecklingen för fyra av de fem teststräckorna.

Modellparametrarna har tagits fram enbart från accelererade försök med kontrollerat klimat. Ofta när resultat från laboratorieförsök ska överföras till verkligheten behövs en korrektionsfaktor. För att få en indikation om en sådan korrektionsfaktor är nödvändig för dessa modeller, utfördes en validering på två olika sätt. Först beräknades spårdjupsutvecklingen för teoretiska konstruktioner. Sex olika konstruktioner dimensionerades enligt ATB Väg (SNRA, 2001). Denna validering kunde ge en antydan om beräkningarna med de framtagna modellparametrarna ger rimliga värden för spårdjupet eller om en korrektionsfaktor skulle bli nödvändig för att kunna föra över laboratorieresultaten till verkligheten. Materialparametrarna som användes för dessa beräkningar är tagna från ATB Väg.

De beräknade spårdjupen med energimodellen blir större för de sektioner som har mer trafik. Eftersom alla konstruktioner, enligt ATB Väg, har obundna lager på sammanlagt minst 500 mm, är det möjligt att vägar med lite trafik, ur spårdjupssynpunkt, blir överdimensionerade och därför får mindre spårtillväxt. Alla beräknade spårdjup är dock rimligt stora.

Med energimodellen är skillnaden i spårtillväxt mellan olika årstider inte så tydlig, men med plastisk töjningsmodellen är det en tydlig skillnad, med kraftigare spårtillväxt under sommaren. Det verkar som om den modellen är mer klimatkänslig.

Med plastisk töjningsmodellen är skillnaden mellan de olika konstruktionerna ganska liten. Största delen av spåret uppkommer under första året. Efter det är spårtillväxten mycket mindre. Spårtillväxten är mer linjär med energimodellen.

Även om det totala spårdjupet i dessa beräkningar är rimligt stora, är det inte säkert att beräkningar med dessa parametrar alltid är rimliga. I beräkningarna med plastisk töjningsmodellen är det endast en liten del av spåret som kommer från undergrunden.

Modellparametrarna validerades även mot två verkliga vägar. Båda dessa vägar är motorvägar med mycket starkare vägkonstruktioner än de accelererade försök som använts för att ta fram modellparametrarna. Den ena

teststräckan ligger nära Hirtshals i norra Danmark på väg M90. Den andra ligger i södra Sverige på väg E4, nära Eket.

Båda modellerna överskattar spårdjupet på dessa sträckor. Det kan bero på flera olika saker. Med de modellparametrar som använts för plastisk töjningsmodellen blir det större deformationer i vägkroppen, och mindre i undergrunden än vad som troligen är fallet i verkligheten. Det betyder att den beräknade deformationen av bärlagret och förstärkningslagret troligen är större än den verkliga deformationen i dessa två lager. Därför kommer troligen beräkningar för konstruktioner med tjocka obundna lager att ge för stor deformation. Eftersom dessa två lager är tjockare i de två verkliga vägarna än i de teststräckor som använts för kalibrering av modellerna blir det totala beräknade spårdjupet för stort för dessa vägar. Det är möjligt att de framtagna parametrarna skulle ha fungerat bättre på lågtrafikerade vägar.

I valideringen mot verkliga vägar gav energimodellen större spårdjup för de högtrafikerade vägarna. I valideringen mot verkliga vägar gav den modellen för stora spårdjup för högtrafikerade vägar. Parametern α beskriver modellens känslighet för trafikmängden. Det är möjligt att denna parameter borde vara lägre än de föreslagna 0.344. Det är också möjligt att den, eller någon annan parameter, inte ska vara konstant, utan variera med antingen trafikmängd eller bärighet.

Slutsatser

Båda modellerna klarar av att beskriva spårdjupsutvecklingen för alla provsträckorna, och det är inte uppenbart at den ena ger en bättre beskrivning än den andra.

Modellparametrarna varierar mycket mellan sektionerna, så ett medelvärde av par metrarna är troligen inte en bra skattning av de verkliga parametervärdena.

När samma modellparametrar används för alla sektioner ger energimodellen bäst resultat för fyra av de fem teststräckorna.

Den bästa anpassningen av modellparametrar för plastisk töjningsmodellen resulterar i stora deformationer i asfaltlagret. Genom att sätta en av parametrarna för asfalten till ett bestämt värde kan man få ett rimligare resultat, även om deformationen i undergrunden fortfarande är mindre än förväntat.

Den relativt lilla deformationen i undergrunden med plastisk töjningsmodellen indikerar att de modellparametrar som tagits fram från denna studie troligen inte beskriver den verkliga deformationen. För att få

bättre värden på parametrarna är det troligen nödvändigt att använda mätningar av permanenta deformationer i olika delar av vägkroppen.

De teoretiska vägarna dimensionerade med ATB Väg (SNRA, 2001), resulterar i rimliga nivåer på spårdjupet för båda modellerna. Det indikerar att det inte behövs någon korrektionsfaktor för att överföra resultaten från de accelererade försöken till verkliga vägar. Med de modellparametrar som använts i denna studie ger energimodellen större spårdjup för vägar med mycket trafik. Det antyder antingen att värdet för parametern α är för högt eller att modellparametrarna bör variera med antingen trafikmängden eller vägens bärighet.

Båda modellerna överskattar spårdjupet på de två verkliga vägar som använts för validering. Åtminstone för Hirtshalsvägen kan en anledning vara att den trafikvolym som använts för beräkningarna inte är den verkliga trafikvolymen. För energimodellen kan en annan anledning vara att modellparametrarna togs fram från lågtrafikerade vägar, och det är möjligt att parametern α har överskattats.

Modellparametrarna togs fram från accelererade försök på relativt svaga konstruktioner, och resultaten från dessa test kan inte direkt överföras till starka vägar med verklig trafik. Eftersom det är två skillnader mellan de vägar som använts för kalibreringen av modellerna och de vägar som använts för valideringen, kan anledningen till skillnader finnas på två ställen. Antingen finns den viktiga skillnaden i vägkonstruktionernas styrka, eller finns den viktiga skillnaden i de skilda förutsättningarna mellan accelererade försök och verkliga vägar. Viloperioden mellan belastningarna på verkliga vägar kan ge längre livslängd för vägen. Försök vid Vejprøvemaskinen i Danmark visar att bärigheten ökar under viloperioder (Zhang et al., 1998).

Mätningarna som använts i denna studie var inte tillräckliga för att ge en bra kalibrering av plastisk töjningsmodellen. Mätningar av permanenta deformationer av enskilda lager eller delar av vägkroppen borde ha använts för att få en bra kalibrering.

Energimodellen kan troligen användas för normala flexibla överbyggnader. Den viktigaste modellparametern (α) har fått nästan samma värde i två olika studier, vilket indikerar att det värdet ligger nära bästa möjliga värde. Å andra sidan indikerade valideringen mot verkliga vägar att det är möjligt att parametern a borde vara lägre än det föreslagna värdet. För de andra två parametrarna skiljer denna studie sig från den andra, och kalibrering mot fler provvägar kan troligen förbättra värdena för dessa parametrar.

1 INTRODUCTION

1.1 Background

In the European Union approximately 15% of GNP is spent on mobility (COST 324, 1997). Road transport is the most important mode of transport in Europe (COST 333, 1999). Since enormous amounts of money are spent on roads it is important to try to use this money as efficiently as possible. A Pavement Management System (PMS) is a helpful tool in planning how to spend the money for constructing and maintaining roads in the best way possible. To get a normal PM System to work well, it is important to have an accurate deterioration model. Unfortunately, the deterioration of a pavement is a complex process and therefore not easy to predict.

> *"The Achilles heel of most pavement management systems is their inability to accurately predict pavement deterioration". (Madanat, 1997)*

To improve the PM systems the most important enhancement is to find better deterioration models.

Deterioration models are used not only in PM systems, but also for design purposes. Since the development of the AASHTO Design Guides from the AASHO Road Trials, most design methods have been empirical and often based on either in-service roads or more controlled tests, such as AASHO Road Trials. (Huang, 1993)

Parallel to the purely empirical design methods, more analytically based methods were also developed. About 25 years ago Shell Petroleum International (Claessen et al., 1977) and Asphalt Institute (Shook et al., 1982) released pavement design methods based on calculations of stresses and strains in the pavement.

A different approach to calculating pavement performance was developed in Denmark that resulted in Mathematical Model of Pavement Performance (MMOPP) (Ullidtz, 1978 and Ullidtz, 1979). The main difference from most other design methods is that the input is not given in single average values, but rather there is a variation along the road in almost every input parameter. The model divides the road into pieces of 0.3 m that all have different thicknesses, material parameters etc.

At the end of the 90's the European Union performed a study on flexible pavement design (COST 333, Development of New Bituminous Pavement Design Method). The design methods from the participating countries were studied and compared. The survey showed that most countries use analytically based design methods. All these methods use a similar concept.

Linear elastic methods are used to calculate stress and/or strain at critical locations in the pavement. The calculated values are then compared to permissible response. The most common critical locations are the horizontal tensile strain at the bottom of the bituminous layers (Saal & Pell, 1960), which is supposed to relate to fatigue cracking, and the vertical compressive strain at the top of the subgrade (Kerkhoven & Dormon, 1953), which is supposed to relate to structural deformation. The design methods are empirically calibrated to accommodate effects like climate, materials used, use of studded tyres and construction practices.

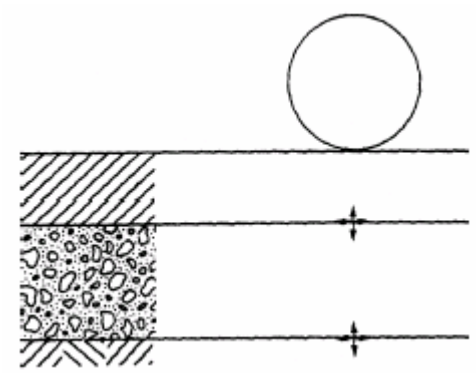

Figure 1.1 The two locations in a pavement where the critical responses normally are assumed to be (Ullidtz, 1987)

Based on a questionnaire handed out to the participants in the COST 333 project, different deterioration mechanisms were ranked according to how commonly observed they were on in-service roads. The ranking gave the following result:

1. Rutting originating in the bituminous layers
2. Cracking initiated at the surface
3. Longitudinal unevenness
4. Loss of skid resistance
5. Longitudinal cracking in the wheel path
6. Cracking initiated at the bottom of the base course
7. General surface cracking
8. Raveling
9. Rutting in the subgrade
10. Frost heave
11. Wear due to studded tyres
12. Low temperature cracking

The last three deterioration mechanisms are only present in cold climates. This poll involved many different European countries, most of which have

relatively warm climates. In northern Europe these three mechanisms should probably have a higher rank.

Most design methods primarily consider the cracking initiated at the bottom of bituminous layers, which was ranked number 6, and rutting in the subgrade, which was ranked number 9. However, other deterioration mechanisms are often indirectly included in the design method by empirical calibrations.

The source of information for developing deterioration models is often collection of data from in-service roads (COST 333, 1999). The data is often gathered for several decades, and the models are revised when needed. One disadvantage with that type of design model is that the new roads are designed for historical conditions and not for present or future conditions. The development of road constructions is not encouraged when historical data are used for design.

Some models are developed from data that are more systematically collected from special test roads or accelerated test facilities. More than one third of the design methods studied in COST 333 still use the AASHO Road Trials to calibrate the models, which shows the great importance of those tests (COST 333, 1999).

Most design models today have an analytically based approach, where linear elastic theory is used to calculate response under a standard axle load at critical locations in the pavement structure. The values of the response are then compared to permissible response for the actual traffic load and climate.

The COST 333 project recommends that an incremental calculation procedure should be used for calculating the future performance of a new design method. This means that the model should be able to describe the increment of damage for each layer under each loading cycle. A flow chart for that kind of design is shown in Figure 1.2. As seen in the flow chart, the method consists of two different models: a response model and a performance model. A similar concept is used in the 2002 Design Guide (NCHRP, 2004).

Based on knowledge about pavement material behaviour, the response in the pavement can probably be calculated with analytical models. Even though a normal pavement structure has a simple geometry, the deterioration of a pavement is a very complicated process, and therefore the pavement performance has to be calculated with empirically obtained relationships.

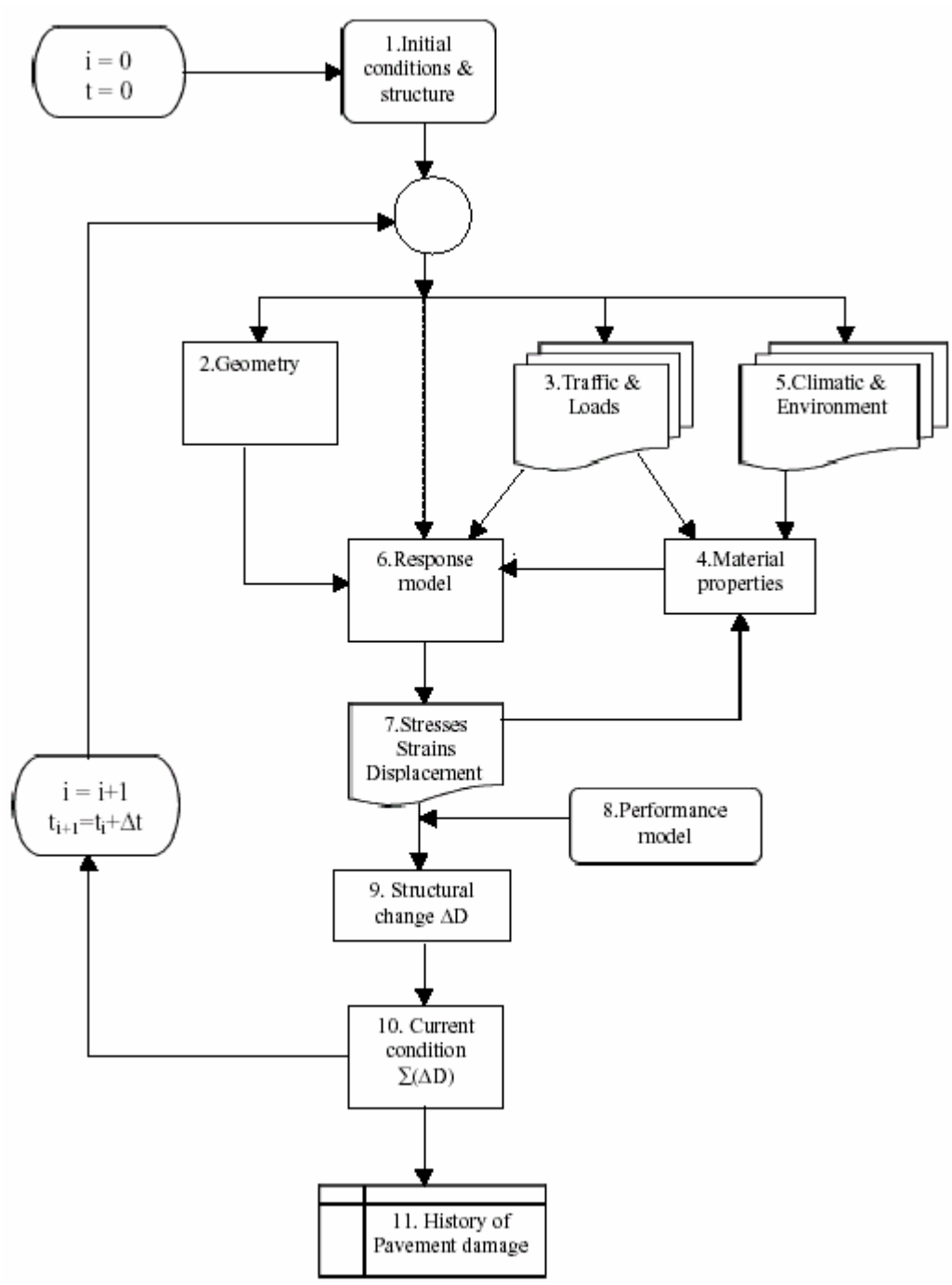

Figure 1.2 Design flow chart (AMADEUS, 2000)

Improvements from the current situation have to be made on both response models and performance models for such a design method. (Hildebrand, 2002)

1.2 Objective

The objective is to evaluate different types of pavement deterioration models that can be used in an incremental design process. The research is limited to flexible pavements, and the main focus is on rut depth development. The evaluation will lead to recommendations for the types of models that should be further developed to be used for real pavements with reasonably accurate results. Finding a solution for how to accurately predict rutting can be a major step towards improving PM Systems. Improved PM Systems can support maintenance planning and save money for both users and owners of roads.

All the models tested are empirical. Probably they cannot be used under conditions that differ too much from those of the data that were used to develop the model without further studies.

1.3 Organization of the thesis

The organization of this thesis can be described with Figure 1.2. **Chapter 2** describes the factors that affect pavement deterioration, which are boxes no 2, 3 and 5 in the figure. In that chapter also different ways of calculating pavement response are described (box no 6). The material parameters that are needed as input to the different models (box no 4) are also discussed. **Chapter 3** is a description of different kind of deterioration models (box no 8) and the input data that is needed for these models (box no 7). The rest of the thesis is an evaluation of different types of deterioration models (boxes no 9, 10 and 11), and starts with a description of how the evaluation is performed in **Chapter 4**. The data used in the evaluation are described in **Chapter 5**. A quality control of the data is executed in the same chapter. **Chapter 6** is the evaluation of the chosen models. The thesis ends with a discussion and conclusions in **Chapter 7**.

2 DETERIORATION FACTORS AND RESPONSE MODELS

A pavement is geometrically a very simple engineering structure. Unfortunately, however, the materials in a normal pavement and their behaviour are not simple. Therefore it is not easy to analyze the deterioration of a pavement. The deterioration consists of different parts and depends on many different factors.

2.1 Pavement condition

The condition of a pavement can be described in several different ways. Normally the damages to the pavement are divided into three groups (Ullidtz, 1998):

- Longitudinal unevenness (roughness)
- Transversal unevenness (rutting)
- Cracking

The cracking and rutting can then be divided into several subgroups, as was done in the COST 333 project see Chapter 1. The condition can also be described using a combined index that gives an overall value of the condition by combining the different damages with weight factors.

2.1.1 Longitudinal unevenness (roughness)

The longitudinal unevenness can be described using various methods. The most common method is the International Roughness Index (IRI). The IRI value is not dependant on a special measurement method, but is a property of the true profile of the pavement. Therefore, all measurement tools that measure the longitudinal profile can be used to determine IRI value. The value of IRI is the length of the movements of a quarter car model (see Figure 2.1) divided by the distance travelled (often in the unit of mm/m). The movements should be calculated with a travel speed of the model of 80 km/h. The quarter car model used is called the "Golden Car", with parameters that are typical for normal vehicles except that it has higher dampening coefficient to minimize the effect of the model to tune in on certain wavelengths and thus increase the movements. (Gillespie, 1992)

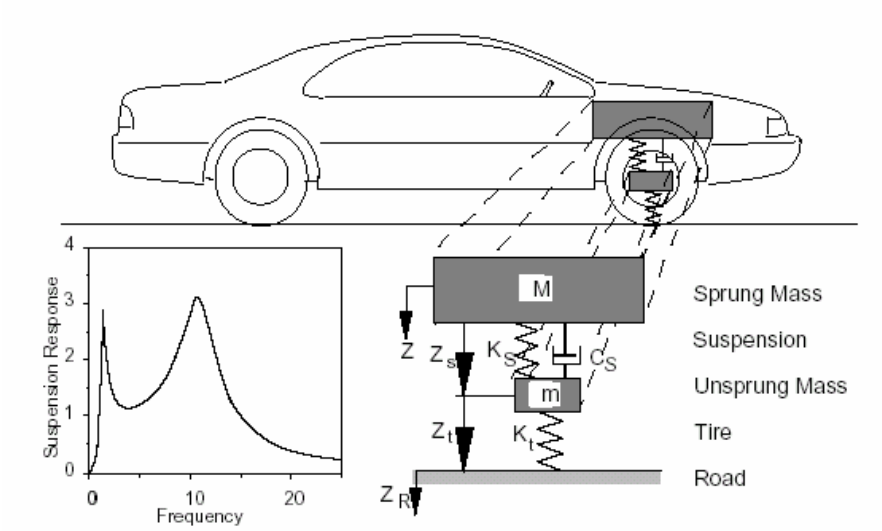

Figure 2.1 Quarter car model (Gillespie, 1992)

The "Golden Car" model is affected by wavelengths between approximately 1.2 m and 30.5 m (which is equal to 0.03 to 0.83 cycles/m in Figure 2.2).

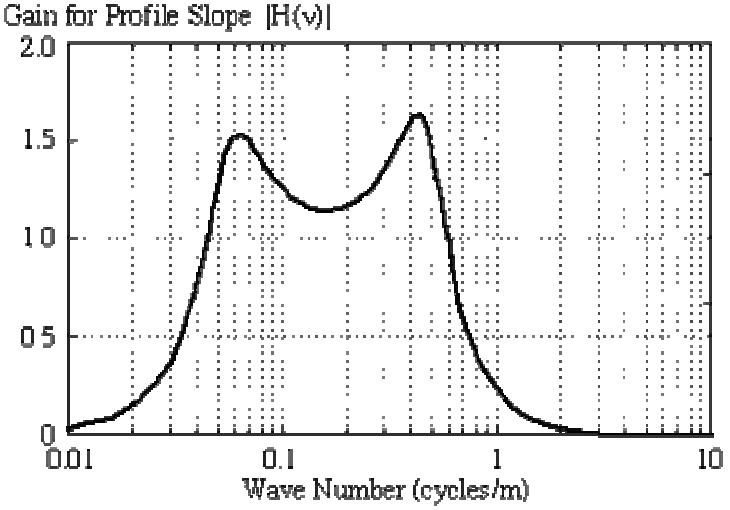

Figure 2.2 Effect of the IRI Golden Car model on different frequencies (sinusoidal movements) (Sayers & Karamihas, 1998)

Another value of pavement roughness is Slope Variance (SV), which was developed during the AASHO Road Test (Carey & Huckins, 1962). The roughness is measured with a CHLOE Profilometer that consists of a small beam with two small wheels 229 mm (9 in) apart on a 7.8 m (25.5 ft) long trailer. The angle between the beam and the trailer is measured at 0.3 m (1 ft)

intervals. The value of Slope Variance is the mean squared deviation from the mean angle of the pavement section.

The gain from the CHLOE Profilometer is close to one for wavelengths between 0.010 m and 17 m. That means that it describes the true profile very well. However, most normal vehicles filter the roughness of the pavement, so only a small span of frequencies affect the ride quality. Therefore, roughness at frequencies that are not noticeable in a car affects the value of SV (Gillespie et al., 1980).

2.1.2 Transverse unevenness (rutting)

Rut depth may seem to be easy to measure and define. Unfortunately, even rutting can be defined and measured in several different ways. The most common definition is from a wireline reference (Figure 2.3). The rut depth can then be measured either as the maximum vertical distance between wireline and pavement or as the maximum distance perpendicular to the wireline.

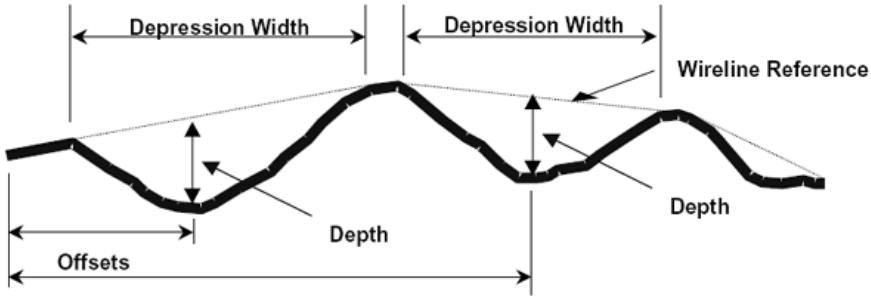

Figure 2.3 Rutting measurement with wireline reference (Elkins et al., 2003)

One advantage of this method is that it is relatively easy to calculate the rut depth from a transverse pavement profile. It is therefore often used when large amounts of data are analyzed.

One problem with rutting is the risk of aquaplaning. To take that risk into consideration, one definition of rut depth can be the theoretical maximum water level (Figure 2.4).

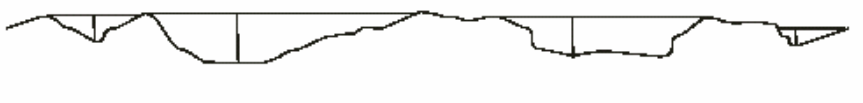

Figure 2.4 Rut depth as the maximum theoretical water depth (Nygårdhs, 2003)

The wireline rut depth can be calculated from normalized profiles, where the crossfall has been removed from the data. The theoretical water depth has to be calculated from the true profile, including crossfall.

2.1.3 Overall condition indices

Many different ways to provide an overall description of the pavement condition have been developed over the years. The most widely spread is probably the Present Serviceability Index (PSI). That method was developed during the AASHO Road Test (Carey & Irick, 1960). Serviceability of a pavement is its ability to serve traffic in its present condition. For the development of PSI, a panel of road users was asked to rate different pavement sections. The average value of the panel members' rating was called Present Serviceability Rating (PSR).

This PSR was then compared to measurable damages of the pavement, and a relationship between these damages and the PSR was established. The serviceability calculated with this relationship is the PSI of the pavement. For flexible pavements that relationship is:

$$PSI = 5.03 - 1.91\log\left(1 + \overline{SV}\right) - 1.38\overline{RD}^2 - 0.01\sqrt{C + P}$$

where

SV = Slope Variance

RD = Rut Depth

C = Cracking

P = Patching

Since the PSI is mostly affected by the roughness, it is possible to develop relations between PSI and IRI:

$PSI = 5e^{-0.18(IRI)}$ (Paterson, 1986)

$PSI = 5e^{-0.26(IRI)}$ (Al-Omari & Darter, 1992)

2.2 Deterioration factors

Odermatt (1997) divided the factors that affect pavement deterioration into five groups:

- Vehicles
- Traffic
- Pavement
- Climate
- Time

Many of these factors are difficult to determine, and sometimes even difficult to define. It can also be both difficult and expensive to collect information on some of the factors on a regular basis. Hence no model includes all of these factors. A deterioration model that is supposed to be applicable on a road network has to choose which factors are most important, and ignore the rest.

2.2.1 Vehicles

Axle load

The most important feature of the vehicle that affects the pavement deterioration is its axle weight. The effect of different axle load is often described with the fourth power law that was developed from the AASHO Road Test (AASHTO, 1981).

$$N_x = N_i \left(\frac{P_i}{P_x} \right)^4$$

where

N_x = number of axle loads with axle type x

N_i = number of axle loads with axle type i

P_x = weight of axle type x

P_i = weight of axle type i

This equation is only a simplification of reality and the fourth power should probably be changed when conditions change. Axle loads within a range of 3 to 13 tons were used to develop the equation. Thus the equation should probably not be used for axle loads outside of that range. The power law was developed for change in serviceability. Therefore it is not certain that it is applicable to other distresses such as cracking or rutting. Nonetheless, it is often used for all types of deterioration.

A later study (Prozzi, 2001) of the same data suggests that the power of 4 should be changed to a power of 4.15 for serviceability. Based on data from both AASHO Road Test and MnRoad, the same study suggests a power of 3.85 for roughness.

Most heavy vehicles use both single axles and tandem axles, and sometimes tridem axles. The damage that different axle types cause on the pavement cannot be evaluated with the above mentioned fourth power law. If the damage occurs close to the surface, it is reasonable to believe that a tandem axle can be treated as two single axles. Further away from the surface, the response (stress and strain) of the pavement is a combined effect from wheels at the same time (see Figure 2.5). If the deterioration is connected to the response, damage in the lower layers of the pavement will not be the same from a tandem axle as from two single axles.

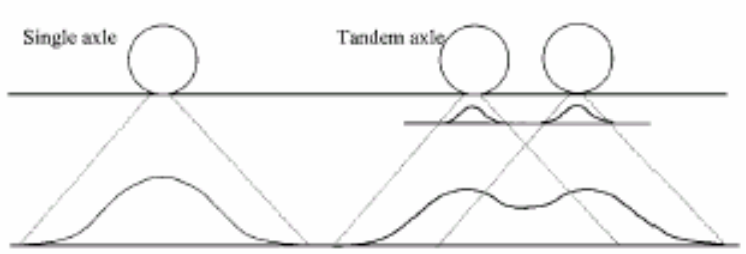

Figure 2.5 Superposition of stress distributions under tandem axle (Archilla & Madanat, 2001)

Since the individual axles in a tandem or triple axle configuration interact, each axle type should be treated separately (Prozzi 2001).

$$EDF = \left(\frac{FA}{P_s\lambda_1}\right)^{\lambda_2} + m_1\left(\frac{SA}{P_s}\right)^{\lambda_2} + m_2\left(\frac{TA}{P_s\lambda_3}\right)^{\lambda_2}$$

where

EDF = equivalent damage factor

FA = load of the front axle

SA = load of the single axles with dual wheels

TA = load of the tandem axles with dual wheels

P_s = standard axle load

$\lambda_1, \lambda_2, \lambda_3$ = regression parameters

m_1, m_2 = number of single and tandem rear axles per truck

This equation uses three axle types. These three are probably the most common types, but it is easy to expand the equation to include other axle configurations such as tridem axles. The load equivalency exponent is the same for all three of the axle types in this model. It is also possible to take the

consequences of different damage factors at different depths one step further, using different exponents for different axle types.

Another way of going into more detail of the origin of deterioration is to use different equations for damage factors for different layers in the pavement (Archilla & Madanat, 2001). For rut depth originating in the AC layer, the following equation was suggested:

$$\Delta RD^{AC} = m * e^{b*N} \Delta N$$

where

m = a function of mix characteristics and loading

N = accumulated number of loads

b = regression parameter that describes hardening

and for rutting originating in the underlying layers:

$$\Delta RD^{U} = a * e^{b*N} \Delta N$$

where

a = a function of layer thicknesses and freeze - thaw periods

N = accumulated number of loads

b = regression parameter that describes hardening

The maximum axle load allowed is different in different countries, and has also been changed several times since the first regulations. Heavier and heavier vehicles have been allowed. This of course affects the existing pavements. Pavements that were designed for one maximum load will deteriorate faster when the load increases.

Example

In 1993 the maximum axle load allowed in Sweden increased from 10 tons to 11.5 tons. Assuming that the fourth power law can describe the effect on the deterioration from the load, it is easy to calculate the increase in deterioration when the load increases.

$$N_x = ?$$
$$N_i = 1\,axle$$
$$P_x = 11.5 ton$$
$$P_i = 10 ton$$
$$N_x = 1\left(\frac{11.5}{10}\right)^4 = 1.75$$

This means that with the increased load of 15% (from 10 to 11.5 tons) the damage to the pavement increases by 75%. That is not the same as the deterioration of the Swedish pavements increasing by 75% when the regulations changed, since it is only a small number of the vehicles that take advantage of the new regulations. This calculation example shows, however, that even a small increase in axle load will have a noticeable effect on pavement deterioration.

Studded tyres

Studded tyres are one source of rutting. The studs cause abrasion of surface material. As opposed to the rutting caused by permanent deformation, the rutting from studded tyres is influenced not only by trucks. Even ordinary cars have a significant effect on the surface wear (Ekdahl, 1997).

In some cold areas, many roads are covered with snow most of the winter. The snow protects the asphalt from the studded tyres, and in those areas the problem of surface wear from studded tyres is only minor. In areas where the roads are covered with snow only occasionally during the winter, many cars are using studded tyres on roads without the snow protection. In those areas the surface wear can be a big problem. In Sweden, the law mandates using winter tyres when winter conditions prevail. Therefore, almost every vehicle uses winter tyres for several months. Many roads are only very rarely covered with snow, but they are nonetheless exposed to studded tyres.

The amount of wear from studded tyres depends on several different factors. Based on observations from both real test sections and laboratory tests, Jacobsson et al. (1997) list the following factors that impact on the wear:

- AADT
- use of studded tyres
- stone material in wearing course
- binder content
- climate
- use of salt in winter maintenance

The use of salt affects the wear in two ways. The purpose of the salt is to melt the snow and ice on the pavement. Hence it removes the protecting snow layer. After the snow has melted, the salt binds water so that the surface is almost constantly wet. A wet surface increases the wear of the pavement by a factor of two to three (Fredriksson et al., 1989).

Another factor that affects wear is speed. As opposed to the permanent deformation, it is high speed that causes the wear from studs. If the speed

increases from 80 km/h to 100 km/h, the wear increases by approximately 100% (Fredriksson et al., 1989).

The surface wear from studded tyres has decreased during recent years. The development of lighter studs that are gentler to the pavement surface has had a great effect. Since the problem of wear was observed, greater attention has been devoted to the stone material in the wearing course. The stone material now used in Sweden is more resistant to studs.

2.2.2 Traffic

Speed

Since most materials that are normally used in pavements have time-dependant response behaviour (plastic, viscous or visco-elastic), speed affects the response in the pavement and so, probably, also the deterioration. The effect of speed can often be seen at intersections or at bus stops where the traffic stands still or drives slowly. Here large permanent deformations (rutting) are often found.

Tests conducted at a test road outside Malmö in southern Sweden show a difference in pavement response, both the horizontal strain at the bottom of the AC layer and the vertical strain in the subgrade, between 30 km/h and 50 km/h. The difference is much smaller between 50 km/h and 70 km/h. This indicates that the effect on the deterioration of the pavement of variations in speed is probably quite small with speeds that are normally used on roads outside rural areas. In rural areas and at intersections, speed is probably an important variable. (Ullidtz & Ekdahl, 1998)

The effect of speed increases when the pavement surface is uneven. The combination of high IRI and high speed increases the effect of the dynamic load from the vehicles (Magnusson 1987, Ullidtz 1998).

2.2.3 Pavement

One of the main purposes of the pavement is to spread the load from the vehicles over an area that is large enough for the subgrade material to be able to carry the load without damaging the subgrade. At the same time, the pavement materials must have sufficient strength to deal with the stress at the level where they are placed. It is therefore obvious that the pavement structure and the properties of the materials have a significant effect on pavement deterioration.

Since the influence from the load (stress) is larger close to the surface, the materials must be stronger at the surface and the demand on the materials can be lower at lower levels. Normally there is a relation between strong material and price. Therefore, the high quality materials, i.e. asphalt concrete, are used in as thin layers as possible, and then progressively weaker materials further down in the pavement.

To get an approximate picture of the size of influence of layer thickness and material properties, some calculations of response are made and presented in graphs below. All calculations are based on a pavement section with a bound layer of 100 mm, and an unbound layer of 500 mm. The E-modulus of the bound layer is assumed to be 5000 MPa, and for the unbound layer 500 MPa. The subgrade is supposed to have an E-modulus of 50 MPa. The load is a plate load with a radius of 150 mm, and a magnitude of 50 kN.

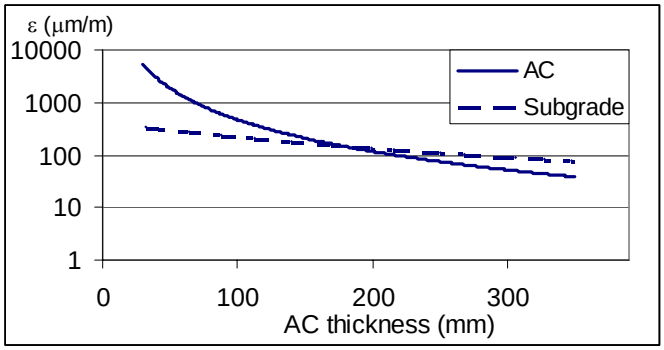

Figure 2.6 Calculated horizontal AC strain and vertical strain in subgrade with different AC thickness (logarithmic scale on y-axis)

As seen in Figure 2.6 the AC strain is strongly affected by the thickness of the AC layer. The AC strain is often supposed to be connected to fatigue cracking that starts at the bottom of the AC layer. Therefore it is reasonable to believe that a thicker AC layer is much better for avoiding fatigue cracking. The subgrade strain is not affected as much as the AC strain.

The relationship between AC thickness and strain is not linear for either horizontal AC strain or vertical subgrade strain. Hence the thickening of the AC layer is most effective when the AC layer is thin, and the increasing AC layer thickness is not always cost efficient.

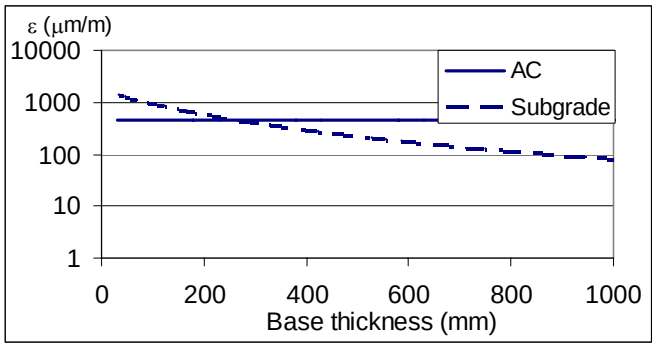

Figure 2.7 Calculated horizontal AC strain and vertical strain in subgrade with different base thickness (logarithmic scale on y-axis)

The calculations in this chapter are made with the method of equivalent thickness (MET) (Odemark, 1949), further described in Chapter 2.3. That method assumes that the material below the level where the response is calculated does not affect the response. That is why the AC strain is not affected by the thickness of the base in Figure 2.7. If the strain is calculated with the multilayer elastic model, the strain decreases by approximately 20% when the base course thickness changes from 200 to 800 mm. As can be seen, the subgrade strain is highly affected by the base thickness, and the relationship is not linear.

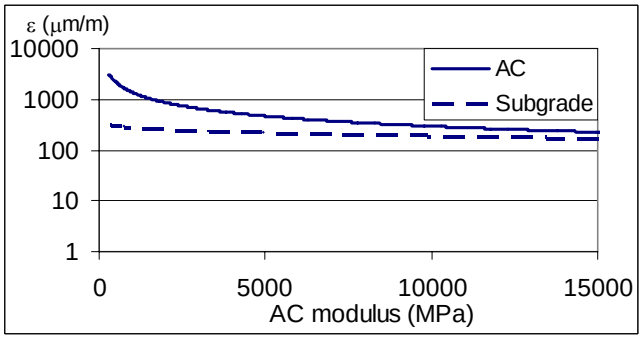

Figure 2.8 Calculated horizontal AC strain and vertical strain in subgrade with different AC modulus (logarithmic scale on y-axis)

Just as for the change in thicknesses, the relationship between AC modulus and strain is not linear. In the normal range of moduli the effect on subgrade strain is relatively small.

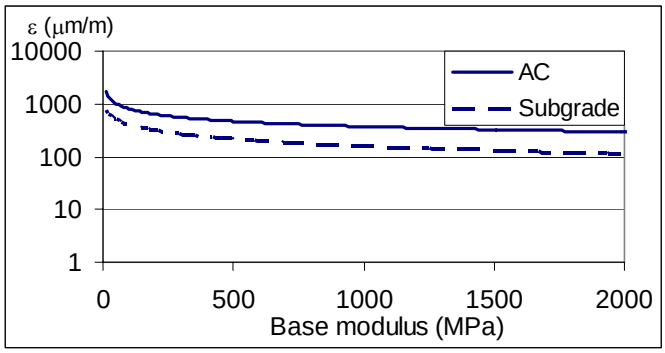

Figure 2.9 Calculated horizontal AC strain and vertical strain in subgrade with different base modulus (logarithmic scale on y-axis)

When comparing the results in Figure 2.8 and Figure 2.9, it can be seen that a change in base course modulus has a greater effect on the subgrade strain than a change in AC modulus. The AC strain is affected by both AC modulus and base course modulus. According to Odemark's (1949) assumptions, the stress distribution depends on the rate between AC modulus and base course modulus, but not on the level of the moduli. Consequently, not only the level of base course moduli, but also the rate between AC and base course moduli has a great influence on the AC strain.

2.2.4 Climate

Stiffness of bituminous layers is highly sensitive to temperature. Unbound layers are affected by moisture and frost. The temperature in the pavement often varies with depth and depends on both air temperature and wind. To simplify calculations, it is often required to find a temperature that is representative of the whole pavement or for a certain layer. One way to calculate a temperature that is representative for the bituminous layers is suggested by George & Husain (1986):

$$T_{asp} = T_{air}\left(1 + \frac{76.2}{h_{asp} + 304.8}\right) - \frac{84.7}{h_{asp} + 304.8} + 3.3$$

where

T_{asp} = effective surface layer temperature (°C)

T_{air} = mean air temperature (°C)

h_{asp} = thickness of surface layer (mm)

A graphical solution is presented in the Shell Pavement Design Manual.

At high temperatures the bituminous materials are soft and sensitive to permanent deformations. When it is cold, the material is stiff and the risk of

cracking increases instead. The change in E-modulus of the material can be expressed with a logarithmic equation (Ullidtz & Ekdahl, 1998).

$$E_t = E_{ref} e^{a(t - t_{ref})}$$

where

E_t = modulus at temperature t

E_{ref} = modulus at reference temperature

a = regression parameter

t = temperature

t_{ref} = reference temperature

The value of a is suggested to be -0.083 (Ullidtz & Ekdahl 1998), but that is based on measurements from only one test site with three different pavements, and it is possible that the parameter should be changed for different materials.

Temperature has an effect specifically on bituminous materials. Back calculation from FWD measurements at two different test sites in southern Sweden has shown that the E-modulus for the base course also depends on the temperature (Ullidtz & Ekdahl 1998, Ekdahl 1998). The reason for this is not clear. The material itself should not be temperature dependent, but it is possible that the contacts between the particles in the interface between the layers are strong, and the two layers interact and almost work as a composite material. When analysed with linear elastic theory, that can cause the base course to seem to be temperature dependant.

While the bituminous materials are sensitive to temperature, the unbound materials are instead sensitive to moisture. Measurements in the Danish Road Testing Machine (RTM) have shown that the E-moduli for unbound materials change approximately 35-40% when the moisture level is changed (Krarup, 1994).

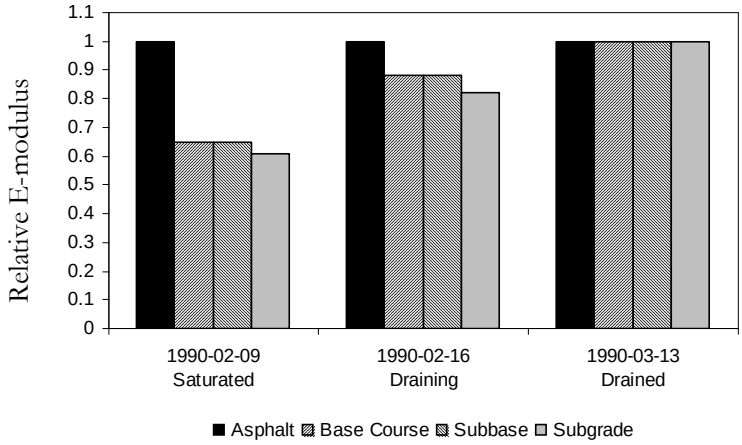

Figure 2.10 Variation of layer modulus at different moisture levels (Krarup, 1994)

In Figure 2.10 the subgrade seems to be most sensitive to moisture. In this case the subgrade consisted of sandy till. The sensitivity to moisture is of course highly dependant on the material content. The content of fine material is especially important.

2.2.5 Time

Aging of bituminous materials occurs in two stages. The first stage is during manufacturing and laying. The main component of this stage is loss of volatile components and oxidation in hot mixes (Collop & Cebon, 1995). The second stage is mainly long-term oxidation. Shell (1990) divides the first stage into two parts where the first, and most important, is the aging during mixing. The second part is the aging during storage, transportation and application (see Figure 2.11).

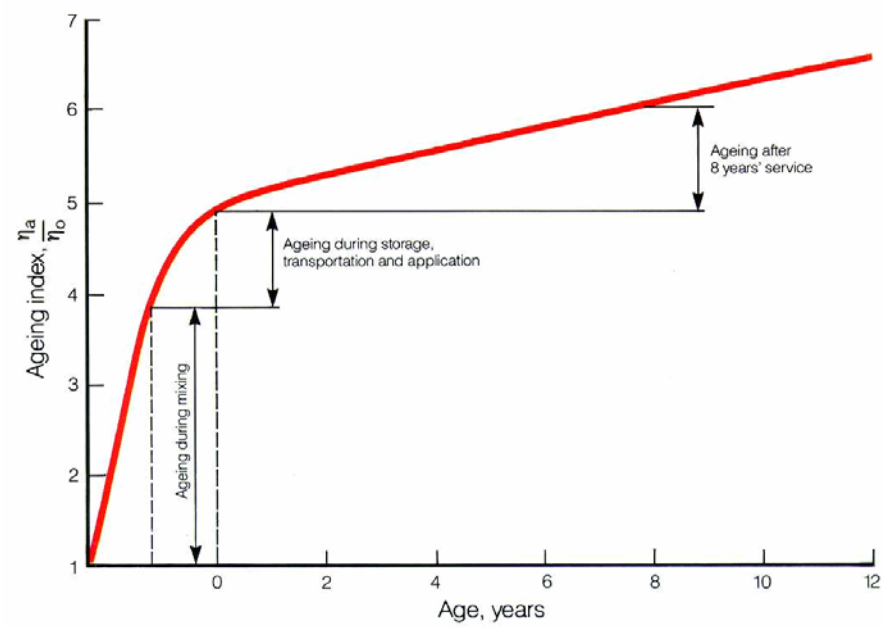

Figure 2.11 Aging of bituminous materials by time (Shell, 1990)

In the example in Figure 2.11 the viscosity of the bitumen has increased approximately 5 times its original value when the pavement is constructed. The reason for the fast aging during mixing and construction is that the bitumen is highly exposed to the oxygen in the air. After construction it is mainly the surface that is exposed to the oxygen. The void content is an important factor for the speed of aging. Tests carried out by Shell (1990) showed that with void content of 10% the penetration dropped from 70 to 25 in five years. With void content of only 5%, the change in penetration was rather small.

One way to deal with the aging in a deterioration model is to calculate the change in Ring and Ball softening point (Verhasselt & Choquet, 1993):

$$T_{RB}^{(R)}\Big|_{t=t1} = T_{RB}^{(R)}\Big|_{t=0} + \sqrt{\Lambda t}$$

where

$T_{RB}^{(R)}\Big|_{t=t1}$ = Ring and Ball temperature at time t = t1

$T_{RB}^{(R)}\Big|_{t=0}$ = initial Ring and Ball temperature at time t = 0

Λ = reaction constant (C^2/h)

t = time (h)

The reaction constant (Λ) depends strongly on the temperature of the bitumen. Verhasselt & Choquet (1993) used the mean annual temperature as

the effective temperature at which the constant was determined. They obtained reasonable agreement with measured aging with constants between $1.2*10^{-3}$ and $2.1*10^{-3}$ $^{o}C^{2}$/hour. The tests were obtained in climates typical of Belgium. Collop & Cebon (1995) used a value of $1.65*10^{-3}$ $^{o}C^{2}$/hour for UK Pavements.

2.3 Material models

There are many ways to calculate pavement response. The most common method is to assume that the materials are homogenous, isotropic and linear-elastic. These assumptions are not true for most pavement materials. The unbound materials are obviously not homogenous since they consist of particles. It is, however, possible that despite the fact that the basic assumptions are false, the theories can still be used with reasonably accurate results. At least for granular materials it has been known for a long time that the linear-elastic theory does not fit very well with measured values (Frölich, 1934). In the last century, many models have been developed to make the calculated stresses and strains fit better with the measured values.

2.3.1 Elastic Models

At the end of the 19th century Boussinesq derived equations for calculating stresses, strains and deformations under a point load in a linear-elastic semi-infinite half-space (Boussinesq, 1885). Using polar coordinates (see Figure 2.12) the equations are:

Normal stresses:

$$\sigma_z = \frac{3P}{2\pi R^2}\cos^3\theta$$

$$\sigma_r = \frac{P}{2\pi R^2}\left(3\cos\theta\sin^2\theta - \frac{1-2\nu}{1+\cos\theta}\right)$$

$$\sigma_t = \frac{(1-2\nu)P}{2\pi R^2}\left(-\cos\theta + \frac{1}{1+\cos\theta}\right)$$

$$\sigma_1 = \frac{3P}{2\pi R^2}\cos\ \theta$$

$$\sigma_v = \frac{(1+\nu)P}{3\pi R^2}\cos\theta$$

Shear stresses:

$$\tau_{rz} = \frac{3P}{2\pi R^2}\cos^2\theta\sin\theta$$
$$\tau_{rt} = \tau_{rz} = 0$$

Strains:

$$\varepsilon_z = \frac{(1+\nu)P}{2\pi R^2 E}\left(3\cos^3\theta - 2\nu\cos\theta\right)$$
$$\varepsilon_r = \frac{(1+\nu)P}{2\pi R^2 E}\left(-3\cos^3\theta + (3-2\nu)\cos\theta - \frac{1-2\nu}{1+\cos\theta}\right)$$
$$\varepsilon_t = \frac{(1+\nu)P}{2\pi R^2 E}\left(-\cos\theta + \frac{1-2\nu}{1+\cos\theta}\right)$$
$$\varepsilon_v = \frac{(1+\nu)P}{\pi R^2 E}(1-2\nu)\cos\theta$$

Deflections:

$$d_z = \frac{(1+\nu)P}{2\pi RE}\left(2(1-\nu) + \cos^2\theta\right)$$
$$d_r = \frac{(1+\nu)P}{2\pi RE}\left(\cos\theta\sin\theta - \frac{(1-2\nu)\sin\theta}{1+\cos\theta}\right)$$
$$d_t = 0$$

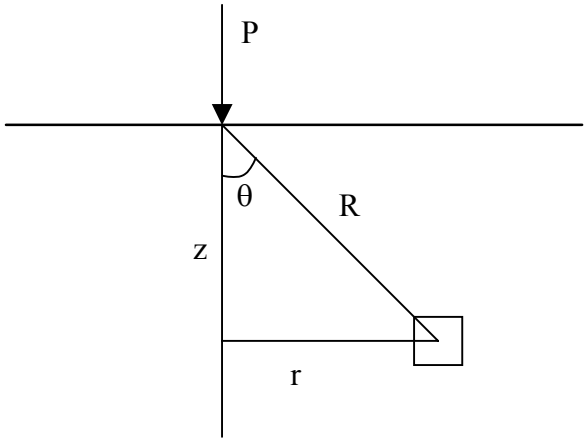

Figure 2.12 Polar coordinates used in the equations above

For calculations under a distributed load, numerical methods are normally necessary. However, for the centreline under a circular load, closed form solutions are available:

$$\sigma_z = \sigma_0 \left(1 - \frac{1}{\left(\sqrt{1 + \left(\frac{a}{z} \right)^2} \right)^3} \right)$$

$$\sigma_r = \sigma_t = \sigma_0 \left(\frac{1+2\nu}{2} - \frac{1+\nu}{\sqrt{1 + \left(\frac{a}{z} \right)^2}} - \frac{1}{2\left(\sqrt{1 + \left(\frac{a}{z} \right)^2} \right)^3} \right)$$

$$\varepsilon_z = \frac{(1+\nu)\sigma_0}{E} \left(\frac{\frac{z}{a}}{\left(\sqrt{1 + \left(\frac{z}{a} \right)^2} \right)^3} - (1-2\nu) \left(\frac{\frac{z}{a}}{\sqrt{1 + \left(\frac{z}{a} \right)^2}} - 1 \right) \right)$$

$$\varepsilon_r = \frac{(1+\nu)\sigma_0}{E} \left(\frac{-\frac{z}{a}}{\left(\sqrt{1 + \left(\frac{z}{a} \right)^2} \right)^3} - (1-2\nu) \left(\frac{\frac{z}{a}}{\sqrt{1 + \left(\frac{z}{a} \right)^2}} - 1 \right) \right)$$

$$d_z = \frac{(1+\nu)\sigma_0 a}{E} \left(\frac{1}{\sqrt{1 + \left(\frac{z}{a} \right)^2}} + (1-2\nu) \left(\sqrt{1 + \left(\frac{z}{a} \right)^2} - \frac{z}{a} \right) \right)$$

These equations apply to a uniformly distributed load. Equations for a rigid plate can be found in (Ullidtz, 1998).

Since the linear-elastic theory cannot accurately describe the behaviour of pavement materials (i.e. Frölich, 1934), many attempts have been made to find a better model. Some of these models are described below.

Stress concentration

One of the earliest modifications of the linear-elastic theory was made by Frölich (1934). From stress measurements in granular materials, he noticed that the stress was more concentrated than linear-elastic theory predicted. He assumed that no tangential stress exists, and that the major principal stress is in the direction of the vector pointing towards the load point (Veverka, 1973). The stress decreases with the square of the distance to the load point (R in Figure 2.12).

If the concentration factor (n) is 3, the Boussinesq equations with ν=0.5 are obtained.

Anisotropy

Since the materials in a pavement are not compacted isotropically, it may be reasonable to assume that the material is not isotropic. The modulus in horizontal direction can be expected to differ from the modulus in vertical direction.

The relation between stresses and strains in a cross-anisotropic body are described as

$$E\varepsilon_x = n\sigma_x - n\nu\sigma_y - \mu\sigma_z$$
$$E\varepsilon_y = -n\nu\sigma_x + n\sigma_y - \mu\sigma_z$$
$$E\varepsilon_z = -\mu\sigma_x - \mu\sigma_y - \sigma_z$$

where

$$E = E_z$$
$$n = \frac{E_z}{E_x}$$
$$\mu, \nu = \text{poisson' s ratio in different directions}$$

(van Cauwelaert, 1977)

Assuming that $\nu=\mu$ and considering the centreline of the load where $\varepsilon_x=\varepsilon_y=\varepsilon_h$, and $\sigma_x=\sigma_y=\sigma_h$ this will give

$$E_v\varepsilon_v = -2\nu\sigma_h + \sigma_v$$
$$E_v\varepsilon_h = -n\nu\sigma_h + n\sigma_h - \nu\sigma_v$$

From the first line in the equation above it is possible to calculate the horizontal stress by

$$\sigma_h = \frac{\sigma_v - E_v \varepsilon_v}{2\nu}$$

and with that equation inserted in line two, the horizontal strain can be calculated by

$$\varepsilon_h = (1-\nu)\frac{\sigma_h}{E_h} - \frac{\nu\sigma_v}{E_v}$$

Shear sensitivity

In granular materials, displacements occur because of particles sliding against each other. Therefore it is likely that the resistance to shear should be lower for a granular material than for a solid material with the same compression strength (Misra & Sen, 1975). For an ideal elastic material, the ratio E/G (compression modulus/shear modulus) is equal to 2(1+ν). For granular materials, the ratio should be larger than that.

Probabilistic stress distribution

Granular materials do not have actual stresses and strains. The load is only transferred within the medium in the form of forces between particles. Therefore there cannot be any tensile stresses in the material, and stresses and strains only exist as average values over an area.

Based on probabilistic (random walk) theory (see Figure 2.13), it can be shown that the stress distribution under a line load will follow a normal distribution (Harr, 1977).

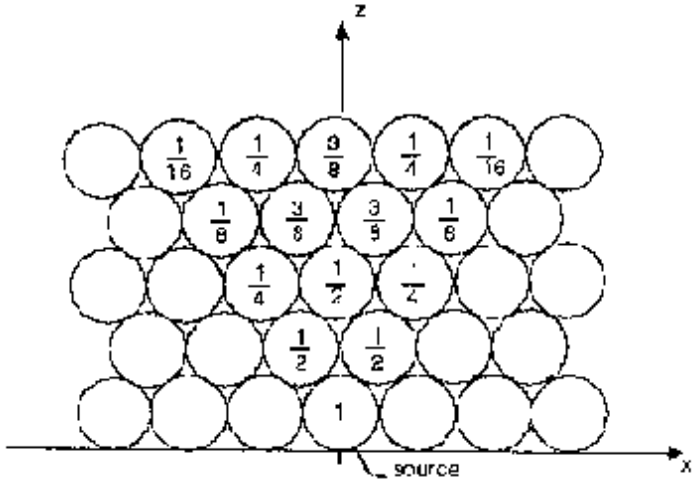

Figure 2.13 The concept of random walk (Stiady, 1999)

Therefore the vertical stress can be calculated with the equation for normal distribution.

With probabilistic theory, it is not only possible to calculate one expected value of the response. This theory also gives the opportunity to calculate the risk that the stress or strain exceeds a certain value. This can be useful for design purposes if there is a certain level of maximum response that must not be exceeded. In incremental deterioration models, however, the mean values best represent the probable deterioration.

One advantage of this method compared to the other elastic methods is that no tensile stress appears in the material. This is also the only elastic method described in this thesis that is not based on the assumption that the medium is a continuum. Since deflections are calculated by the sum (integral) of the strains, the deflection calculation is a bit more time consuming than for the other models. This mainly affects the calculation of material data from FWD measurements. Therefore it is not necessarily a big disadvantage for use in design purposes. If FWD measurements are used to obtain material data for the deterioration model, this time consuming back calculation is only done once, at the beginning of the calculations. For the deterioration calculations, most often only stress and strain is necessary.

2.3.2 Visco-elastic Models

It is well known that most materials in normal pavements are not purely elastic. A part of the deformation under load is not immediately recovered, and the deformation increases with longer loading time. Especially for asphalt materials, different attempts have been made to deal with this. Deformation can be divided into three different kinds of deformation:

1. Momentanous elastic deformation
2. Recoverable creep (primary creep)
3. Permanent viscous deformation (secondary creep)

The simplest model that can describe all three kinds of deformations is Burger's (Hult, 1966). It has been suggested (i.e. Nilsson, 2001b) that this visco-elastic model can be used for asphalt mixes. Burger's model consists of four elements, two springs and two dampers, according to Figure 2.14.

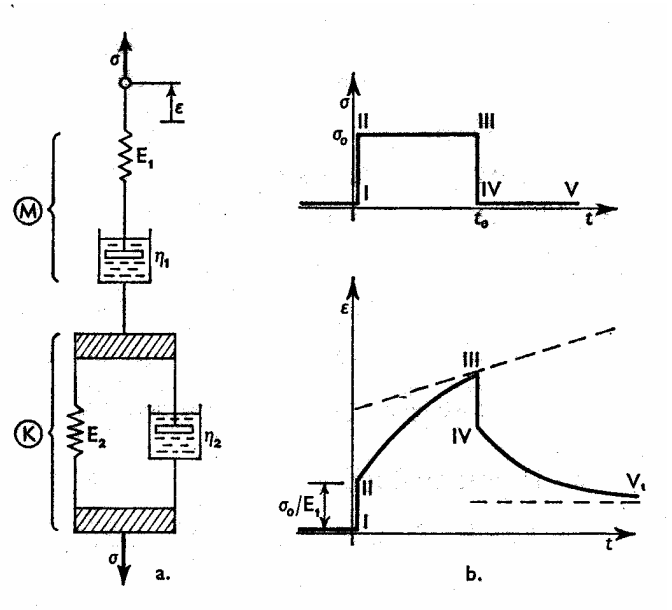

Figure 2.14 Burger's material model (Hult, 1966)

Each element has one material parameter, and hence four material parameters are needed for this model. By combining the constitutive equations for each element, the constitutive equation for the model will be (Hult, 1966):

$$\ddot{\varepsilon} + \dot{\varepsilon}\frac{E_2}{\eta_2} = \frac{\ddot{\sigma}}{E_1} + \dot{\sigma}\left(\frac{1}{\eta_1} + \frac{E_1 + E_2}{E_1\eta_2}\right) + \frac{\sigma E_2}{\eta_1\eta_2}$$

notation according to Figure 2.14.

It is possible to obtain different linear visco-elastic models by combining springs and dampers in different ways. A general constitutive equation for these kinds of materials is (Hult, 1966):

$$\sum_{r=0}^{q} q_r \frac{d^r \varepsilon}{dt^r} = \sum_{r=0}^{p} p_r \frac{d^r \sigma}{dt^r}$$

where d_r and p_r are functions of the material parameters (E, η).

With more elements in the material model, it is possible to get a better description of the material behaviour, but this also requires more material parameters. With more material parameters it can be difficult to interpret the parameters, and also more difficult to determine accurate values of the parameters.

2.3.3 Distinct Element Method

All of the models described above, except possibly the probabilistic stress distribution model, assume that the materials are homogenous. The distinct element method (DEM) describes each particle in the material individually, and therefore it describes granular material in a way that is closer to reality than other material models.

This theory assumes that the deformation within the particles is small compared to the deformation in the whole particle assembly. Therefore it is not important to model the deformation inside the particles (Cundall & Strack, 1979).

The basis of DEM is a couple of simple and well-known equations. Assume two lines that are approaching two discs as in Figure 2.15.

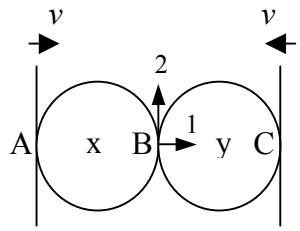

Figure 2.15 Simple example of DEM (1/2)

At the time $t_1=t_0+\Delta t$ the lines will have moved onto the discs as in Figure 2.16.

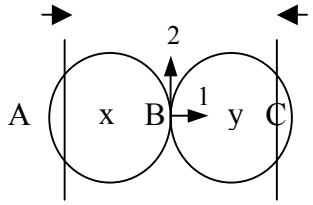

Figure 2.16 Simple example of DEM (2/2)

The force acting between the particles can be calculated by

$$\Delta F_n = k_n(\Delta n)_{t1} = k_n v \Delta t$$

where

k_n = stiffness of the discs

$$F_{(x)1} = k_n(\Delta n)_{t1},\ F_{(y)1} = -k_n(\Delta n)_{t1}$$

When the forces are known, the accelerations can be calculated with Newton II:

$$\ddot{x}_1 = \frac{F_{(x)1}}{m_{(x)}},\ \ddot{y}_1 = \frac{F_{(y)1}}{m_{(y)}}$$

Assuming that the accelerations are constant from t_1 to t_2, the speeds of the particles can be calculated by

$$\left[\dot{x}_1\right]_{t2} = \left[\frac{F_{(x)1}}{m_{(x)1}}\right]\Delta t\ ,\ \left[\dot{y}_1\right]_{t2} = \left[\frac{F_{(y)1}}{m_{(y)1}}\right]\Delta t$$

With known speeds the movements of the locations A, B and C can be calculated by:

$$\left(\Delta n_{(A)}\right)_{t2} = \left(v - \frac{F_{(x)1}}{m_{(x)}}\Delta t\right)\Delta t$$

$$\left(\Delta n_{(B)}\right)_{t2} = \left(\frac{F_{(x)1}}{m_{(x)}}\Delta t - \frac{F_{(y)1}}{m_{(y)}}\Delta t\right)\Delta t$$

$$\left(\Delta n_{(C)}\right)_{t2} = \left(\frac{F_{(y)1}}{m_{(y)}}\Delta t - \left[-v\right]\right)\Delta t$$

where compression is represented by positive values. (Cundall & Strack, 1979)

These calculations have to be made again for each time step. Forces are calculated by some kind of relation between deformation and force.

Since the assumption that accelerations are constant during each time step is not true, there is a risk that the sum of the calculated forces inside he

assembly will not be equal to zero. To avoid this problem, an iterative procedure has to be applied for each time step. When the assembly contains a large number of particles, the number of calculations will be very large. Therefore this calculation procedure can be quite time consuming. However, all calculations do not have to be made after each other. Many of them can be made at the same time, so with parallel processors the calculation time can be reduced considerably (Ferrez et al., 1996).

2.3.4 Layered system

The equations presented above in section 2.3.1 are all based on the assumption that the material is a semi-infinite half-space. A pavement consists of several layers of different materials. Calculations of response cannot be made with exact closed form solutions of the linear-elastic theory.

Method of Equivalent Thicknesses

In 1949, Odemark provided a simple, and therefore fast, method of calculating response in a multi-layer model with linear-elastic materials (Odemark, 1949). The first step in this method is to convert the layers into one single layer. Then Boussinesq's equations can be used. The conversion is made by replacing the thickness and E-modulus of a layer with the E-modulus of the underlying layer and a new equivalent thickness. Therefore the method is often called Method of Equivalent Thicknesses (MET).

Odemark made the assumption that the response in a layer is independent of what lies beneath the layer. If the thickness and E-modulus of a layer are changed, but the stiffness of the layer is constant, then the response in that layer also remains constant. The stiffness is supposed to be proportional to:

$$\frac{IE}{1-\nu^2}$$

where

I = moment of inertia

E = Elastic modulus

ν = Poisson's ratio

This leads to the transformation equation:

$$\frac{h_1^3 E_1}{1-\nu_1^2} = \frac{h_e^3 E_2}{1-\nu_2^2}$$

where

h_e = equivalent thickness

h_1 = thickness of the upper layer

E_1 = elastic modulus for the upper layer

E_2 = elastic modulus for the lower layer

ν_1 = Poisson's ratio for the upper layer

ν_2 = Poisson's ratio for the lower layer

which leads to the following equation for calculating equivalent thickness:

$$h_e = h_1 \sqrt[3]{\frac{E_1\left(1-\nu_2^2\right)}{E_2\left(1-\nu_1^2\right)}}$$

This method is not a mathematically correct solution of linear-elastic theory. To obtain values that are closer to the mathematically correct solution, it is possible to add a correction factor (f). There are many suggestions of what correction factors should be used. Often f=0.9 is used for two-layer systems, and for multi-layer systems f=1 for the first layer and f=0.8 for the other layers are used (Ullidtz, 1998). These correction factors are suggested in order to get closer agreement with linear-elastic theory. Since most pavement materials are not linear-elastic, these correction factors do not necessarily improve the agreement with the real response.

It has also been suggested that the correction factors should vary with the thickness of the layers. One way to achieve that is to calculate the correction factor in the form:

$$f = A + Bh_e^{-C}$$

where

f = correction factor

h_e = equivalent depth

A, B and C = constants

Typical values for A, B and C can be 0.8, 0.7 and 1.4 respectively (Busch, 1991).

Based on tests with the Danish road testing machine, a correction factor of 1.3 for the AC strain and 0.9 for the vertical strain in the subgrade has been suggested to get better agreement with the measured values (Baltzer et al.,

1998). However, the general applicability of these factors has not been studied.

Burmister's method

Burmister (1943) developed mathematically correct solutions for a two-layer system, for example full-depth pavements. Later he also developed solutions for a three-layer system that allowed both an AC layer and an unbound layer in the pavement (Burmister, 1945). With increased computer power, it became possible to also solve the equations for a system with an infinite number of layers (Huang, 1967). The assumptions made for these solutions are (Huang, 1993):

- Each layer is homogenous, isotropic and linear-elastic
- The material is weightless and infinite in horizontal directions
- Each layer has a finite thickness, except the lowest layer, which has infinite thickness
- A uniform pressure is applied over a circular area
- Continuity equations are satisfied at the layer interfaces in the form of same vertical stress, shear stress and both vertical and horizontal displacements

These solutions are used in many of the computer programs commercially available and in the public domain for calculating response in pavements, such as BISAR, mePADS and PCASE.

2.4 Back Calculation

The most common purpose of the back calculation is to determine material parameters (e.g. E-moduli) for different layers in a structure from a deflection basin. The calculation of these parameters often involves a trial-and-error process. The calculation starts with a set of parameters and the deflection basin is calculated with this set. If the calculated basin does not agree with the measured basin, the parameters are adjusted and a new deflection basin is calculated. The process is repeated until the calculated and measured deflection basins are reasonably close.

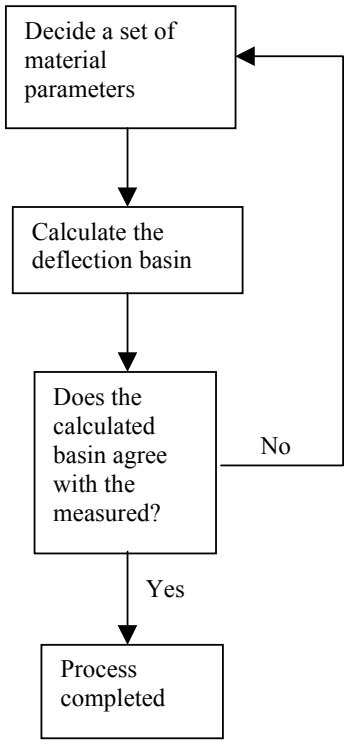

Figure 2.17 The Back Calculation process

Each measured deflection gives one deflection to calculate, and therefore one equation. All the deflections form a system of equations. Often all layer thicknesses are known, and therefore only the layer moduli are unknown parameters. In most cases there are more measured deflections than layers in the structure, and the system of equations is then mathematically over-determined. The upper layers of the pavement primarily influence the deflection close to the load. Therefore the outermost geophones in most FWD measurements measure mostly a deflection in the subgrade, and do not provide much information about the material parameters of the upper layers. This means that not all deflection measurements contribute new information to the equation system. Instead of an over-determined equation system it is in reality more like an under-determined system. There are therefore many sets of moduli that give reasonable fit with the measured deflection basin. This makes it important that the initial set of layer moduli is as close to the real values as possible. More geophones do not provide much new information to the equation system, but do contribute to minimizing the effect of measurement errors.

There are several ways to decide the initial set of parameters. The easiest way is to just guess the values. In order to get a good result from the back calculation, it is important that these guesses are as intelligent as possible.

Some simple calculations often make it possible to get an idea of the layer moduli. Since the deflection at a greater distance from the load is more influenced by the lower layers, the outermost geophones can often be used to determine the modulus of the subgrade.

Assuming that the construction is just one homogenous layer (Boussinesq case), the E-modulus of the material can be calculated from:

$$E_0 = 2(1-\nu^2)\frac{\sigma_0 a}{d_0}$$

$$E_r = (1-\nu^2)\frac{\sigma_0 a^2}{r d_r}$$

where

E_r is the surface modulus at distance r from the load centre

ν is Poisson's ratio

σ_0 is the contact stress under the loading plate

a is the radius of the loading plate

d_r is the deflection at distance r

If the half-space is linear-elastic, E_r will be the same for all distances from the load (r). Since the real pavement is never just one homogenous layer, this value can only be used to compare different parts of the same object. This surface modulus can be considered as a weighted mean value of the moduli of all layers (Ullidtz, 1987).

At a distance r from the load, the surface deflection ($d_{r,0}$) is equal to the deflection at a certain depth ($d_{r,z}$). This depth z depends on Poisson's ratio. If Poisson's ratio is 0.40, the depth (z) is equal to the distance from the load (r). Normally Poisson's ratio is close to 0.40 and a small deviation from that value does not influence the deflection much. Therefore it is a reasonable assumption that the deflection at the depth z is equal to the surface deflection at the distance r=z from the load (see Figure 2.18).

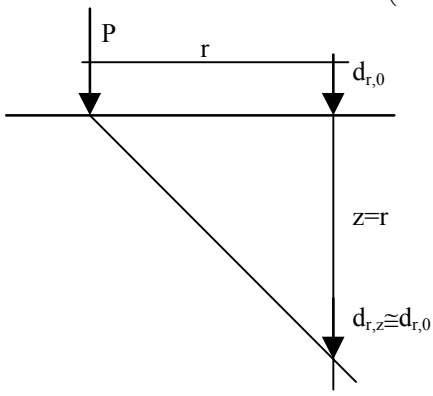

Figure 2.18 Deflection on semi-infinite half-space (Ullidtz, 1998)

As mentioned above, the surface modulus can be considered as a weighted mean value of the moduli of all layers in the structure. Since the deflection at the surface is equal to the deflection at the 45° line, the surface modulus can also be considered as a weighted mean value of the moduli of all layers under the 45° line. If the subgrade is linear-elastic, geophones at a greater distance from the load than the subgrade level can be used to determine subgrade modulus and give one unknown parameter less in the equation system. With a linear-elastic subgrade, all these deflections should give the same modulus. Unfortunately that is not always true. Very often the surface modulus varies with distance as shown in Figure 2.19. Theoretically the values to the right in the figure should all be at the same level.

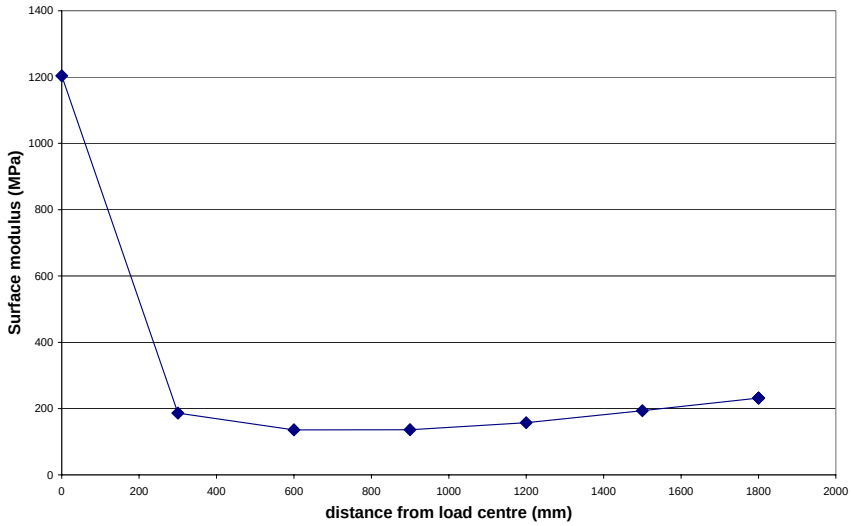

Figure 2.19 Typical surface modulus versus distance from load

The greater the distance from the load, the greater will a stiff underlying layer affect the calculated subgrade modulus. Therefore the innermost geophone that is outside the pressure bulb from the load should be used. Darter et al. (1991) recommend a way to determine from which geophone the subgrade modulus should be determined:

$$d \geq 0.7 \frac{r}{\sqrt{a^2 + \left(\sum_{i=1}^{n} D_i \sqrt{\frac{E_p}{M_r}}\right)^2}}$$

where

d_{sg} = distance where the subgrade modulus should be determined

a = load plate radius

D_i = thickness of pavemant layer i

n = number of pavement layers

E_p = effective pavemnet modulus

M_r = backcalculated subgrade resilient modulus

The effective pavement modulus can be derived from:

$$d_0 = 1.5pa\left(\frac{1}{M_r\sqrt{1+\left(\frac{D}{a}\sqrt[3]{\frac{E_p}{M_r}}\right)^2}} + \frac{1-\frac{1}{\sqrt{1+\left(\frac{D}{a}\right)^2}}}{E_p}\right)$$

where

d_0 = *deflection at center of the load*

p = *load plate pressure*

D = *total thickness of the pavement layers above the sugrade*

2.5 Verification of Calculated Response

Several attempts have been made to validate different response models. Some of them are mentioned below.

Chatti et al. (1999) have compared responses calculated with the MICHBACK-MICHPAVE system with measurements of strain at the bottom of the AC layer from a test site in Michigan. MICHPAVE is a FEM-based program for calculating pavement response, and MICHBACK is a back-calculation program for determining E-moduli from FWD measurements. Results show that the calculated strains from FWD load are within 5% of the measured strain, and for truckloads within 20% of the measured data. (Chatti et al., 1999)

Visco-elastic models have been validated with good results by, for example, Hopman et al. (1997). The calculated response was compared to measured

AC strain from LINTRACK (full scale testing in the Netherlands). Good fit was obtained for both longitudinal and transversal strain. The visco-elastic model has the advantage that the asymmetric strain curves under a moving load can be described. Both the shape of the response curve and the size of the response fitted well (Hopman et al., 1997).

Some of the commercially available computer programs that are used to calculate pavement response were evaluated in the AMADEUS (2000) project. Most of the programs are based on elastic multi-layer theory. The results from that study showed that there was little difference between the programs. Most of the programs could predict the AC strain, but the strain, and also the stress, in the subgrade was underestimated by all programs (Table 1). Since all of the tested programs assumed that the materials are homogenous, the project suggests that DEM could be used to improve the understanding of material characteristics for unbound materials. It is also suggested that more studies should be conducted about non-linear and plastic behaviour of the materials.

Table 1 Summary of the findings from phase 2 of the AMADEUS project (AMADEUS, 2000)

Model	Team	CEDEX				DTU			LAVOC		
		ε_x	ε_z	σ_z	d	ε_x	ε_z	σ_z	ε_x	ε_z	d
BISAR	1	⇩	•	↓	⇳	⇩	↓	↓	⇔	↓	⇧
CAPA3D	1	⇩	•	↓	⇧	⇩	↓	↓	⇔	↓	⇔
CIRCLY	1	⇩	•	↓	⇳	⇩	↓	↓	⇔	↓	⇧
	4	⇔	•	↓	⇔	⇩	↓	↓	⇔	↓	⇧
KENLAYER	2	•	•	↓	⇔	•	↓	↓	•	↓	⇳
	3	•	•	•	⇔	•	↓	↓	•	↓	⇩
	4	⇔ (1)	•	↓	⇔	⇔	↓	⇔	⇔	↓	⇔ (2)
MICHPAVE	3	•	•	•	•	•	•	•	⇔	↓	⇔
NOAH	2	⇳	•	↓	⇔	⇔	-	-	⇔	↓	⇧
SYSTUS	2	•	•	•	•	•	•	•	•	•	•
VEROAD	2	•	•	•	•	•	•	•	•	•	•

εx horizontal strain at bottom of the asphalt.
εz vertical strain in the sub-grade.
σz vertical stresses in the subgrade.
d deflection at the surface.
⇩ Underestimate of response.
⇧ Overestimate of response.
↓↑ Large under or overestimate of response.
⇔ Predicted response close to measured response.
⇳ Predicted responses span the measured response.

- • Response not compared.
- - Response yet to be included in Team report.
- (1) Elastic analysis with full friction between layers.
- (2) Smooth interface used between asphalt and granular layer.

The data for the AMADEUS project were measured at three different test sites: the Danish Road Testing Machine, the LAVOC test site in Lausanne and the CEDEX test site in Madrid. Measured data from the first two test sites are also used for the study in this thesis.

The results from the AMADEUS (2000) study showed that the additional features in some of the programs (i.e. anisotropy in CIRCLY, interface slip in BISAR and NOAH or Finite Element Method in SYSTUS and CAPA3D) did not improve the results. At least for anisotropy, this can be due to lack of knowledge about how to use the extra parameters in the most effective way (AMADEUS, 2000).

The elastic material models mentioned earlier in this chapter have also been evaluated by Agardh (2002). That study was performed in three steps, where the first step evaluated the potential of the models by trying to find material parameters that could make a good fit between calculated and measured response. Seven test sections, four full-scale laboratory sections and three instrumented real pavements, were included in the evaluation. All calculations were done with the Method of Equivalent Thicknesses (MET). A summary of the results from the first step is shown in Figure 2.20.

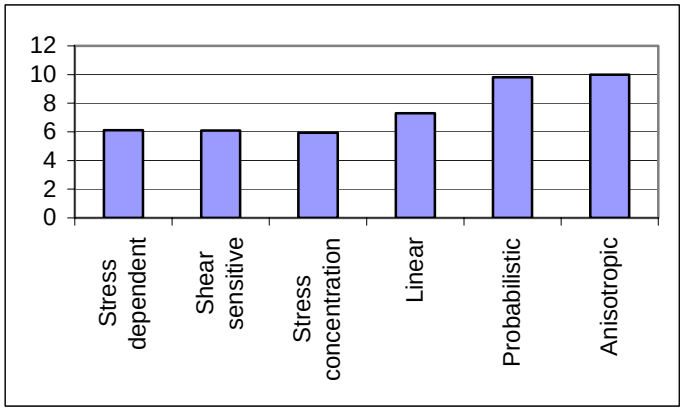

Figure 2.20 Deviation between measured and calculated response in "number of standard deviations of the measured response" (Agardh, 2002)

The three models that gave the best results in the first step of the evaluation were chosen for further studies. In the next step, the material parameters were obtained only from FWD measurements, and the response was

calculated for the same load. Also calculations with BISAR were included in this study. The material parameters for the BISAR calculations were obtained with the computer program MODULUS 5.1. Material parameters from FWD can be obtained in two ways. Either a back calculation is performed for each measurement and then the parameters are averaged, or the measured deflections are averaged and then just one back calculation is performed. This study showed that the calculated responses were closer to the measured responses when the deflections were averaged and only one back calculation was performed (Figure 2.21).

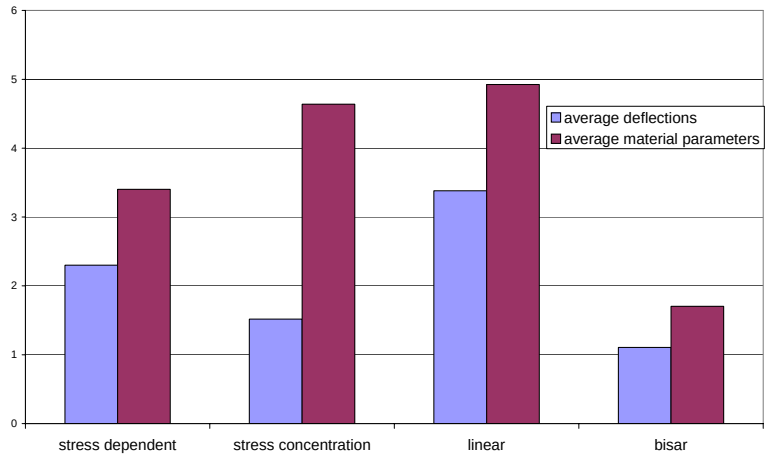

Figure 2.21 Average RMS for the different models from FWD analysis. (Agardh, 2002)

The model with stress dependant subgrade resulted in calculated responses that were closest to the measured responses.

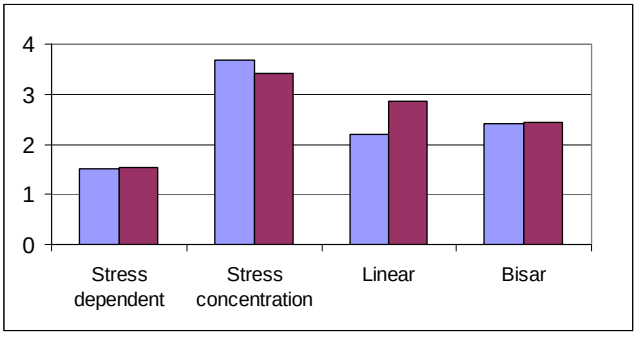

Figure 2.22 Average differences between measured and calculated response in the unit "number of standard deviations". The left (light) bars are calculated from average deflections, and the right (dark) bars are calculated from average parameters. (Agardh, 2002)

The third step of the evaluation was to compare the calculated response to measured response under a dual wheel load. Even in these calculations it seems that the stress dependant subgrade enhances the calculations (Figure 2.23).

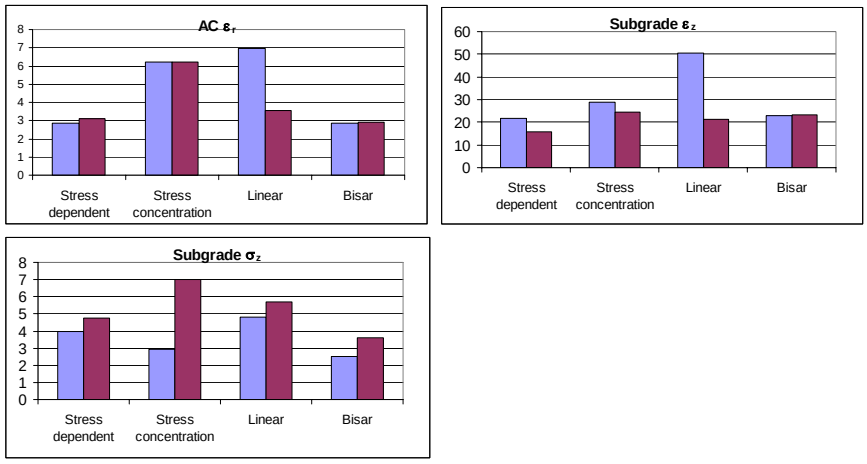

Figure 2.23 Difference between calculated and measured response in the unit "number of standard deviations". The left (light) bars are calculated from average deflections, and the right (dark) bars are calculated from average parameters. Note that the charts use different scales on the y-axis. (Agardh, 2002)

2.6 Remarks on further work in this thesis

In an incremental-recursive deterioration model, many calculations of stresses and strains are performed. If there is a fast and simple calculation method that is as accurate as a more complex method, the simple method should be preferred. The study of material methods mentioned earlier (Agardh 2002) showed that the model with stress dependant subgrade and calculations with Method of Equivalent Thicknesses was at least as accurate as the more complex method that BISAR uses. Therefore, MET is used with stress dependant subgrade for all response calculations in this thesis.

Some of the factors that affect pavement deterioration are not included in this study. Only accelerated tests are used to obtain model parameters, and the limitation of these tests excludes some of the factors. Due to constant climate during the tests, the effect of climate has not been studied. The magnitude of the wheel load has also been constant during most of the tests. Since only accelerated tests are used, aging is also excluded.

3 DETERIORATION MODELS

There are a great many different deterioration models. They can be divided into groups in different ways. One way can be to divide them according to what kind of output they give. Some models (e.g. ATB Väg) give the remaining service life, while others give continuous or incremental change in pavement condition.

Another grouping of models can proceed from how they describe the pavement condition or damage. The different kinds of damage, such as rutting or cracks, can be described separately. Another way to describe the pavement condition is to combine the various kinds of damage into one index, such as PSI (Present Serviceability Index) or OPI (Overall Pavement Index).

Pavements deteriorate in several different ways, and the condition of the pavement can be described in many ways. According to the EU project COST 324 (1997) there are seven indicators for pavement condition:

- Longitudinal profile
- Transverse profile
- Surface cracking
- Structural cracking
- Structural adequacy
- Surface defects
- Skid resistance

Deterioration models should be developed for each of the seven indicators (COST 324, 1997). The first four indicators are the most commonly used.

Longitudinal profile is often expressed as IRI (International Roughness Index). Other ways of describing the longitudinal profile are Bump Integrator or Slope Variance. In most models that predict longitudinal profile, the age of the pavement, traffic and measured roughness are the most important explanatory variables. The roughness, in the form of IRI, is often seen as the most economically important condition indicator. The World Bank's Highway Development and Management system (HDM), which is a requisite tool in most international financing schemes, uses the IRI as input for economical analysis.

Transverse profile is most commonly addressed as rut depth. The most important explanatory variables in most models are the age of the pavement, traffic and measured rut depth.

Surface cracking means cracks that start at the surface and progress downwards (top-down cracking). This is mostly seen on pavements with relatively thick AC layer.

Structural cracking means cracks that start at the bottom of the bituminous layer and progress upwards (bottom-up cracking). This is the most common way of describing cracks in the pavement, and there are several models available for this distress indicator. The cracks are supposed to occur because of fatigue in the bituminous material while exposed to repeated tension under heavy loads. Most models use the horizontal strain at the bottom of the AC layer and accumulative traffic loading as explanatory variables.

Structural adequacy can be described for the whole pavement as deflection of the surface or for the different layers in the pavement individually as elasticity moduli or other material parameter. The structural adequacy of the pavement does not affect the road user directly but has an effect on the rate of development of the other indicators.

Surface defects can be raveling, potholes or asphalt bleeding. Since these defects mainly occur because of faulty materials and are often very local, they are hard to model.

Skid resistance is connected to the micro and macro texture of the pavement surface. The skid resistance often varies during the year. Especially in countries where studded tyres are commonly used, the skid resistance can be low during summer and autumn and then increase during winter. The explanatory variables are often age of the pavement and number of vehicles with studded tyres.

3.1 Empirical models that calculate combined damage

Based on the AASHO road test, an equation for calculating loss in Present Serviceability Index (PSI) was derived (Highway Research Board, 1962):

$$g_t = \frac{p_0 - p_t}{p_0 - p_f} = \left(\frac{N_t}{\rho}\right)^{\varpi}$$

where

g_t = damage parameter

p_t = servicability at time t (PSI)

p_0 = initial servicability (PSI)

p_f = terminal servicability (PSI)

N_t = cumulative number of equivalent standard axle loads (80 kN) until time t

ρ, ϖ = regression parameters

The parameter ρ is number of equivalent standard axle loads at failure. This can be seen by substituting p_t=p_f.

The two regression parameters were obtained for each test section using step-wise linear regression. The parameters from all test sections were then expressed as a function of design variables (Highway Research Board, 1962):

$$\varpi = \varpi_0 + \frac{\beta_0 (L_1 + L_2)^{\beta_2}}{(a_1 D_1 + a_2 D_2 + a_3 D_3 + a_4)^{\beta_1} L_2^{\beta_3}}$$

where

ϖ_0 = minimum value of ϖ

L_1 = axle load

L_2 = 1 for single axle, 2 for tandem axle

$D_1 - D_3$ = thickness of surface, base and subbase layers

$a_1 - a_4$ = regression parameters from analyses of variance

$\beta_1 - \beta_3$ = regression parameters

$$\rho = \frac{\beta_0 D^{\beta_1} L_2^{\beta_3}}{(L_1 + L_2)^{\beta_2}}$$

where

$D = a_1 D_1 + a_2 D_2 + a_3 D_3 + a_4$

The same notations as in the equation above except that the values of the regression parameters are not necessarily the same

The unit of the regression parameters in the above equation cannot be determined since the addition of L_1 and L_2 is addition of different units. There have been discussions about the way the parameters were determined because pavement sections that had not failed when the test ended were excluded from the regression analysis (Prozzi, 2001). These equations, or

modifications of them, have been used in the AASHTO Design Guide for many years (AASHTO, 1981, 1993).

Another example of an empirical model that determines the overall pavement condition is a model developed from 25 years of observations. From that study, time was the only deterioration parameter that was statistically significant (Karan, 1983):

$$RCI_t = \beta_0 + \beta_1 \ln(RCI_0) + \beta_2 \ln(t^2 + 1) + \beta_3 t + \beta_4 t \ln(RCI_0)\beta_5 \Delta t$$

where

RCI_t = Riding Comfort Index (0 – 10)

RCI_0 = Initial RCI

t = age (years)

$\beta_1 - \beta_5$ = regression parameters

Since this kind of model often fits network level data quite well, it can be used in Pavement Management Systems to predict future condition of pavements. Such models are often good at estimating the deterioration for the average road. They underestimate the deterioration as often as they overestimate it. On a network level, an error in the estimation of deterioration of a single road is not a big problem. Therefore these models are suitable for pavement management systems on network level. However, they cannot be used for design purposes. Therefore a PM System that is based on such a model needs another model to be able to make the design and determine how to rehabilitate the pavements.

3.2 Empirical models that calculate specific damage indicator

Transportation Road Research Laboratory (TRRL) performed a study on real in-service roads in Kenya that gave data to improve the AASHO models (Hodges et al., 1975). As opposed to the AASHO tests, these tests included mixed traffic loading and pavements with different ages. The analysis of the tests resulted in the following model:

$$R_t = R_0 + f(SN)N_t$$

where

R_t = roughness at time t

R_0 = initial roughness

SN = Structural number (D in the above equation)

N_t = cumulative number of standard axle loads (80kN) applied until time t

Since most of the test sections had cement-treated base layers and were located in Kenya, it is doubtful whether the model is applicable for normal flexible pavements in northern Europe.

Studies of in-service roads often fail to quantify the effect of pavement strength and/or traffic loading. This is due to the fact that pavements that are subjected to higher traffic load also are designed with higher strength. Therefore it can be difficult to distinguish between the effects of these two parameters. The same problem occurs with traffic loads and pavement age, since cumulative traffic loading and age normally increase almost proportionally. Because of these problems, many models exclude one or more of these parameters. For example, a model based on a ten-year data series of 51 pavement sections that resulted in a relation between only roughness and time (Way & Eisenberg, 1980):

$$\Delta R_t = \beta_1 R_t \Delta t - \beta_2$$

where

ΔR_t = change in roughness at time t

Δt = time increment

β_1, β_2 = regression parameters

This kind of model has almost the same advantages and drawbacks as the models described previously. Often only time is included as a factor that affects the deterioration, and therefore these models can only be used on network level.

Since the different kinds of damage of the pavement are described individually, it is possible to use these models for maintenance planning and for choosing rehabilitation methods. The completely empirical nature of the models has the drawback that they can only be used under the conditions of the roads they were developed from. Since two roads very seldom are constructed under completely similar conditions, probably a lot of models, or at least a lot of model parameters, have to be used to be able to describe all roads. All possible combinations of climate (temperature and moisture), traffic load and subgrade material can probably not be described with one model. The former Swedish design standards, Väg 94 (SNRA, 1994), contained more than 1000 different pavement sections for different variations of surrounding conditions (Ekdahl, 1999).

3.3 Analytical-empirical models that calculate overall damage

All of the models described above are purely empirical models. They do not try to explain the physical phenomenon that causes the deterioration. Most design methods used today are based on critical response at a certain location in the pavement. One example of that is the Swedish pavement design standard, ATB Väg (SNRA, 2001), where there are two criteria for calculating the time to failure for the pavement. The first criterion is based on the strain at the bottom of the AC layer:

$$N_{bb,i} = f_s \frac{2.37 \cdot 10^{-12} \cdot 1.16^{1.8T_i+32}}{\varepsilon_{bb,i}^4}$$

where

$N_{bb,i}$ = maximum number of standard axle loads at season i

f_s = correction factor for cracking, for newly constructed pavemnts $f_s = 1.0$

T_i = temperature at season i

$\varepsilon_{bb,i}$ = largest horizontal strain at the bottom of the AC layer at season i

The second criterion is based on the vertical strain at the top of the subgrade:

$$N_{te,i} = f_d \frac{8.06 \cdot 10^{-8}}{\varepsilon_{te,i}^4}$$

where

$N_{te,i}$ = maximum number of standard axle loads at season i

f_d = correction factor for moisture

$\varepsilon_{te,i}$ = maximum vertical strain at the top of the subgrade at season i

ATB Väg does not mention anything about the terminal condition of the pavement. It is often suggested that the strain at the bottom of the AC layer induces cracking and the vertical strain at the top of the subgrade induces rutting. If that is the case with these design criteria, the design standard does not take roughness into account. Roughness is one of the main problems of flexible pavements in Europe (AMADEUS, 2000).

Assuming linear deterioration it is possible to reformulate the design criteria to an incremental form:

$$dD_i = \frac{N_{bb,i}}{2.37 \cdot 10^{-12} \cdot 1.16^{1.8T_i+32}} \varepsilon_{bb,i}^4 \Delta D$$

where

dD_i = increment of damage at season i

ΔD = Damage at failure

and

$$dD_i = \frac{N_{te,i}}{8.06 \cdot 10^{-8}} \varepsilon_{te,i}^4 \Delta D$$

An attempt to use an incremental deterioration model based on physical deterioration principles was made by Prozzi (2001). Data from the AASHO road test were used and resulted in the following equation for calculating pavement serviceability:

$$p_{it} = \beta_1 + \beta_2 e^{\beta_3 H_{1i}} + \sum_{l=0}^{t-1} \left(1 + \beta_4 H_{1i} + \beta_5 H_{2i} + \beta_6 H_{3i}\right)^{\beta_7} e^{\beta_8 G_l} N_{il}^{\beta_9} \Delta N_{i,l+1}$$

where

p_{it} = PSI for section i at time t

H_1, H_2, H_3 = thickness of surface, base and subbase layer

G_t = frost penetration gradient

$N_{il} = \sum_{q=0}^{l} \Delta N_{iq}$

ΔN_{iq} = traffic increment (ESALs)

$\beta_1 - \beta_9$ = regression parameters

This model can be divided into parts that describe physical properties of the deterioration process. Some parts of the model are described in more detail in Chapter 2.

The analytical-empirical methods can be used in incremental design methods, but by considering only overall pavement condition, they cannot be used for choosing rehabilitation method. The models try to explain the deterioration in terms of physical properties of the pavement. That probably makes these models usable under a wider range of conditions than purely empirical models.

3.4 Analytical-empirical models that calculate specific damage indicator

Since different kinds of damage to a road often have different causes, it is probably necessary to calculate each damage indicator separately.

One of the first attempts to develop a model that is partly based on mechanistic principles was made by Queiroz (1983). The deterioration in these models is based on calculated response in the pavement. The critical responses are surface deflection, horizontal tensile stress, strain and strain energy at the bottom of the AC layer and vertical compressive strain at the top of the subgrade. By regression analyses, a set of linear models was suggested. The roughness of the pavement is predicted from the following equation:

$$\log(QI_t) = \beta_0 + \beta_1 t + \beta_2 ST + \beta_3 D_1 + \beta_4 SEN \log N_t$$

where

QI_t = roughness at time t measured by the quarter car index (counts/km)

t = pavement age in years

ST = dummy variable (0 for original surface, 1 for overlaid surfaces)

D_1 = Thickness of AC layer

SEN = Strain energy at the bottom of AC layer

N_t = cumulative equivalent single axle loads until time t

$\beta_0 - \beta_4$ = regression parameters

In this study the response was calculated using multi-layer linear-elastic theory.

From another study in Brazil (Paterson, 1987), incremental models were developed. An incremental model gives the advantage of a possibility for a non-linear model. Since the calculated value in one time step is input in the next time step, the rate of deterioration can change during the lifetime of the pavement.

Paterson (1987) categorized the mechanisms that caused roughness into three categories. The categories were chosen from at what depth the source for the roughness came from. The first category is plastic deformation that normally occurs in the lower pavement layers. This deformation depends on pavement strength, traffic loading and also some environmental effects (moisture). The second category is the mechanical damages at the surface such as cracking, potholes, raveling etc. The third category consists of environmental effects that do not involve direct structural damage, such as temperature and moisture effects.

The study found several parameters that had a statistically significant effect on pavement deterioration:

$$\Delta R_t = \beta_1 e^{\beta_2 t} S^{\beta_3} \Delta N + \beta_4 \Delta D + \beta_5 \Delta C + \beta_6 \Delta P + Z + \beta_7 R_t \Delta t$$

where

ΔR_t = increase in roughness during time period t

S = a function of SN, H and C

SN = modified structural number

H = thickness of cracked layer

C = percentage area cracking

ΔN = number of equivalent 80 kN single axles in period t

ΔD = increase in rut depth standard deviation

ΔC = increase in area cracking in period Δt

ΔP = increase in area of surface patching

Z = dummy intercept estimate for sections with potholes

R_t = roughness at time t

Δt = time increment

$\beta_1 - \beta_7$ = regression parameters

One advantage of that model is that it is at least partly based on the physical principles that cause the deterioration and not only on statistical analysis. Therefore, parameters such as pavement strength (SN), rutting and cracking are input to the model.

Based on data from an accelerated pavement testing (APT) facility in Denmark, a model for deterioration has been developed. It is assumed that the deterioration depends on the internal energy density at the top of the subgrade. The same equation, but with different value of the regression parameters, is assumed for calculation of slope variance, roughness and rut depth (Ullidtz et al., 1999).

$$\Delta SV = AN^{\alpha}\left(\frac{1}{2}\varepsilon_z \frac{\sigma_z}{p}\right)^{\beta}$$

where

SV = slope variance, may be substituted by roughness (IRI) or rut depth (RD)

N = number of load repetitions

ε_z = vertical resilient strain at the top of the subgrade

σ_z = vertical stress at the top of the subgrade

p = reference stress

A, α, β = regression parameters

This equation can be expressed in an incremental form:

$$dSV = \alpha \Delta SV \left(\frac{A\left(\frac{1}{2}\varepsilon_z \frac{\sigma_z}{p}\right)^{\beta}}{\Delta SV} \right)^{\frac{1}{\alpha}}$$

Models where the deterioration was based on only stress or strain were also tested in the same study, but the strain energy model seemed to fit the measured data best. Ullidtz et al. (1999) found good agreement with the measured data from the Danish Road Testing Machine (RTM) with the following set of parameters:

Table 3.1 Regression parameters for the energy density model from RTM (Ullidtz et al., 1999)

	A	α	β
SV	$1.92*10^{-4}$	0.341	0.868
IRI	$5.92*10^{-5}$	0.341	0.868
RD	$3.03*10^{-4}$	0.341	0.868

In the 2002 Design Guide (NCHRP, 2004), the IRI is calculated with an equation that does not seem to be based on any response in the pavement:

$$IRI = IRI_0 + \beta_1 SF\left(e^{age/20} - 1\right) + \beta_2 FC + \beta_3\left(\frac{COV_{RD}}{100}\right) + \beta_4 TC + \beta_5 BC + \beta_6 SLCNWP_{MH}$$

where

SF = Site Factor

FC = Fatigue Cracking

RD = Rut Depth

COV_{RD} = Coefficient Of Variance for rut depth

TC = Length of Transverse Cracking

BC = Area of Block Cracking

$SLCNWP_{MH}$ = Length of Sealed Longitudinal Cracks outside Wheel Path

$\beta_1 - \beta_6$ = regression parameters

Even though there is no pavement response in this equation, in practice it is response based. Some of the input data, i.e. rut depth and fatigue cracking, are calculated based on pavement response.
Instead of using a critical response at a certain depth as input in the rut depth calculation, the rut depth can be calculated as the integral of plastic strains:

$$RD = \int_0^{\infty} \varepsilon_p$$

In practice, the 2002 Design Guide calculates the rut depth as the sum of the permanent deformations in sublayers. Each material layer is divided into sublayers, where those closest to the surface are thinner, and the thickness increase with depth.

$$RD = \sum_{1}^{nsublayers} \varepsilon_p^i h^i$$

The rut depth is calculated as the sum of the permanent deformations in the different layers plus the permanent deformation of the subgrade.

The plastic strain in the AC layer is calculated with:

$$\frac{\varepsilon_p}{\varepsilon_r} = \beta_0 + \beta_1 \log(N) + \beta_2 \log(T)$$

where

ε_p = Plastic strain

ε_r = Resilient strain

N = Number of load cycles

T = Temperature

$\beta_0 - \beta_2$ = regression parameters

The permanent deformation in unbound layers is calculated with:

$$\delta_a(N) = \beta_{UB}\left(\frac{\varepsilon_0}{\varepsilon_r}\right) e^{-\left(\frac{\rho}{N}\right)^{\beta}} \varepsilon_v h$$

where

$\delta_a(N)$ = Deformation for N load repetitions

$\varepsilon_0, \rho, \beta$ = Material parameters

ε_r = Resilient strain

ε_v = Vertical strain

N = Number of load repetitions

β_{UB} = Calibration factor

These kinds of models are what the COST 333 (1999) project describes as desirable for future design standards. They can be used on both network and object level. One drawback is that several deterioration models are needed to cover all kinds of damage. According to COST 324 (1997), 7 different models are needed (see the beginning of this chapter). On network level there will be a lot of calculations if these models are used. Therefore, it is possible that on network level empirical models are more efficient.

3.5 Concluding remarks

The design procedure suggested by COST 333 (1999), shown in Figure 1.2, requires a model based on pavement response. According to COST 324 (1997), the different kinds of damage to the pavement should be treated separately to make it possible to plan maintenance activities. Therefore, models of the type described in section 3.4 (Analytical-empirical models that calculate specific damage indicator) should be used, at least for the object level of the PM system. On network level, models that use a combined damage indicator can sometimes be used to save computing time.

Analytical-empirical deterioration models are based on the assumption that the deterioration depends on some response somewhere in the pavement. The location of that critical response is different in different deterioration models, even though most models use either the bottom of the AC layer or the top of the subgrade. Often the critical response is strain, but sometimes stress, often in combination with elastic modulus, is used.

Two models with different approaches to the rut depth development are chosen for further studies:

Rut depth development based on energy

- The critical response is located at the top of the subgrade
- The critical response is the strain energy

Rutting occurs because of permanent deformation in some part of the pavement. It is often assumed that most of the rutting occurs in the subgrade. Therefore it is reasonable to believe that the critical response for rutting should be at the top of the subgrade. Based on tests at the Danish Road Testing Machine, an evaluation of deterioration models with stress, strain and strain energy as the critical response was conducted (Zhang et al., 1998). The result showed the energy model as the best at predicting the pavement performance. It also sounds reasonable to believe that the damage (rutting) is due to the internal energy and not only the resilient strain.

Rut depth development based on plastic strain

- The rut depth is the sum of the deformations of the pavement layers
- The plastic strain is related to the resilient strain

This way of calculating rutting is used in the 2002 Design Guide (NCHRP, 2004). Instead of using a certain location for the critical strain, the plastic strain through the whole pavement is calculated. Since rutting occurs in all pavement layers, and not only in the subgrade, this method is one more step

towards analytical design. The models used are based on the assumption that the plastic strain depends on the resilient strain.

The two models used in the study can be seen as representatives for two different approaches to rut depth development. The model from the 2002 Design Guide is used as a representative of the plastic strain through the whole pavement approach, and the strain energy model is used as a representative of the approach with critical response at a certain location.

4 METHOD

The study of deterioration models in this thesis consists of three parts:

1. Selection of models for further investigation
2. Test of the potential of the models and calibration
3. Validation of the calibrated models

4.1 Selection of models for further investigation

Chapter 3 presents a survey of existing deterioration models. Two models are chosen for further studies according to the following criteria:

- **Ability to fit in the design process shown in Figure 1.2**
  This is the most important criterion. Since it is most probable that the future design process will work that way, all models chosen must have the ability to fit in that process. This means that they have to be, or be able to be transferred to, an incremental procedure. It must be possible to calculate the gradual deterioration of the pavement and not just its lifetime. One of the supposed advantages of the incremental design process is that the same way of calculating deterioration can be used for both new and existing pavements. Therefore, the calculations of the deterioration during one time step of the incremental procedure have to be based on the pavement conditions calculated from the former time step, and not only on the conditions of the newly built pavement.
- **Simplicity of the model**
  Since all the models are empirical, they include empirical parameters that must have a value. The more regression parameters the model includes, the easier it is to adjust parameter values to fit calculated deterioration with measured deterioration at a test site. Unfortunately, with more parameters it is harder to determine the correct value of the parameters. It also requires more data to get statistically significant results. Therefore, the model should have as few regression parameters as possible but still be able to describe reality.
- **Interpretation of parameters**
  To make it easier to use and understand the model, it is important that all parameters are understandable. All parameters should have a specified unit. In some empirical models, qualities with different units are added, thereby ruining the unit interpretations in the model. All parameters should have a defined unit, and it should be easy to understand the effect of each parameter. It should easily be seen if

raising the value of one parameter increases or decreases the deterioration rate.

According to the first criterion above, the input data for the chosen models consist of responses somewhere in pavement. Response is seldom measured in real roads. To get as much information as possible about the response in the pavement, only accelerated tests with response measurements are used when calibrating the models.

Often in accelerated tests, cracking does not occur in the same way as it does on real roads. The accelerated nature of the test eliminates aging (oxidation) of the bituminous materials. The two other kinds of damage that occur on roads, rutting and roughness, are often connected to each other and can be considered as two parts of the same deterioration mechanism. They both occur because of deformations in the pavement, and are therefore related to the strength of the materials.

Many accelerated tests, for example the tests used in this study, use a relatively short test area. It is hard to get relevant measurements of roughness with only a few metres of loaded pavement. Normally roughness is not measured at such test sections, even though it has been done, for example at the Danish Road Testing Machine (Zhang et al., 1997). The most relevant and accurate measurement of deterioration from accelerated tests probably is the rutting. Therefore only models for rutting are studied. Since roughness often is connected to rutting, the calculated rut depth can then be used as input in models for roughness as is done in the 2002 Design Guide (NCHRP, 2002).

4.2 Test of potential of the models and calibration

Different performance model needs response from different locations in the pavement as input. Since it is impossible to measure the response at all possible locations in the pavement, most of the accelerated pavement tests have not measured the required response. To be able to use these tests in evaluation of performance models, the responses have to be calculated in some way.

The potential of the model is tested by obtaining one set of model parameters (calibrating the model) for each test section. This test will show whether the models are able to accurately describe the rut depth development of the pavements. Then the models are calibrated to all test sections at once.

Calculating pavement response

The calculation of the response can be done in several ways. If the same kind of response (stress or strain) is measured at two locations close to the desired response, it is possible to interpolate or extrapolate for the desired response. If only stress is measured and strain is required (or vice versa), it is possible to calculate the strain if the elastic modulus of the material is known. That modulus can be found either from laboratory or FWD measurements or from standard values.

One method that always can be employed is to use all measured data to obtain material parameters and then calculate the response from those parameters. The advantage of this method is that an error in one measurement will not have such a great influence on the assumed response. The main problem with this method is that the calculated response will not be better than the response model that is used. Therefore this method is only usable if the response model is trustworthy.

According to other studies (Agardh, 2002 and Hildebrand, 2002), it is important to treat the subgrade as if it has a stress dependant elastic modulus. To be able to easily use non-linear subgrade, the Method of Equivalent Thicknesses (see Chapter 2) has been used for all response calculations. All subgrades have been assumed to have stress dependant moduli. All other material layers are assumed to be linear-elastic.

The elastic moduli used for the calculations have been obtained by considering both deflections from an FWD and measured response in the pavement according to the description in Section 6.1. The measured response is measured under a wheel load, which often has a considerable longer loading time than the FWD. Since at least bituminous materials are visco-elastic, the modulus differs with loading time. Therefore, the modulus of all AC layers has to be adjusted between the two load types. The sensitivity to loading time for the AC layer is not tested at any of the test sites used in this study. Therefore, a master curve from a typical Swedish AC layer is used for the load time adjustment. This material is thoroughly tested by Nilsson (2001a).

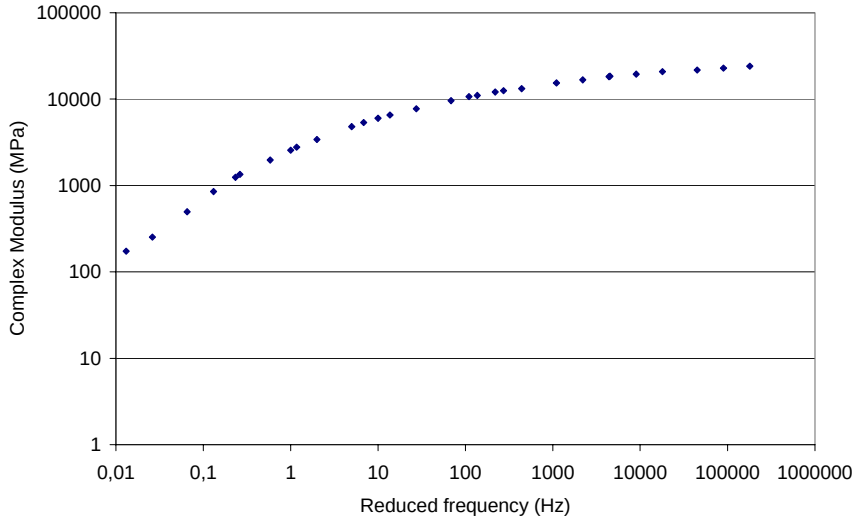

Figure 4.1 Master curve used for load time adjustment for all AC layers, log-log scale (Agardh, 2002)

The load time is calculated based on the assumption that the area shown in Figure 4.2 is affected by the wheel load. The load time is calculated for the centre of the layer.

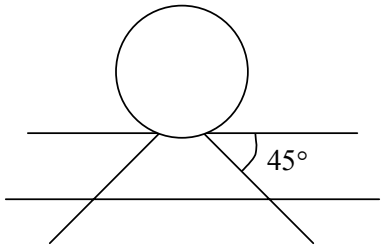

Figure 4.2 Volume that is assumed to be affected by the wheel load (Agardh, 2002)

Calculation of deterioration

Most deterioration models calculate the total damage of the pavement (e.g. rutting or roughness) and not the increment of damage. When the conditions (temperature, moisture, traffic etc.) change, it is necessary to calculate the increment of damage for each season. One way to do that is to reformulate the deterioration equation, as it is done with the strain energy model in section 3.4. Another way to do it is to use the strain hardening approach (NCHRP, 2004).

The strain hardening approach is used for all deterioration calculations in this thesis.

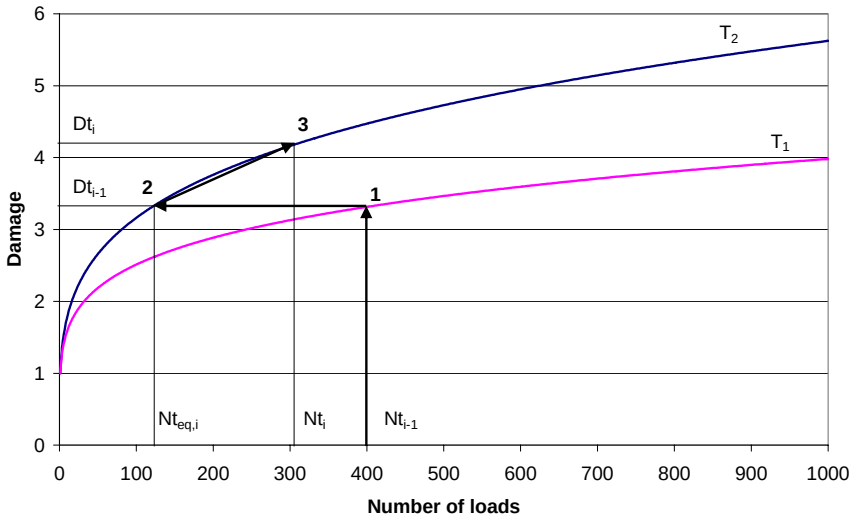

Figure 4.3 Strain hardening approach

With the conditions during season i-1 (T_1) the total damage after season i-1 is calculated (1 in Figure 4.3). In season i the damage development is different (T_2). The same damage (D_{t-1}) will, with these conditions, occur after $N_{teq,i}$ loads (2 in Figure 4.3). The damage after season i can then be calculated by adding the number of loads during that season to $N_{teq,i}$. (3 in Figure 4.3)

Potential of the models

The purpose of this step of the evaluation is to determine whether the model is able to describe the deterioration behaviour of the pavement. A set of model parameters is obtained to get best fit to the measured rut depth for each test section individually.

Calibration of the models

The purpose of this step is to evaluate whether it is possible to find a set of model parameters that are general for all test sections. If that is the case, it is an indication that the parameters are fairly general and can be used on different pavement sections, which is necessary if the model is to be used for real pavements.

A simple sensitivity analysis of the calibrated models is also performed. This is done for each parameter individually. The parameter is increased and

reduced 10% from the calibrated value, and the rut depth development is calculated with these new parameter values.

4.3 Validation of the calibrated models

Often when laboratory tests are transformed for use in reality, a correction factor has to be used, because of the differences between laboratory and reality. In this case, all test sections are full-scale pavements, but they are all accelerated tests under a controlled environment, and therefore not reality. To see if such a correction factor will be needed for these deterioration models, a validation to reality is carried out.

Validation to theoretical roads

Six pavements with different traffic and different subgrade materials are designed according to Swedish standards (SNRA, 2001). The rut depth development is then calculated for these sections. All input data, such as climate and material properties, are taken from ATB Väg (SNRA, 2001).

The purpose of this evaluation is to determine whether the calculated rut depths are on a reasonable level, or if a large correction factor is needed. All sections used for the calibration of the models are relatively weak pavements (see Chapter 5), and this validation can also give an indication of whether the same model parameters can be used for stronger pavements with more traffic.

Validation to real roads

If the models are to be used for real roads, they have to be validated to real roads. Such a validation can be another indication of the general applicability of the model parameters, and also whether a correction factor is needed.

The models are also validated to two real roads. Both are located in southern Scandinavia where frost heave will probably have only minor impact on the rutting. Except for that, there is at least one significant difference between these sections and the sections for the accelerated tests from which the model parameters are obtained. Both sections are highways with relatively high traffic load, and therefore also considerably stronger than the sections in the accelerated tests.

5 MEASURED DATA

In this chapter the measured data used in this thesis are described, and for some measurements a quality control is also performed. The first three parts of the chapter (5.1 to 5.3) describe the test sites for the accelerated tests that are used for the calibration of the models. The next two parts (5.4 and 5.5) describe the two in-service roads that are used for the validation.

All stress measurements have been controlled with the following method. Under a load from a Falling Weight Deflectometer (FWD) or a single wheel, the stress distribution in the pavement can be assumed to be approximately axial symmetric. This assumption can be used to calculate the stress concentration caused by the stress gauges. By integrating the measured stress over the plane where the gauges are installed, it is possible to calculate how much of the load is actually passing the gauge. Theoretically, the integrated stress should be equal to the applied load. Divergence between the integrated force and the applied force can be due to either a gauge problem, or that the gauge itself disturbs the stress distribution.

One way to perform the integration is to use Boussinesq's equation for vertical stress:

$$\sigma_z = \frac{3P}{2\pi} \frac{(f_z z)^3}{\left((r + f_0)^2 + (f_z z)^2\right)^{\frac{5}{2}}}$$

P = the force on the plane at depth $f_z z$

f_z = a factor used to obtain good fit with the measured stress

z = the depth where the gauge is placed

r = the radial distance between the load and the gauge

f_0 = a factor used to adjust radial distance between the load and the gauge

If there is a good fit between the measured and calculated stress, the integrated force is equal to P in the equation above. (Zhang et al., 1997)

One problem with this method is that in the integration of the function the stress at large distance from the load is more important for the calculated force than the stress close to the load. Therefore, the stress measured quite far away from the load has a great influence on the calculated force. Since this stress is relatively small, it is hard to measure with great accuracy. Consequently, this method can probably not be used to determine exactly how much of the applied force passes through the gauges, but only to give a hint if there is reason to believe that the measured stresses are larger or smaller than the expected stress.

Placing a gauge in a particulate medium will disturb the stress distribution. Even if the material is not homogenous, it will be even less homogenous with a gauge of another material inside. A good pressure cell affects the stress distribution as little as possible. The size and the stiffness of the pressure cell affect the measured stresses. According to Sparrow & Tory (1966), the theoretical difference between cell reading and true pressure is:

$$\frac{P_e}{P} = 1.1\frac{B}{D} - 0.022\frac{E_s}{E_c}\left(\frac{d}{t}\right)^3$$

P_e = the difference between cell reading and true pressure

B = half of the thickness of the cell

D = the diameter of the cell

E_s = soil modulus

E_c = cell modulus

d = the diameter of the diaphragm

t = thickness of the diaphragm

The equation above is applicable if the B/D ratio is below 0.4. An ideal pressure cell should have a large diameter, and be thin but still stiff.

5.1 Copenhagen

The test track in Copenhagen is a linear accelerated pavement testing facility. The test track is 27 m long, in which 9 m are the actual test track with the same depth. The instruments are placed in the central 6 m of this part. The depth of the instrumented track is 2 m. Two sections from this test site are included in this study.

5.1.1 The design of the test roads

The asphalt concrete consists of a densely graded mix with maximum aggregate size of 16 mm. The base course consists of a partly crushed natural aggregate. The maximum particle size is 32 mm. The subgrade soil is clayey silty sand. Under the subgrade layer there is a porous drainage layer consisting of natural gravel with a particle size between 16 and 22 mm. This layer is separated from the subgrade by geotextile. (MacDonald & Zhang, 1998)

Figure 5.1 Design of RTM 2

Figure 5.2 Design of RTM 3

5.1.2 Instrumentation

The track is instrumented by:
Asphalt strain gauges (ASG) that measure horizontal strain at the bottom of the asphalt layer. Four gauges measure the longitudinal strain and another four gauges measure the transversal strain. The gauges were placed on the base course before the paving.

Soil pressure cells (SPC) that measure dynamic stress in unbound layers. Twelve soil pressure cells measure the vertical stress in the subgrade at three different depths.
Soil deformation transducers (SDT) that measure both dynamic and permanent strain in unbound layers. Fourteen soil deformation transducers are placed at different locations and different directions in the pavement.

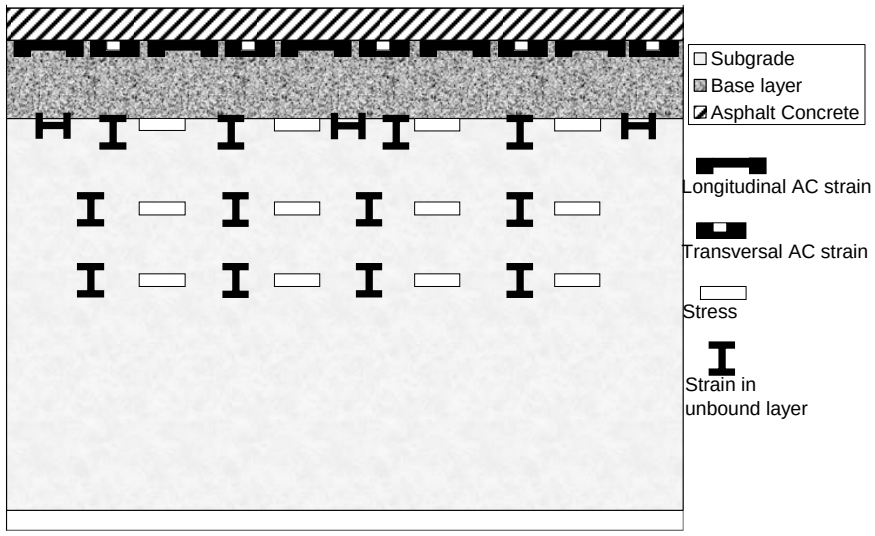

Figure 5.3 Instrumentation of the test pit in Copenhagen

The measurements from the stress gauges have been tested according to the method described at the beginning of this chapter. The load is an FWD load of 500 kPa, which equals 35.4 kN.

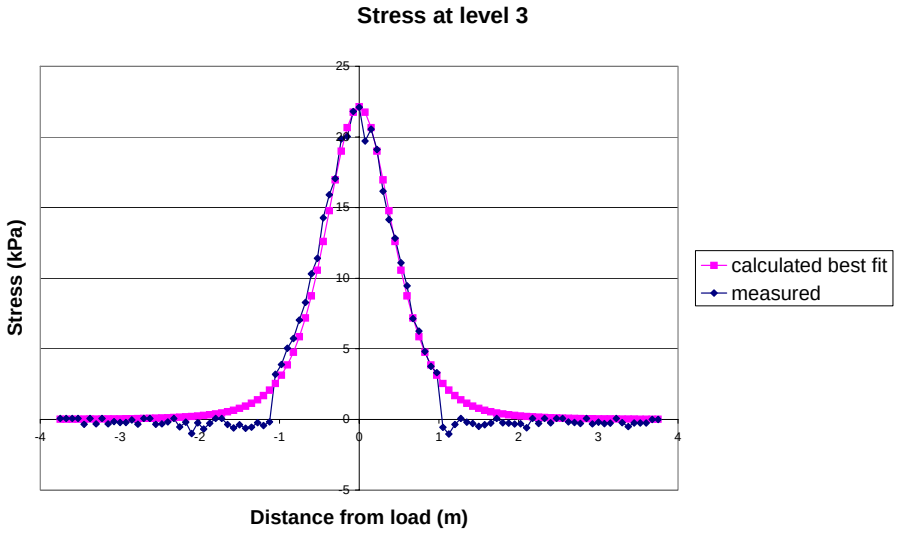

Figure 5.4 Example of calculated stress fitted to the measured stress (gauge SZ3H482)

Table 5:1 Calculated force that passes the stress gauges

	Gauge	Force (P) kN	P/35.4 kN	f_z
Subgrade level 1	SZ1V150	21.3	0.60	2.11
	SZ1H270	41.8	1.18	2.87
	SZ1V480	25.5	0.72	2.23
	SZ1H570	24.9	0.70	2.24
Subgrade level 2	SZ2H149	18.2	0.51	1.58
	SZ2V449	17.0	0.48	1.69
	SZ2H539	17.6	0.50	1.69
	SZ2V750	19.8	0.55	1.47
Subgrade level 3	SZ3H300	27.1	0.77	1.68
	SZ3V390	28.9	0.82	1.44
	SZ3H482	37.1	1.05	1.66

Most gauges measure lower stress than expected. At level two, only about half of the applied load passes through the gauges. This can also be seen at the measured maximum values. The difference between the measured values at level two and level three is rather small.

5.1.3 Measurements

The performance test was made in three steps with increasing load. Each step contained 50 000 load repetitions. The response was measured at the start and after 1 000, 3 000, 10 000 repetitions and then after each 10 000

repetitions. Response under FWD loading was also carried out at each load increment. The FWD was moved 75 mm between each measurement.

This study used response from FWD measurements that were carried out before the performance test, and the first response test under wheel load.

5.2 Linköping

The test site in Linköping is a concrete pit in a laboratory. The load facility is a Heavy Vehicle Simulator (HVS) that has a test length, with constant load and speed, of 9 m. The depth of the test pit is 3 meters. More information about the test site and the measurements can be found in Wiman (2001). Two sections from this test site are included in this study.

5.2.1 The design of the test roads

The test road is built as two of the weakest constructions in the former Swedish standards (BYA 86). The subgrade consists of fine sand.

The pavement in the first section consists of only two layers: a granular base layer of 89 mm and an AC layer of 49 mm. The base layer is a natural till mixed with crushed material with particle sizes up to 32 mm. The AC layer is a dense asphalt mix with maximum particle size of 16 mm and bitumen with penetration 85.

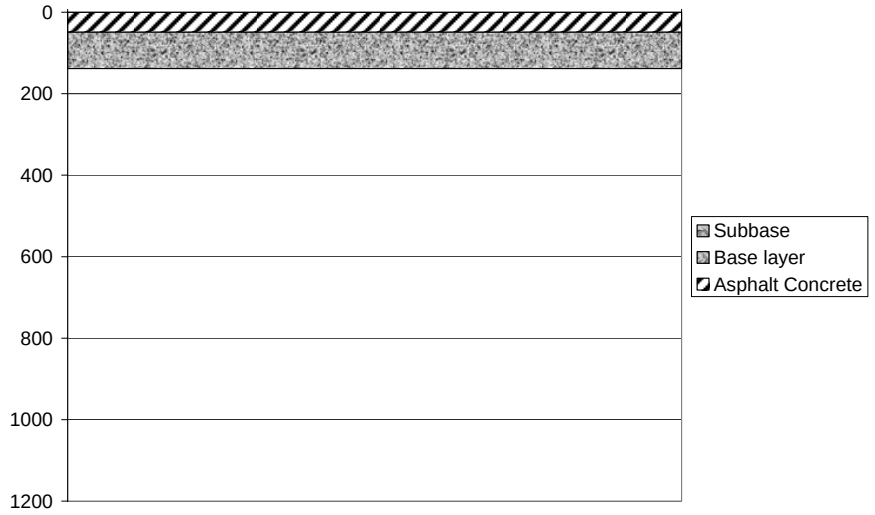

Figure 5.5 Design of test section Se01

The second section is thicker, and 128 mm granular subbase with maximum particle size of 63 mm is added. The thicknesses of the AC layer and the base layer are 62 and 110 mm respectively.

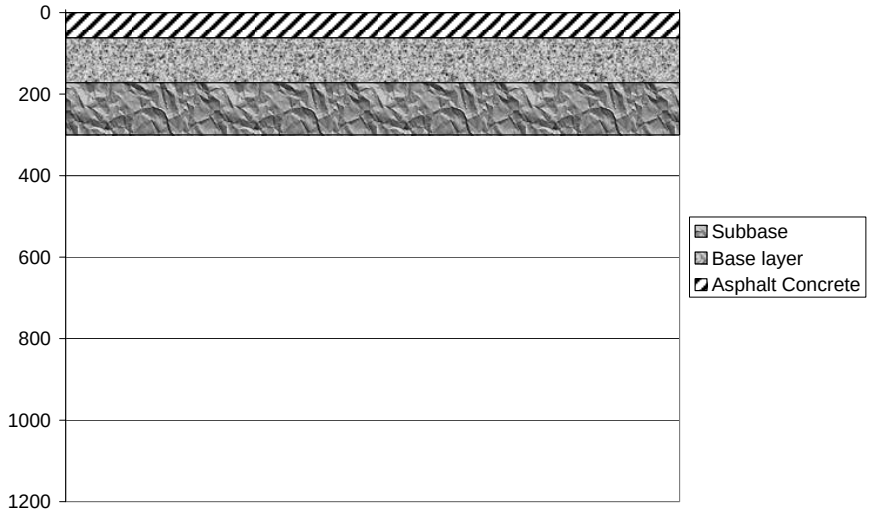

Figure 5.6 Design of test section Se02

5.2.2 Instrumentation

The test track is instrumented with asphalt strain gauges at the bottom of the AC layer, and soil pressure cells in the base layer and on two levels in the subgrade. Three LVDTs (Linear Variable Differential Transformers) were also placed to measure deflections at different depths in the structure, but unfortunately they did not work all the time.

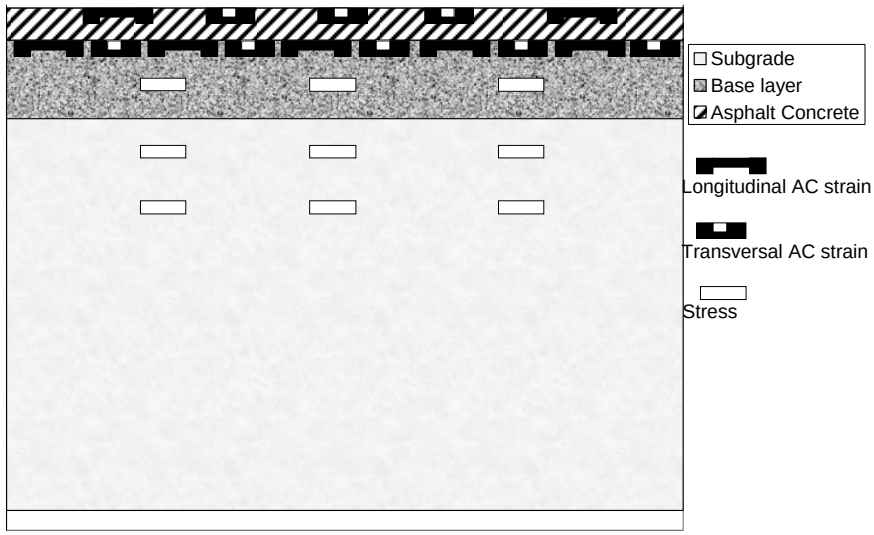

Figure 5.7 Instrumentation of test pit in Linköping

The asphalt strain gauges were installed by removing core samples from the road. The gauges were then fastened on other core samples that were subsequently placed in the road. In order to get good contact between the core sample and the asphalt layer, the core samples with gauges were a little bit bigger than the samples from the place where the gauges were to be placed.

The measurements from the stress gauges have been tested according to the procedure described at the beginning of this chapter. It is shown that only a part of the applied stress passes the gauges. The calculations were made for a single wheel load of 60 kN.

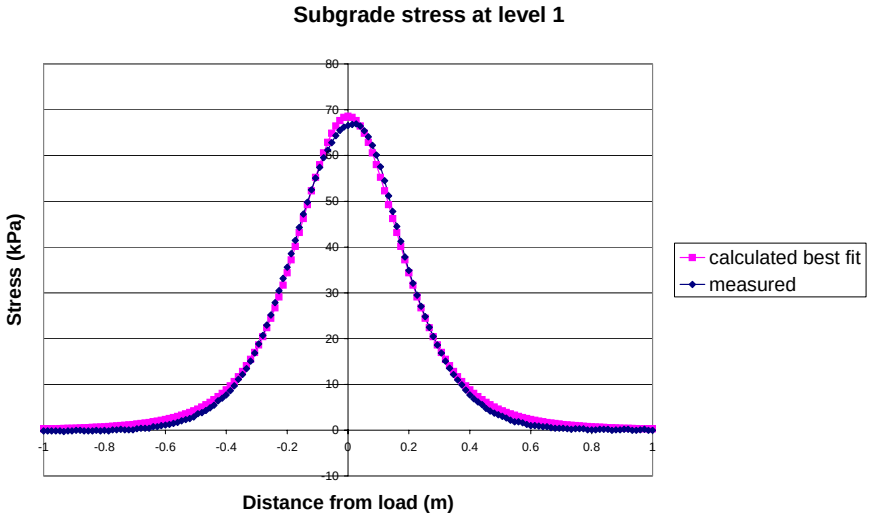

Figure 5.8 Stress curve fitted to measured stress (gauge SPC 17)

Table 5:2 Calculated force that passed the stress gauges at test section Se01

	Gauge	Force (P) kN	P/60 kN	f_z
Base	SPC 37	36.8	0.61	2.87
	SPC 39	32.9	0.55	2.90
	SPC 40	14.7	0.25	2.35
Subgrade level 1	SPC 17	18.2	0.30	1.44
	SPC 19	24.5	0.41	1.44
	SPC 22	24.2	0.40	1.44
Subgrade level 2	SPC 16	11.5	0.19	1.08
	SPC 18	11.9	0.20	1.01
	SPC 21	21.8	0.36	1.10

Table 5:3 Calculated force that passed the stress gauges at test section Se02

	Gauge	Force (P) kN	P/60 kN	f_z
Base	SPC 41	5.27	0.09	1.82
Subgrade level 1	SPC 26	19.1	0.32	1.20
	SPC 28	24.5	0.41	1.32
	SPC 30	17.4	0.29	1.21
Subgrade level 2	SPC 23	9.69	0.16	0.96
	SPC 27	9.01	0.15	0.98
	SPC 29	8.18	0.14	1.01

For one of the gauges at test section Se02, only a tenth of the applied load passes the gauges. Since all gauges show calculated forces that are smaller

than the applied force, it is reasonable to believe that the average maximum stress at a certain level is larger than the maximum measured stress. It is possible that the reason for this is that during the installation of the gauges, the material surrounding the gauges became less compacted than the rest of the material. If that is the case, the load will not be equally distributed over the plane. A weaker part of the construction will take care of less force than the stronger parts, and therefore the gauges lie in a part of the plane where the stress is less than the average stress at that plane.

For most of the gauges, the measured stress is larger for each measurement although the load is the same. It is possible that the material surrounding the gauges was relatively loosely packed at the beginning of the test, but became increasingly denser because of the load. The same phenomenon occurs in both test sections.

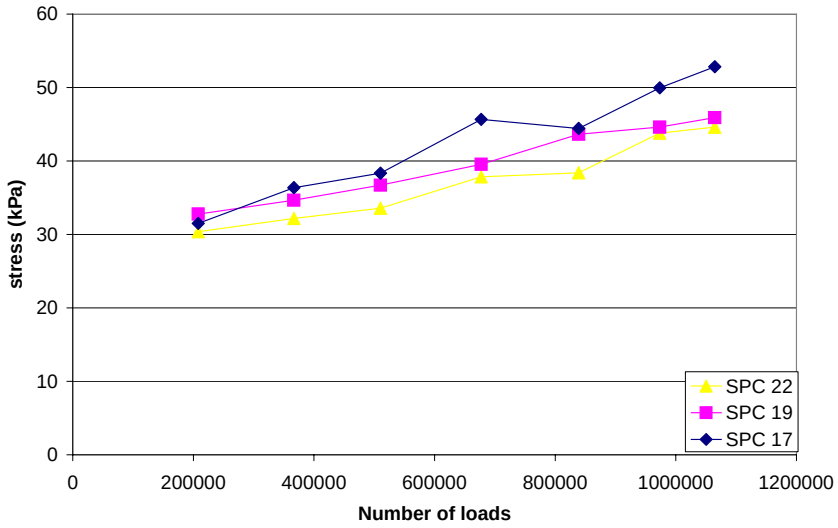

Figure 5.9 Measured stress in the subgrade at test section Se01

5.2.3 Measurements

At the beginning of the accelerated deterioration test, response measurements were made under several different conditions. The load for the performance study was set to a dual wheel load of 60 kN, with tyre pressure of 800 kPa. The temperature of the road was 10°C. Maximum speed of the loading wheel was used (12 km/h). Response measurements under several other conditions were also done, but those measurements are not included in this study. Both single wheel and dual wheel have been used. Variables that were varied for the other measurements were tyre pressure (from 500 kPa to 900 kPa), wheel load (from 30 kN to 80 kN), load speed (from 2 km/h to 12 km/h), lateral

position of the load (from 35 cm on each side of the instrumented line) and temperature (from 0°C to 20°C). These variables were changed one at a time. In all, measurements were made under more than 50 different conditions, and under each condition measurements were made at several different lateral positions.

5.3 Lausanne

The test road from Lausanne was built for the EU project COST 333. The loading device in Lausanne is a linear loading device consisting of a lorry wheel axle with a top speed of 12 km/h.

5.3.1 The design of the test road

The test road is built in a reinforced concrete pit that is 2 m deep and 5 m wide. The actual test length, where the speed of the load is constant, is 4 m. To control the environment, the test road is placed in an insulated tent where the temperature can vary from –20°C to 50°C. The geometry of the test road is shown in Figure 5.10.

Figure 5.10 Design of the test road in Lausanne

5.3.2 Instrumentation

The test road is instrumented with asphalt strain gauges both at the bottom of the asphalt layer (depth 8 cm) and at the interface between the two AC layers (depth 3 cm). These gauges are manufactured by Kyowa. Sixteen gauges were installed, but unfortunately only six of them worked after construction.

Vertical strain gauges were placed at the interface between subgrade and subbase. These gauges were also manufactured by Kyowa and were anchored in the material with a mushroom-shaped plate at the top and bottom of the gauge to obtain a better representation of the strain. Two gauges of this type were installed. (Turtschy & Perret, 1999)

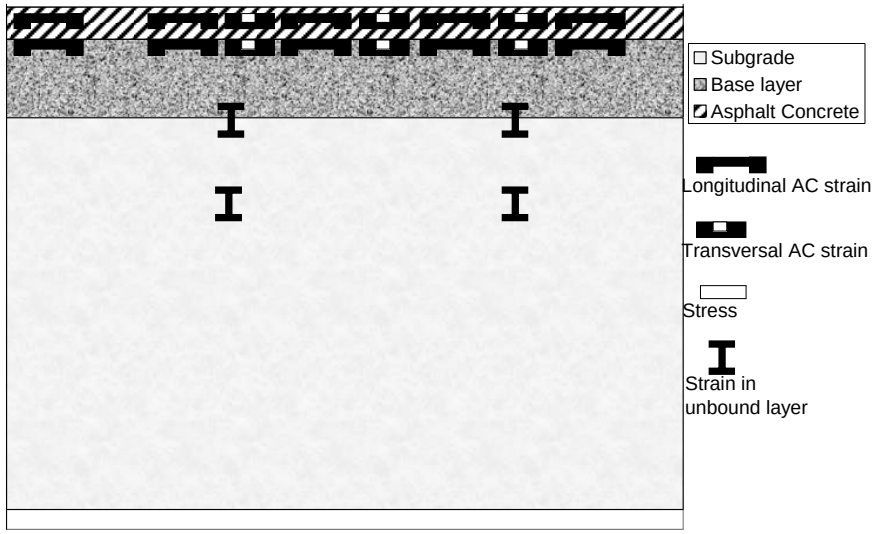

Figure 5.11 Instrumentation of the test pit in Lausanne

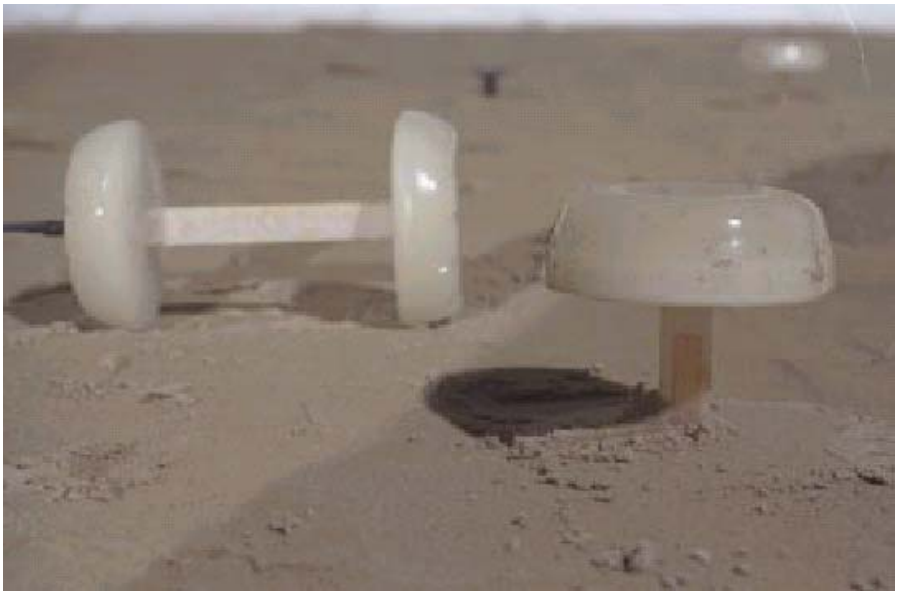

Figure 5.12 Vertical strain gauges at the test site in Lausanne (Turtschy & Perret, 1999)

A control of the measurements was done for the COST 333 project where some of the gauges were found to be unreliable and removed from the database. (Ekdahl, 1999 and Turtschy & Perret, 1999)

5.3.3 Measurements

Tests have been made at different temperatures from –10°C to 30°C. FWD measurements were carried out at 11 points at each temperature. No response measurements were made under FWD.

The wheel load had a speed of 12 km/h, and the load was varied according to Table 5:4. Each load case was repeated at each temperature.

Table 5:4 Load configurations (Turtschy & Perret, 1999)

Dual tyres		Single tyres	
Pressure (bars)	Load (t)	Pressure (bars)	Load (t)
6.5	8.0	8.0	8.0
6.5	10.0	8.0	10.0
6.5	11.5	8.0	11.5
7.5	11.5	8.0	13.0
7.5	13.0	9.0	10.0
8.5	11.5	9.0	11.5
8.5	13.0	9.0	13.0

The transverse position of the wheel was also changed for each loading case according to Table 5:5.

Table 5:5 Transverse position of the wheel (COST 333)

Dual tyres		Single tyres	
Identification of the transverse position	Distance (cm)[1]	Identification of the transverse position	Distance (cm)
0	0.0	0	0.0
1	5.0	1	7.5
2	10.0	2	15.0
3	14.5	3	22.5
4	20.0	4	30.0
5	29.0	-	-
6	34.0	-	-

[1] Distance between the central axis of the gauges and the symmetry axis of the tyres.

5.4 Hirtshals

This test section is located on Highway M90 in northern Denmark. The pavement is designed for approximately 7 million standard axles during 20 years.

Design

The road is built as a test road where two different designs are compared. For this study, only the more traditional section is used. The AC layer of that section consists of three different materials with a total thickness of 275 mm. The base course is 150 mm and the subbase is 750 mm. The total thickness of the pavement is 1175 mm (Hildebrand & Bruun, 2004)

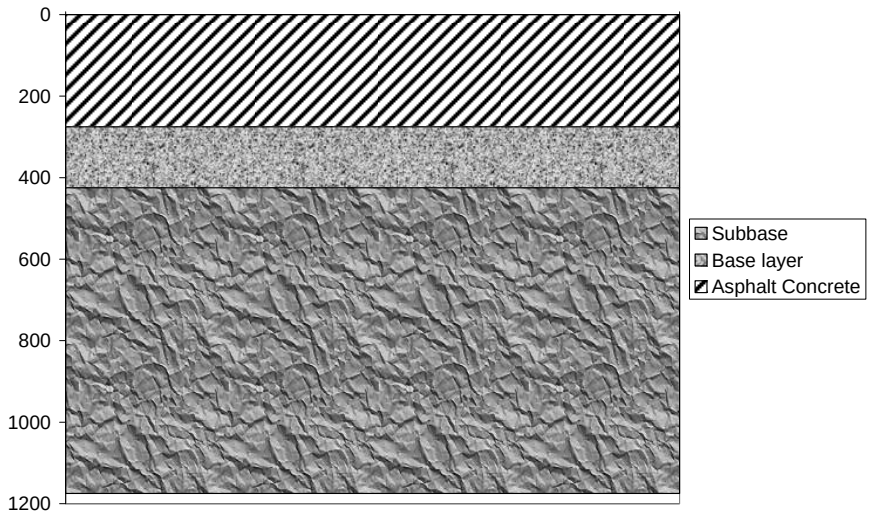

Figure 5.13 Design of the Hirtshals test section

Measurements

FWD measurements have been performed in September each year since the construction in 2001. At the same time, rut depth measurements were also done.

5.5 Eket

The test section at Eket is a part of Highway E4. It was built in 1997. When it opened, the traffic was 7000 vehicles per day, and 17% of them were trucks (Ekdahl, 1997).

Design

The road was built on moraine with 160 mm of Asphalt Concrete, and like all other Swedish roads a base course of 80 mm. The subbase is 470 mm thick.

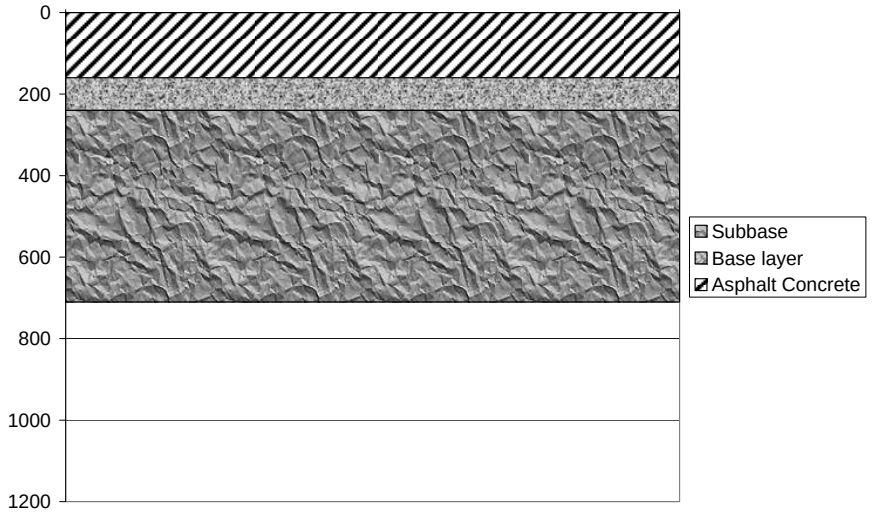

Figure 5.14 Design of the Eket test section

Measurements

FWD measurements have been performed three times. The first measurements were performed on the new road in December 1997. In May 1998 the second set of measurements were carried out, and the third in October 2003.

The surface profile has been measured every year since the road was built. However, the reference system for these measurements was changed in 2001. To be completely sure that the measurements are done at the same place, only measurements after this date are included in the analysis.

5.6 Summary

All sections for the calibration of the models are test pavements that are constructed indoors and have been tested under controlled climate. These sections are built in a concrete pit and therefore have a rigid concrete layer at a certain depth.

Table 5:6 Layer thicknesses at the different test sites (mm)

	Copenhagen RTM 2	Copenhagen RTM 3	Lausanne	Linköping SE 01	Linköping SE 02	Nørresundby	Eket
AC layer	84	120	80	49	62	275	160
Base course	140	140	400	89	110	150	80
Subbase					128	750	470
Rigid layer at depth	1781	1817	2000	2638	2638		
Total thickness of pavement	224	260	480	138	300	1175	710

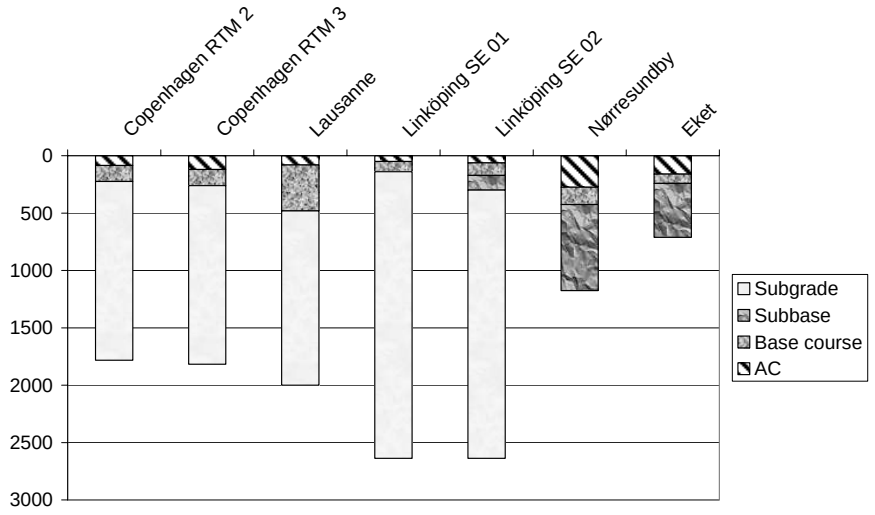

Figure 5.15 Layer thicknesses and depth of the concrete pit of the test sections

All sections used for the calibration are relatively thin pavements, and if they were used under real traffic conditions it would be on low traffic roads. The sections used for the validation are high traffic roads, and therefore noticeably stronger than the calibration sections. Accelerated tests are often done on relatively weak constructions in order to avoid excessively long test times. On real roads, high traffic roads are better controlled than low traffic

roads. That means that high quality measurements of deterioration, bearing capacity and traffic are easier to find from strong roads.

Table 5:7 Number of functioning gauges at each test section

	Copenhagen RTM 2	Copenhagen RTM 3	Lausanne	Linköping SE 01	Linköping SE 02
AC strain longitudinal	5	5	1	5	1
AC strain transversal	5	5		4	
Vertical strain in unbound layers	3 levels 4 at each level	3 levels 4 at each level	2 levels 2 at each level		
Horizontal strain in unbound layers	3	3			
Vertical stress	3 levels 4 at level 1 4 at level 2 3 at level 3	3 levels 4 at level 1 4 at level 2 3 at level 3		3 levels 3 at each level	3 levels 1 at level 1 3 at level 2 3 at level 3
Surface deflection			1		

It is difficult to measure response in a pavement. The gauges have to survive high pressure during the construction of the layer, and then measure small stresses or strains accurately. The asphalt strain gauges also have to survive high temperatures during construction. Therefore, the quality demands on pavement response gauges are very high. It is difficult to live up to these demands. Many things can cause a failure. Unfortunately, many gauges on these test sites could never be used, or failed after a short service life. Especially at the Lausanne test sites and the SE02 section from Linköping, many gauges failed, and only a few could be used. The low number of functioning gauges will of course affect the trustworthiness of the measured responses.

6 MODEL PARAMETERS

For further studies, two of the models described in Chapter 5 were chosen according to the criteria in Chapter 4. Most of the deterioration models fail at the first and most important criterion. Most models cannot be used for incremental rut depth calculations based on pavement response. Two models seem to fit reasonably well with all three criteria. Both are based on pavement response and can be used for incremental calculations. The models are fairly easy to understand, and all model parameters are unit consistent. Hence all model parameters can be interpreted in some way, or at least the consequences of changing the parameter can be described. The chosen models are:

The energy model:

$$\Delta RD = AN^{\alpha}\left(\frac{1}{2}\varepsilon_z \frac{\sigma_z}{p}\right)^{\beta}$$

where

RD = Rut Depth

N = number of load repetitions

ε_z = vertical resilient strain at the top of the subgrade

σ_z = vertical stress at the top of the subgrade

p = reference stress

A, α, β = regression parameters

The plastic strain model:

For AC layers:

$$\frac{\varepsilon_p}{\varepsilon_r} = \beta_0 + \beta_1 \log(N) + \beta_2 \log(T)$$

where

ε_p = Plastic strain

ε_r = Resilient strain

N = Number of load cycles

T = Temperature

$\beta_0 - \beta_2$ = regression parameters

For unbound layers:

$$\delta_a(N) = \beta_{UB}\left(\frac{\varepsilon_0}{\varepsilon_r}\right)e^{-\left(\frac{\rho}{N}\right)^{\beta}}\varepsilon_v h$$

where

$\delta_a(N)$ = Deformation for N load repetitions

$\varepsilon_0, \rho, \beta$ = Material parameters

ε_r = Resilient strain

ε_v = Vertical strain

N = Number of load repetitions

β_{UB} = Calibration factor

Not all of the required input data for the plastic strain model were varied during the tests. For example, the temperature was constant during the loading. As a result, not every model parameter can be determined individually with these measurements. Thus some parameters have been combined into one parameter.

There are of course some differences between the models. One difference is that the plastic strain model has the pedagogical advantage that the rut depth is calculated as the sum of the deformations of the different layers in the pavement. The energy model treats the whole pavement as a unit. On the other hand, the energy model has the advantage of fewer parameters to determine.

Another advantage of calculating the deformation of each layer is that such a model has better chances to fit with unusual or new kinds of pavement constructions. The use of the energy model is probably more limited to the conditions from which the model parameters were obtained.

Different deterioration models require responses at different locations in the pavement as input data. For example, the energy model used in this study requires the vertical stress and strain at the top of the subgrade as input data for the deterioration calculation. To calculate these responses, the material parameters of the pavement have to be known. What kind of material parameters are needed depends on the response model that will be used. These parameters can often be obtained from FWD measurements. For this study, test roads with response measuring devices inside the pavement have been used. Therefore, more responses than surface deflections are available to determine the material parameters.

6.1 Material parameters

Obtaining material parameters from FWD measurements can be described as solving an over-determined equation system. In a simple case where only elastic moduli will be determined, the equation system can look like this:

$$
\begin{aligned}
d_0 &= f(E_1, E_2, E_3, E_4) \\
d_{300} &= f(E_1, E_2, E_3, E_4) \\
d_{600} &= f(E_1, E_2, E_3, E_4) \\
d_{900} &= f(E_1, E_2, E_3, E_4) \\
d_{1200} &= f(E_1, E_2, E_3, E_4) \\
d_{1500} &= f(E_1, E_2, E_3, E_4) \\
d_{1800} &= f(E_1, E_2, E_3, E_4)
\end{aligned}
$$

where

d_0 = deflection at distance 0 mm from the load centre

With measurements of other types of response, the equation system can easily be expanded with a new equation for each measurement location that can add information about the moduli, for example:

$$
\begin{aligned}
\varepsilon_{x,AC} &= f(E_1, E_2, E_3, E_4) \\
\varepsilon_{y,AC} &= f(E_1, E_2, E_3, E_4) \\
\varepsilon_{z,SG} &= f(E_1, E_2, E_3, E_4) \\
\sigma_{z,SG} &= f(E_1, E_2, E_3, E_4) \\
\sigma_{z,BC} &= f(E_1, E_2, E_3, E_4)
\end{aligned}
$$

Even a small error in the measured response can result in quite a large error in the material parameters. With more responses used in the back calculation process, the impact of a single error will hopefully be less significant.

There are always problems when measuring pavement response (see Chapter 4). It is probably harder to measure the stress or strain inside the pavement than the surface deflection, and even different measurements of the same kind are not always equally accurate. Hence some measurements should be considered more important than others when trying to fit material parameters to measured data. The equations above have to be complemented with a weight factor for each equation. Weighting the equations is the same as weighting the measurements.

These weight factors can be determined in several different ways. For example, different responses (stresses, strains, deflections) can be weighted

differently for various reasons. Since it is probably easier to get an accurate value of the deflection than of the other responses, those measurements should have a greater weight.

Another way to determine the weight of different responses is to study the variation of the measurements. Normally each response is measured more than once. If the variation between measurements is large, that is an indication that the measurement is probably not very reliable. Such measurements should have a low weight in the analysis. The weight factor can be a function of a variation parameter. For example, the weight factors can be equal to the inverse of the standard deviation of each measured response.

Often when doing a back calculation from FWD measurements, the Root Mean Square (RMS) of the difference between measured and calculated deflections is minimized. That method is based on the assumption that the error is the same for all measurements. If it is assumed instead that the relative error is the same for all measurements, then the RMS of the relative difference (absolute difference over measured value) is minimized.

It can often be assumed that the measurement error is correlated to the variation of the measured values. Therefore a parameter of variation, such as standard deviation, can be used as the base for weight factors. The standard deviation has the same unit as the measured value. Thus, to be unit consistent, all measurements must have the same unit if the standard deviation is used as the base for weight factors. Normal FWD measurements include only deflections, and therefore the standard deviation could probably be used as the base for the weight factors.

If different types of responses with different units are included in the analysis, the weight factor should be without unit. That can be done by using the inverse of the coefficient of variance (COV) as the base of the weight factors. One difference between using the COV instead of the standard deviation as the base for the weights is that small measured values, for example deflections at a long distance from the load, will have greater weight when the standard deviation is used as the base.

Example:
An FWD measurement is made with two geophones. The one that is closest to the load measures an average of 200 μm. The outermost geophone measures an average of 20 μm. Both measurements have a standard deviation of 2 μm.

Average	*standard deviation*	*COV*	*inverse of standard deviation*	*inverse of COV*
200	*2*	*0.01*	*0.5*	*100*
20	*2*	*0.1*	*0.5*	*10*

With standard deviation as base both measurements will have the same weight, but with COV as base the first measurement will be 10 times more important than the second one.

If the standard deviation is supposed to be the same no matter what the measured average is, then the standard deviation should be used as the base for the weight factors. If the standard deviation is supposed to increase when the mean value increases, then COV should be used as the base.

Another way to give different weights to different measurements is to include the variation (i.e. in the form of standard deviation) in the error value that is minimized. For example, the RMS of the difference between measured and calculated value over the standard deviation $\left(\frac{d_{calc} - d_{meas}}{\sigma}\right)^2$ can be minimized. That means that the optimization process will minimize the deviation from measured value in the unit "number of standard deviations of the measured value". In that way measurements with different units can be used in the same analysis. Material parameters used in this study are obtained with this method.

When several FWD measurements are carried out, the average material parameters can be obtained in two different ways. Often a set of parameters (e-moduli) are calculated for each FWD measurement. Then the average of these parameters is used as representative for that pavement section. It is also possible to use the average of the measured deflections to obtain a representative set of material parameters. The latter method is less time consuming since it doesn't require a lot of back calculation loops. The study mentioned above (Agardh, 2002) also showed that the method of average deflections resulted in better fit to the FWD measurements (lower RMS), and in most cases could give predictions of the response in the pavement that were closer to the measured response. When FWD measurements are used in this study, only the average deflections method is used.

An example from the Lavoc test section of the variation in material parameters during the test is shown in Figure 6.1.

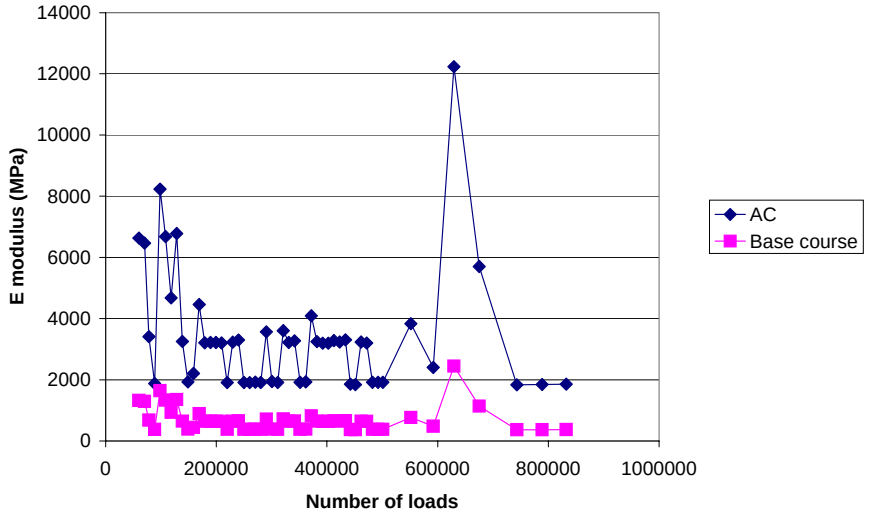

Figure 6.1 Variation of modulus for the AC and base course layer at the Lavoc test section during the test period

6.2 Response

As described in Chapter 4, there are a lot of different response models that can be used to determine response in pavements. All of these models require different material parameters, and also different information to obtain these material parameters. For most of the pavement sections used in this study there is little or no information about the response during a whole load cycle. Often only the maximum value is available. From such data it is hard or even impossible to obtain time dependant material parameters. That is one reason for using an elastic material model in this study.

In a study of different elastic response models (Agardh, 2002), it was shown that a model with stress dependant modulus of the subgrade gave the best fit to measured response. Therefore that model is used in this study.

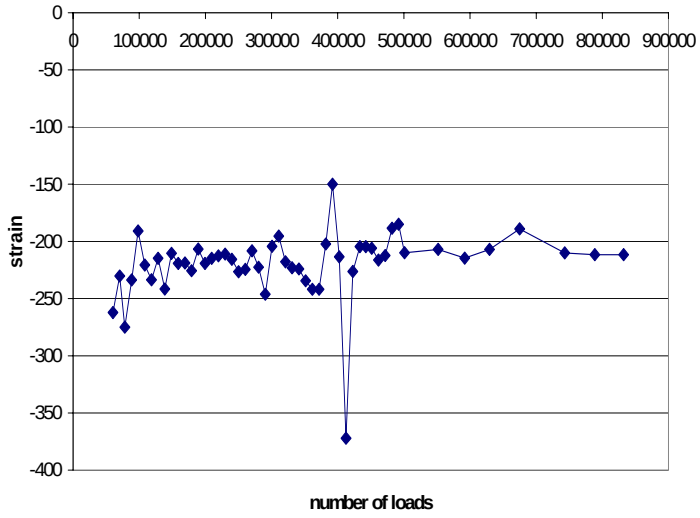

Figure 6.2 Variation in AC strain at the Lavoc test section during the test period

According to Figure 6.1 and Figure 6.2, the variation in the material parameters seems to be larger than the variation in the measured response. No clear trend of a change in modulus can be seen in either of the two layers. The modulus of the base course seems to be correlated to the AC modulus. When the AC modulus is high, the base course modulus is also high. The AC strain depends on the ratio between these two moduli, and not on their absolute values. Since the measured strain is relatively constant, it is reasonable that the AC modulus over the base course modulus is also relatively constant.

6.3 Deterioration model parameters

6.3.1 Part 1: different parameters for each test section

In the first study the model is optimized for each section separately. The results from the optimization for the parameters of the energy model are shown in Table 6:1 and the parameters for the plastic strain model are shown in Table 6:2. The RMS value in the last row of each table is the difference between calculated and measured rut depth.

Table 6:1 Parameter values for the energy model

	Rtm 2	Rtm 3	Se 01	Se 02	La
A (μm)	2.76	0.406	0.331	37.0	249
α	0.307	0.228	0.342	0.436	0.227
β	0.662	1.023	0.742	0.002	0.175
RMS (mm)	**0.13**	**0.16**	**0.31**	**0.18**	**0.29**

Table 6:2 Parameter values for the plastic strain model

		Rtm 2	Rtm 3	Se 01	Se 02	La
AC	$\beta_0+\beta_2\log(T)$	0.00104	0.00124	0.0179	0.598	0.00113
	β_1	1.009	0.928	0.833	0.574	0.0102
Base	$\beta_{ub}*(\varepsilon_0/\varepsilon_r)$	7.942	8.266	43.9	5.01	38.7
course	ρ	2200	2200	2000	2200	2200
	β	0.392	0.670	0.350	0.010	0.001
Subbase	$\beta_{ub}*(\varepsilon_0/\varepsilon_r)$			20.1	1.357	
	ρ			3000	2200	
	β			0.200	0.010	
Subgrade	$\beta_{ub}*(\varepsilon_0/\varepsilon_r)$	10.81	12.3	21.0	11.33	45.9
	ρ	2120	2120	2000	2200	2120
	β	0.344	0.010	0.498	0.079	0.016
RMS (mm)		**0.13**	**0.11**	**0.54**	**0.34**	**1.03**

The measured and calculated rut depths are shown in Figure 6.3 to Figure 6.7.

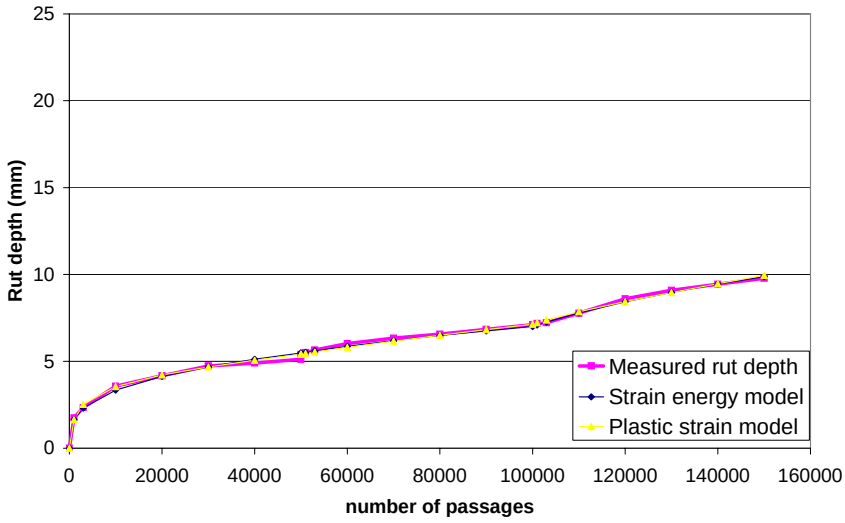

Figure 6.3 Best fit to measured rut depth for RTM 2

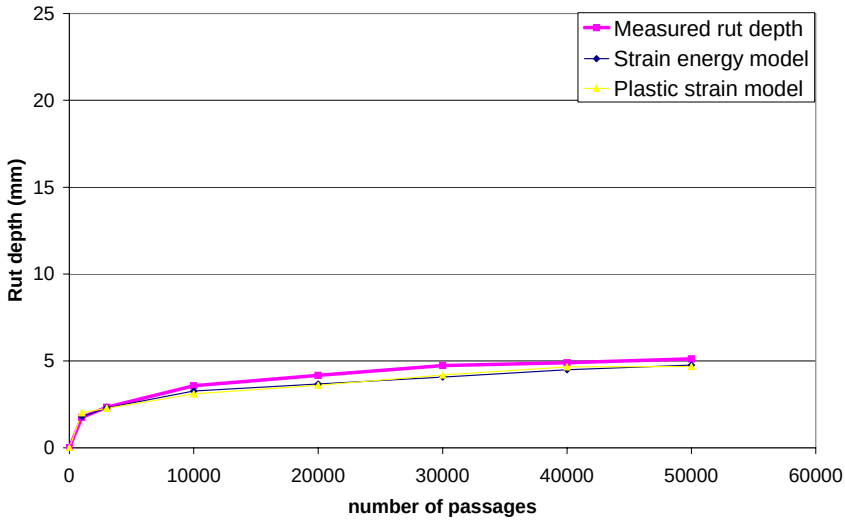

Figure 6.4 Best fit to measured rut depth for RTM 3

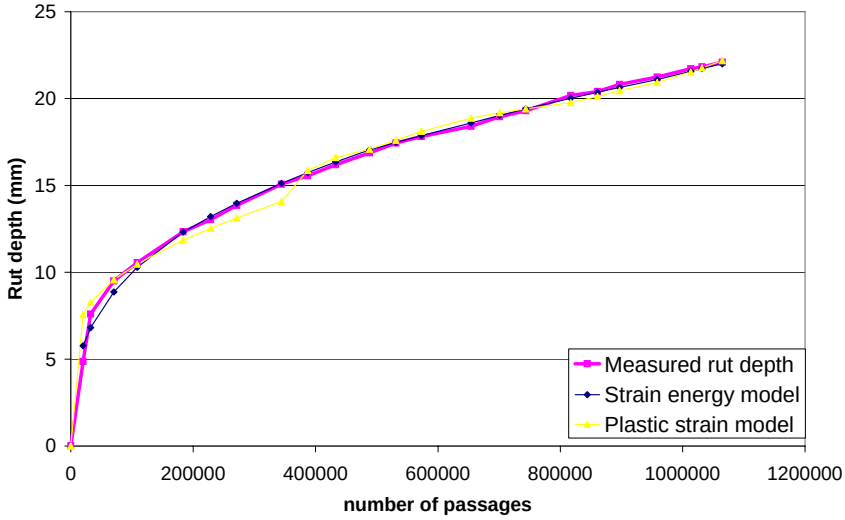

Figure 6.5 Best fit to measured rut depth for Se01

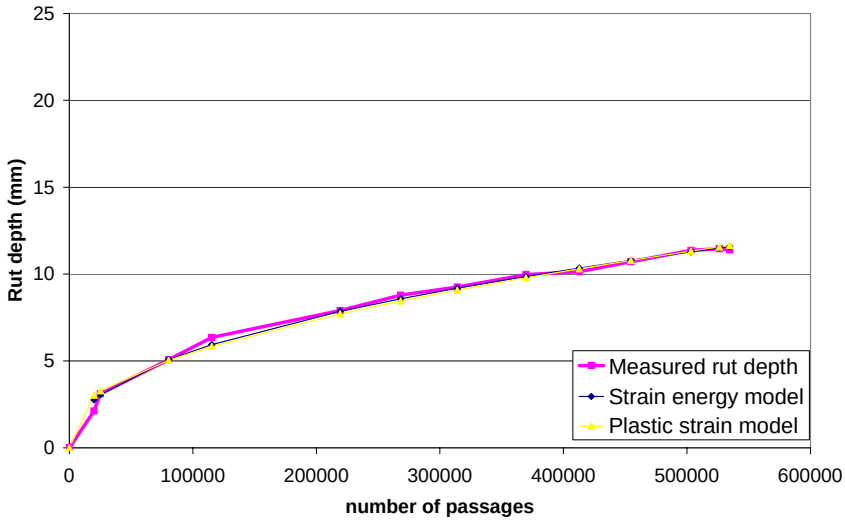

Figure 6.6 Best fit to measured rut depth for Se02

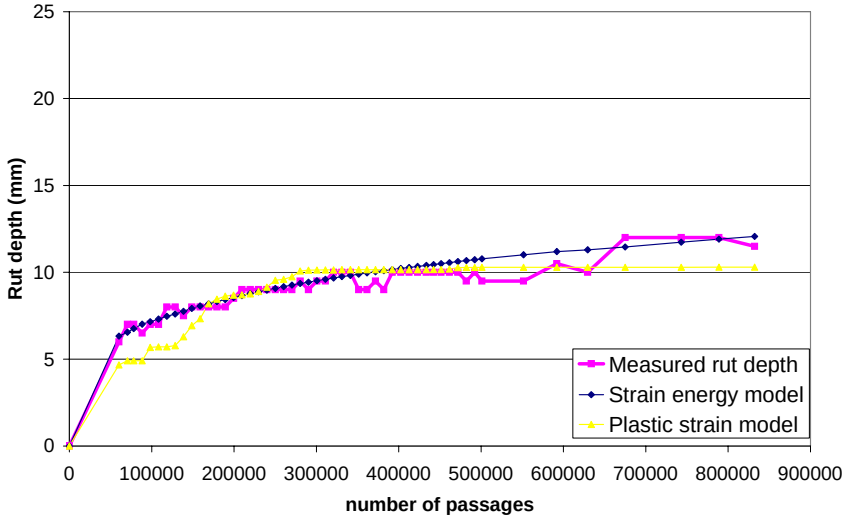

Figure 6.7 Best fit to measured rut depth for Lavoc

Both models can quite accurately describe the deterioration. On some of the sections the difference between measured and calculated rut depth is definitely within the measurement error of the rut depth.

Some of the model parameters show a variation of more than a factor of 10 between the different test sections. Therefore it is probably not a good idea to take only the average value of all test sections as general parameters.

6.3.2 Part 2: Same regression parameters for all sections

For the energy model, one set of regression parameters is supposed to describe all pavements. The only differences between different pavement sections are the layer thicknesses and the E-moduli of the materials, and thus the input data of stress and strain will differ. In the 2002 Design Guide the plastic strain model is supposed to use different parameters for different materials. That means that for the energy model the only material parameter that is required is the E-modulus. For the plastic strain model, parameters for the deterioration model are also required for each material. Therefore material testing for that model also has to include some time dependant test.

In part two of the evaluation of the models, one set of model parameters is determined to fit all test sections. Because of the difference in how the models that are mentioned above have been developed, it is not really fair to the plastic strain model to compare the models in this way. However it is, at least theoretically, possible to use the plastic strain model with one set of parameters, and it is also possible to use the energy model with different model parameters for different pavement sections. The five test sections used in this study are all normal flexible pavements with no major differences in the manner of construction. Even though the materials are not the same, they do not differ very much between the test sites. The model parameters at the different sections should therefore not differ very much between the different test sections, and it can also be possible to use the same set of parameters for all sections.

The material parameters that give the best fit to all sections are shown in Table 6:3 and

Table 6:4

Table 6:3 Model parameters for the energy model

	all sections
A (μm)	68.1
α	0.344
β	0.115
RMS (mm)	**0.87**

Table 6:4 Model parameters for the plastic strain model

		All sections
AC	$\beta_0+\beta_2 \log(T)$	0.0204
	β_1	0.797
Base course	$\beta_{ub}*(\varepsilon_0/\varepsilon_r)$	49.9
	ρ	2200
	β	0.217
Subbase	$\beta_{ub}*(\varepsilon_0/\varepsilon_r)$	81.0
	ρ	2200
	β	0.152
Subgrade	$\beta_{ub}*(\varepsilon_0/\varepsilon_r)$	0.100
	ρ	2200
	β	0.050
RMS (mm)		**2.08**

From looking at the RMS values, it seems that the energy model gives a much better prediction of the rut depth. Most of that difference is from the Lavoc test section where the energy model seems to give noticeably better results. Since that section contains the largest number of rut depth measurements, it also has the largest impact on the overall RMS value.

6.4 Sensitivity analysis

A simple sensitivity analysis is performed for the model parameters. The analysis is based on test section Se01 and the model parameters obtained from all test sections. In the figures below, the rut depth is shown both with the original parameters, and by adding or subtracting 10% to the original value of the parameter. Only one parameter is changed in each figure. All other parameters are as obtained from the "all sections" analysis.

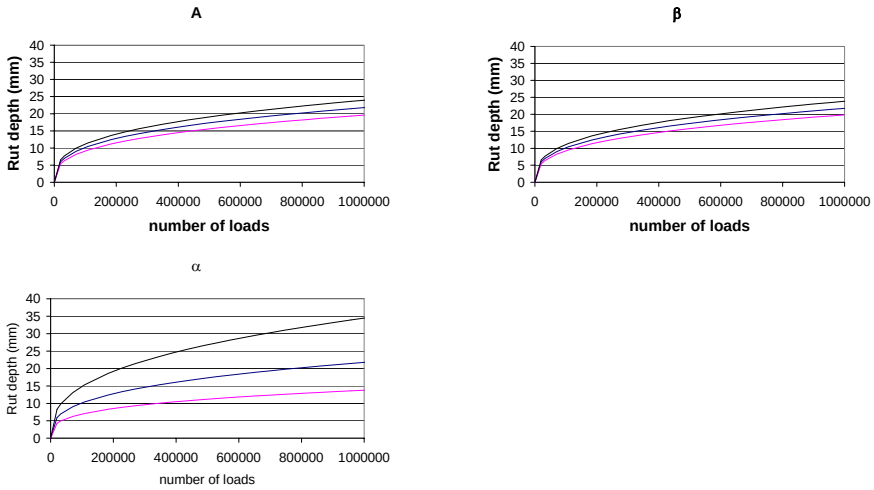

Figure 6.8 Results from the sensitivity analysis for the energy model

It is quite clear that the α-parameter has the greatest impact on the calculated rut depth. A change of the parameter of 10 % will result in almost 60% difference in the calculated rut depth after 1 000 000 loads. In an earlier study (Ullidtz et al., 1999), this parameter has been determined to 0.341, which is almost the same as in this study (0.344).

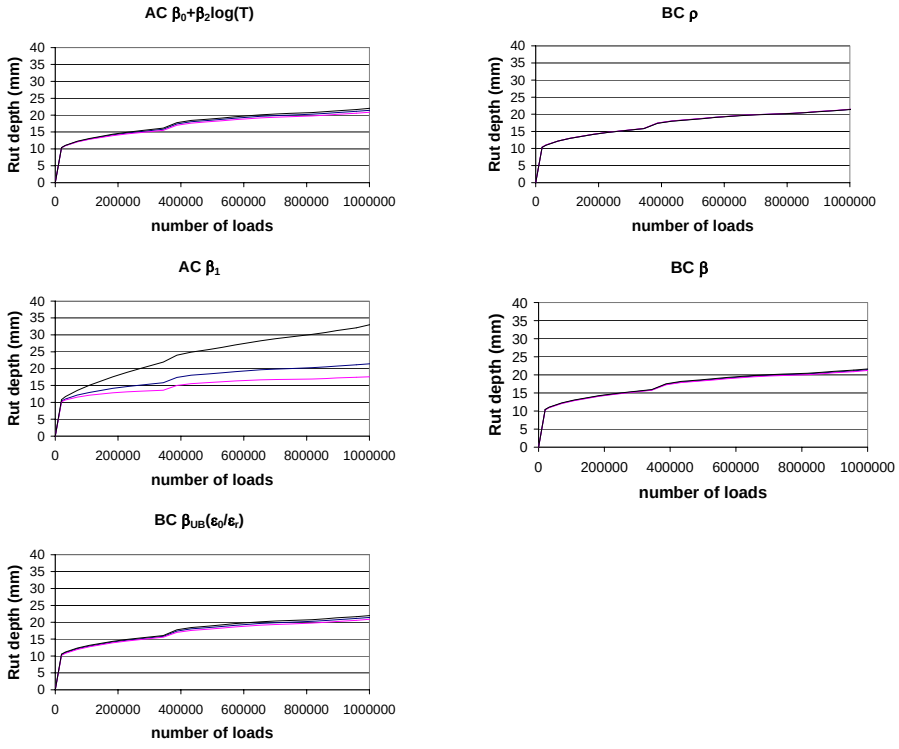

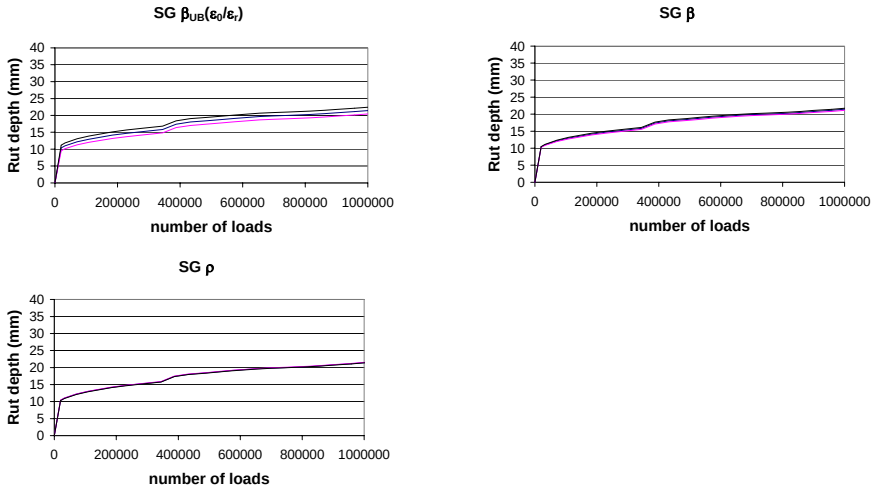

Figure 6.9 Results from the sensitivity analysis for the plastic strain model

The most interesting result from this sensitivity analysis is the great impact of the β_1 parameter for the AC layer. Normally it is assumed that most of the rutting consists of permanent deformation in the subgrade, and that a very small part of the rutting is from the AC layer. With these model parameters, almost half of the rutting is from the AC layer. That is definitely more than expected. To reflect reality, the β_1 parameter probably should be lower than what was obtained from the best fit to all sections.

The ρ parameter for the unbound layers does not have a great impact on the total rut depth. By changing the ρ parameter for the subgrade by 10%, the total rut depth of the pavement after 1 000 000 loads will only be changed by 0.3%. The permanent deformation of the subgrade will change by approximately 0.6%. When this model is used as it is supposed to be used in the 2002 Design Guide, with different parameters for different materials, it is not very important to get an accurate value of that parameter. Probably just a standard value can be used.

Because of the unreasonable results with large deformations of the AC layer, a new analysis was performed where the β_1 parameter was set to the value suggested in the 2002 Design Guide (0.479244). The best fit to all sections resulted in an RMS value of 2.40 instead of 2.08 from the earlier analysis.

Table 6:5 Regression parameters for the plastic strain model with fixed β_1

		All sections
AC	$\beta_0+\beta_2 \log(T)$	0.0552
	β_1	0.479
Base course	$\beta_{ub}*(\varepsilon_0/\varepsilon_r)$	119

	ρ	3440
	β	0.267
Subbase	$\beta_{ub}*(\varepsilon_0/\varepsilon_r)$	147
	ρ	3650
	β	0.370
Subgrade	$\beta_{ub}*(\varepsilon_0/\varepsilon_r)$	0.100
	ρ	2200
	β	0.050
RMS (mm)		**2.40**

With this set of parameters the relative deformation in the different layers is more reasonable, even though it is still only a small part of the rutting that comes from the subgrade.

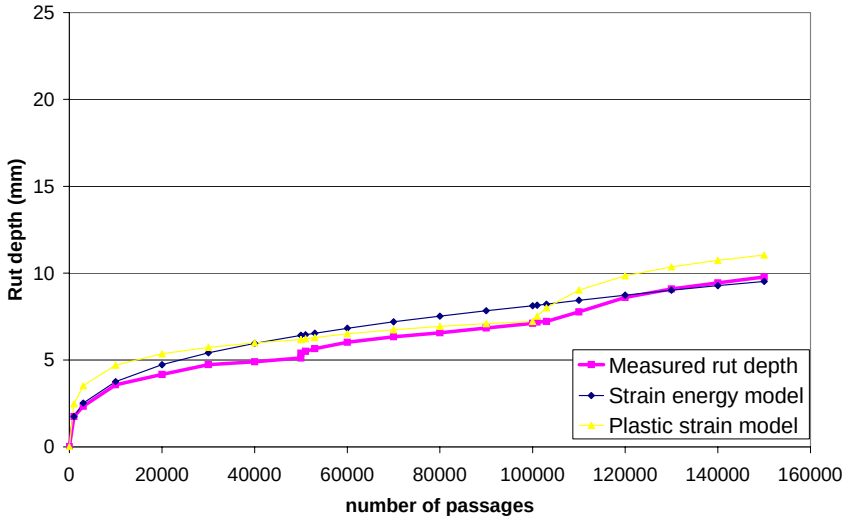

Figure 6.10 Measured and calculated rut depth for RTM 2

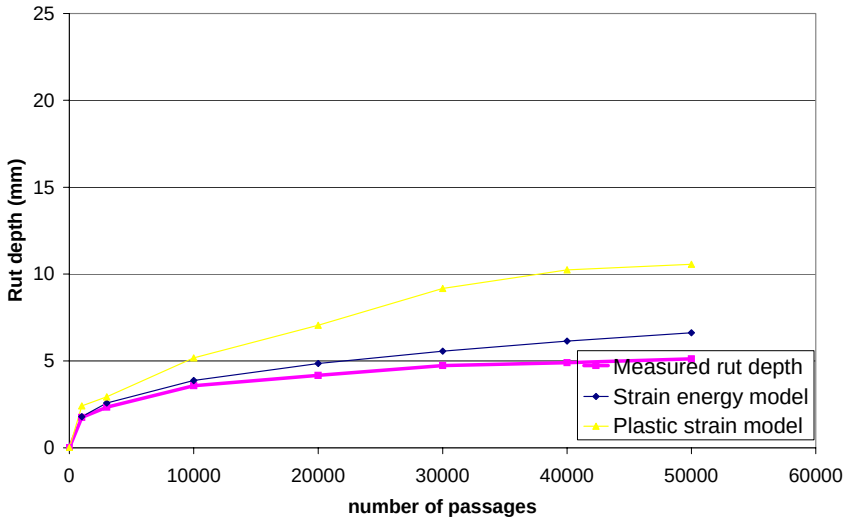

Figure 6.11 Measured and calculated rut depth for RTM 3

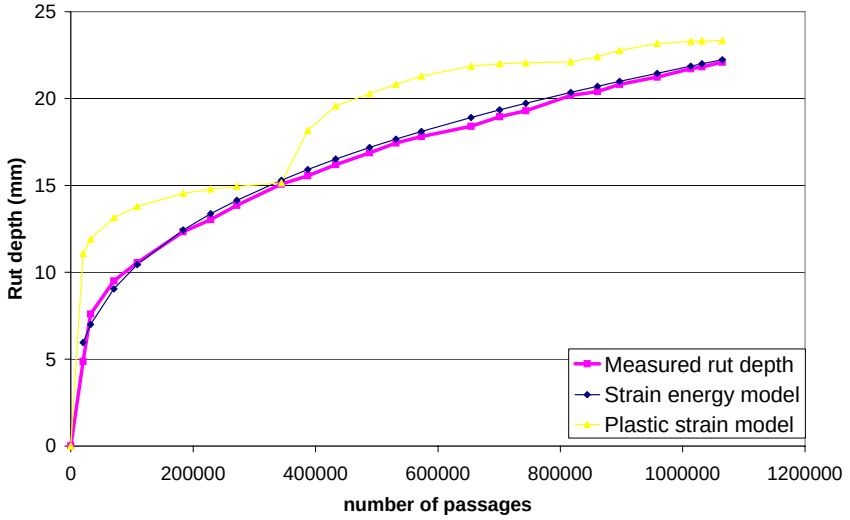

Figure 6.12 Measured and calculated rut depth for Se01

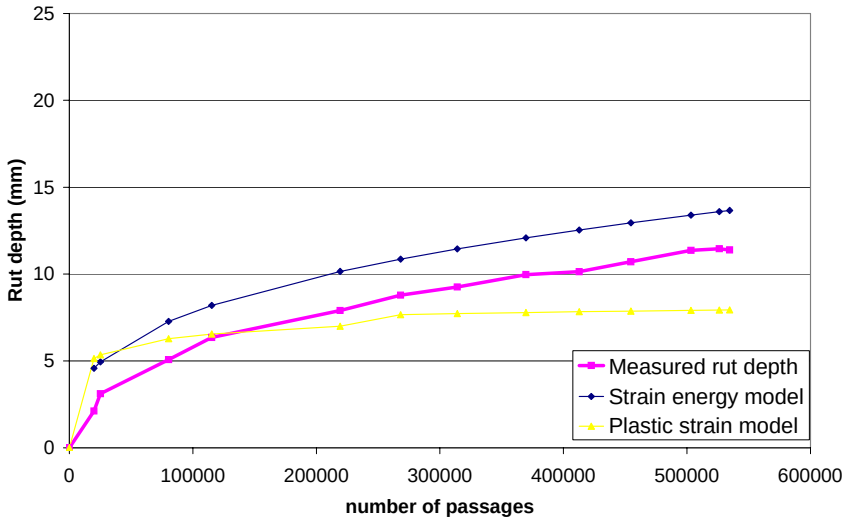

Figure 6.13 Measured and calculated rut depth for Se02

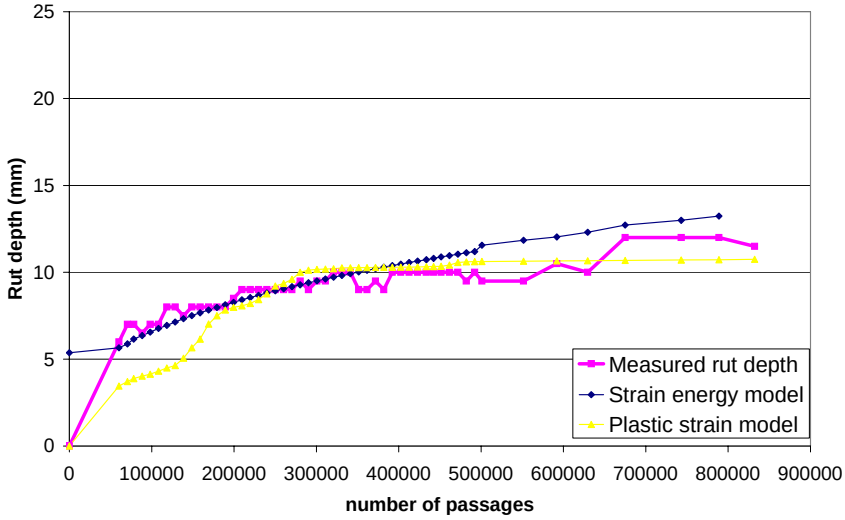

Figure 6.14 Measured and calculated rut depth for Lavoc

Table 6:6 RMS value (mm) between measured and calculated rut depth for each test section

	Rtm2	Rtm3	Se01	Se02	Lavoc
Energy model	0.48	0.87	0.44	1.19	1.14
Plastic strain model	0.74	3.05	1.86	0.65	1.46

The energy model gives the best prediction (lowest RMS) for 4 of the 5 sections. The only section with lower RMS for the plastic strain model is Se02. However, the rut depth development of that section is better described with the energy model. The rut depth calculated with the energy model is 2-3 mm higher than the measured rut depth through the whole test. With the plastic strain model, the calculated rut depth is higher than measured rut depth at the beginning of the test, but lower at the end.

6.5 Validation of the model parameters obtained

The model parameters have been obtained only from accelerated tests with controlled climate. Often when laboratory results are to be transformed to reality a shift factor is needed. To get an indication of whether such a shift factor is needed for these models, a validation is performed in two different ways. First rut depth development is calculated for theoretical pavements. Six different sections were designed according to Swedish standards, ATB Väg (SNRA, 2001). This validation can give a hint as to whether the model parameters obtained give rut depth development of reasonable size for real pavements, or whether a correction factor is needed when the accelerated tests are transformed to real pavements. The material parameters for these calculations are the material parameters used in ATB Väg.

Then the model parameters are validated to two real pavement sections. Both these sections are highways and are considerably stronger pavements than the accelerated test sections used to obtain the model parameters. One section is located close to Hirtshals in northern Denmark on highway M90. The other section is located in southern Sweden on highway E4, close to Eket.

The material parameters used for these calculations are obtained from FWD measurements. The moduli have then been adjusted to different seasons according to VVMB 114 (SNRA, 2000). That means that during winter no change in rut depth was calculated. The moduli for the unbound material were assumed to be the same during summer and autumn, and reduced according to Table 6:7 in the spring.

Table 6:7 Correction factors for unbound materials during spring

	Base course	correction factor
Modulus obtained from back calculation of fwd measurement	>450 MPa	0.9
	250-450 MPa	0.8
	75-250 MPa	0.6
	Subbase	
	>100	0.9

	50-100	0.7
	20-50	0.6
	<20	0.9

The modulus of the AC layer at different temperatures is described by a line with the same shape as the following equation, which is supposed to represent new materials (SNRA, 2000):

$$E_{AC}(T) = 17900e^{-0.071T}$$

The number of standard axles is calculated with the following equation and standard values (SNRA, 2000):

$$N_{ekv} = AADT * A * C * D * E * 3.65 * \sum_{j=1}^{n}\left(1+\frac{l}{100}\right)$$

where

A = Portion of heavy vehicles (14 %)

C = Average number of axles on heavy vehicles (5)

D = Average number of standard axles for each axle on heavy vehicles (0.3)

E = Correction factor for number of lanes and width of lanes (0.8)

n = length of design period (20 years)

j = 1,2,3...n

l = annual change in number of heavy vehicles (0 %)

6.5.1 Validation to theoretical sections

Pavement sections were designed for three different traffic classes, according to Table 6:8, and two different subgrade materials. All sections were designed for the climate in southern Sweden. The traffic for the calculations was chosen in the middle of the interval for each traffic class. The subgrade materials chosen were material types 3 and 5. Material type 3 is moraine with good bearing capacity and less than 30 % clay and silt. Material type 5 is soils with mostly silt and/or clay.

Table 6:8 Traffic classes used for the analysis

Traffic class	Number of standard axles during 20 years
2	0.5-1.0*10^6
4	2.5-5.0*10^6
6	9.0-19*10^6

The thicknesses of the different layers are shown in Figure 6.1.

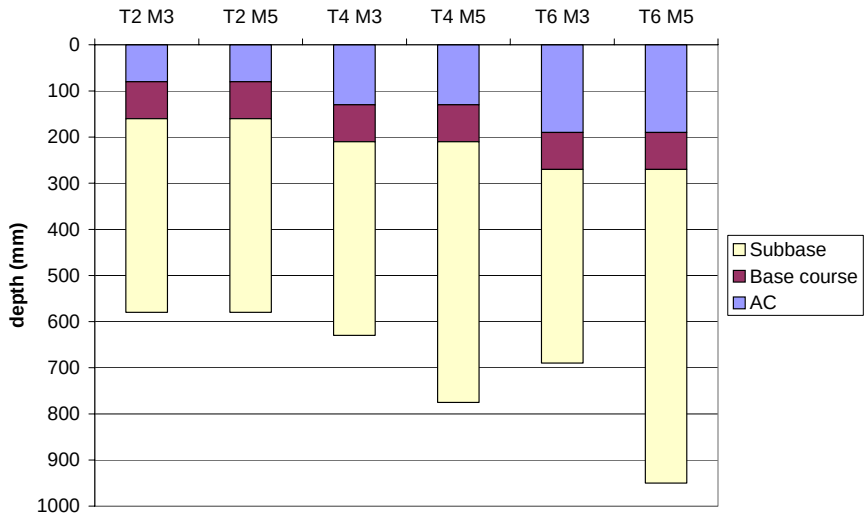

Figure 6.15 Theoretical sections for the analysis

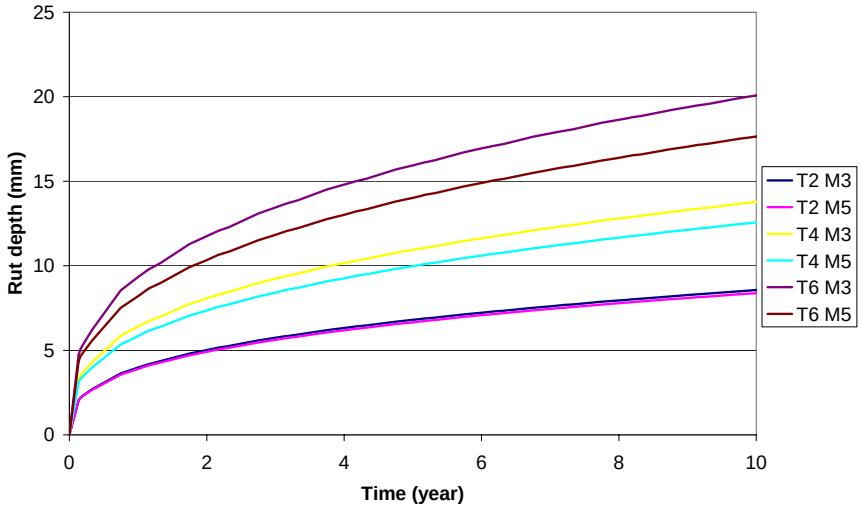

Figure 6.16 Rut depth for the theoretical sections with the energy model

With the energy model, the calculated rut depth will increase with traffic. Since all sections according to the design standard (ATB Väg) have a base and subbase of at least 500 mm, it is possible that sections with lower traffic are a bit thicker than what is necessary to avoid rutting, and therefore get less rutting. All calculated rut depths are of reasonable sizes.

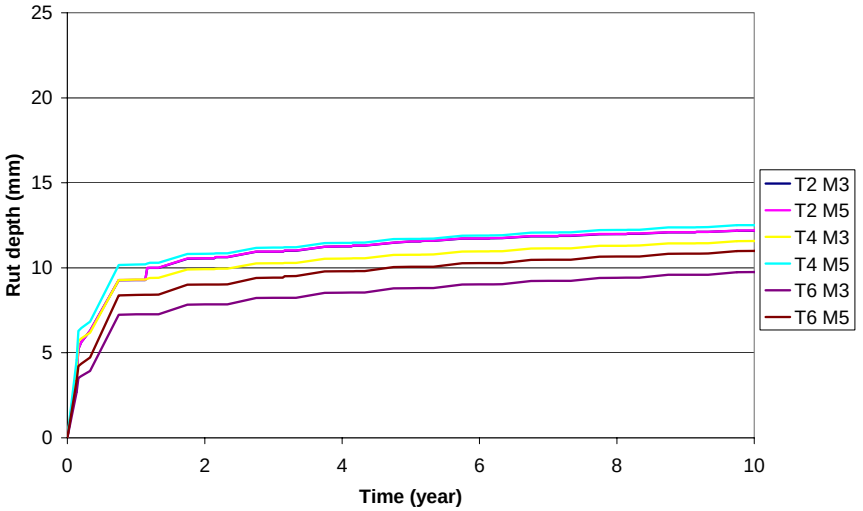

Figure 6.17 Rut depth for the theoretical sections with the plastic strain model

With the energy model it is not easy to see the different seasons in the figure, but with the plastic strain model the seasons are visible with faster rut depth development in the summers. The plastic strain model seems to be more sensitive to climate variations.

For the plastic strain model, the difference between the sections is quite small. Most of the rutting occurs in the first year. After that the rut depth development is considerably smaller. The rutting with the energy model is more linear with the parameters used for these calculations.

Even though the total rut depths from these calculations seem to be of reasonable size, it is not sure that calculations with these parameters will always be reasonable. The calculations with the plastic strain model show that only a small part of the rutting occurs in the subgrade. That is probably not the case for real pavements (Huang, 1993). The deterioration parameters for the subgrade should probably have different values than those obtained in this study. That error has, in this study, been compensated with larger deformations in the other layers. Consequently, these parameters should not be used. Further studies are needed to find a better set of parameters. The conclusion must be that for calibration of the plastic strain model, normal response and performance measurements from accelerated tests are not enough. Probably some deformation measurements for different layers have to be made to determine the model parameters.

6.5.2 Validation to real roads

Hirtshals

The Hirtshals section is located on highway M90 in northern Denmark. The highway was built in 2001, and rut depth measurements and FWD measurements have been conducted in August or September every year since then.

The pavement is designed for 7 000 000 standard axles.

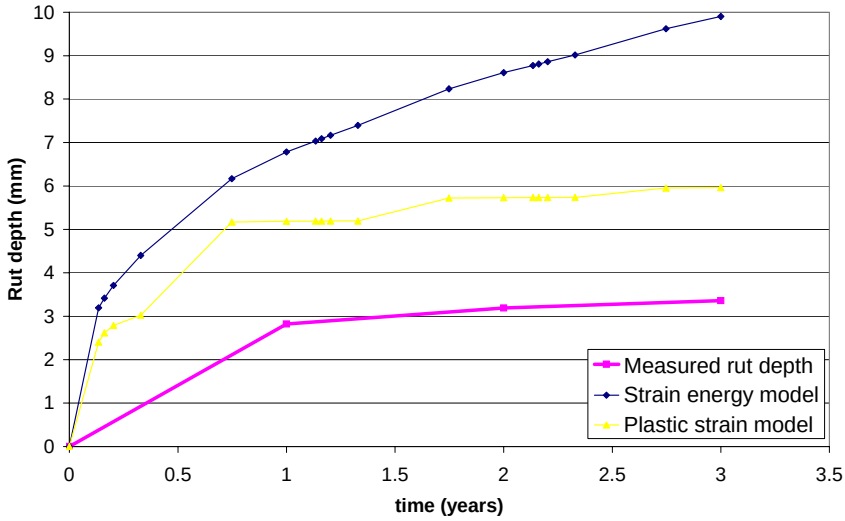

Figure 6.18 Measured and calculated rut depth for the M90 section

The rut depth is calculated with the assumption that the traffic has been what the pavement was designed for. It is possible that there has been less traffic than expected, and that can explain why both models overestimate the rut depth. To get calculated rut depth to equal the measured rut depth after three years, the traffic can be set to approximately 500 000 standard axles for both models. It is, however, not likely that the traffic has been less than 10 % of the expected traffic. The error in traffic assumptions can only be a part of the explanation for the overestimation of the rut depth.

The plastic strain model actually describes the rut depth development very well after the first year, and there is only error in the first year.

Eket

This pavement section is a highway located in southern Sweden. The section is designed according to Väg 94 (SNRA, 1994). The expected traffic was 7000 vehicles per day. It was opened to traffic in 1998, and fwd measurements were made at three different times in the first year.

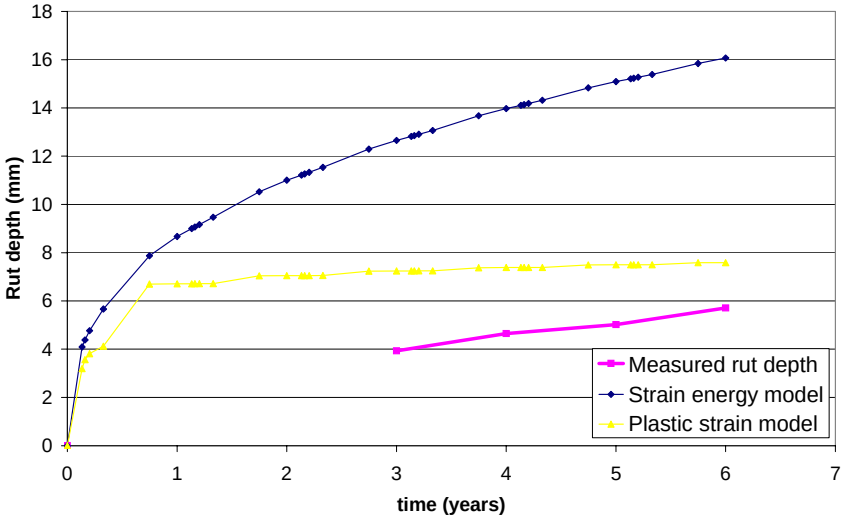

Figure 6.19 Measured and calculated rut depth at Eket

For this section as well, both models overestimate the rut depth. There can be several reasons for this. With the model parameters obtained for the plastic strain model, probably more of the deformation occurs in the pavement and not in the subgrade than it does in real pavements. That means that the calculated deformation of the base course and subbase is larger than the real deformation in these layers. Hence, with thick base course and subbase the calculated deformation is likely to be too large. Since these layers are thicker in these two pavements than in the ones used to obtain the parameters, the calculated total deformation will be too large for these sections. It is possible that these parameters would work better for low traffic roads.

During construction of a road, trucks with building material often drive along the unfinished road. That means that especially the unbound layers have been subject to traffic before the surface layer is done. The deformation of the unbound layers and the subgrade, which should result in rutting, is adjusted by the upper layers. Therefore the unbound layers have been object to loading before the first load that the calculations deal with. One way to deal with this problem is to ignore the calculated deformation of the unbound

layers for the first loads. In the Danish design standards, a correction similar to that is made by ignoring the calculated deformation for the first 1000 vehicles after each thaw cycle. How many vehicles that should be ignored should probably be different for each construction site. If the road is built far from other roads, probably a large number of trucks will use the road that is being constructed, but if there is an older parallel road, there will probably be less traffic on the construction site.

If only the rut depth development after the first rut depth measurement is calculated, then the calculated rut depth will be much closer to the measured rut depth.

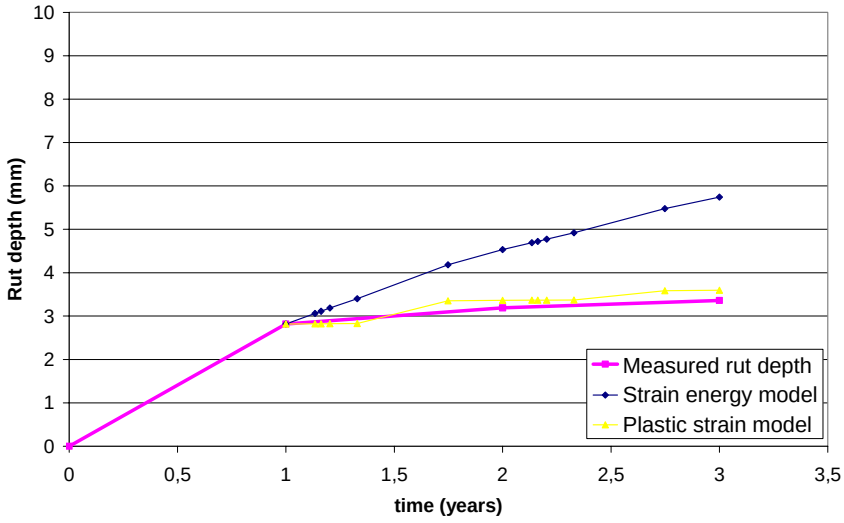

Figure 6.20 Measured and calculated rut depth at Hirtshals when the rutting until the first rut depth measurement is not calculated

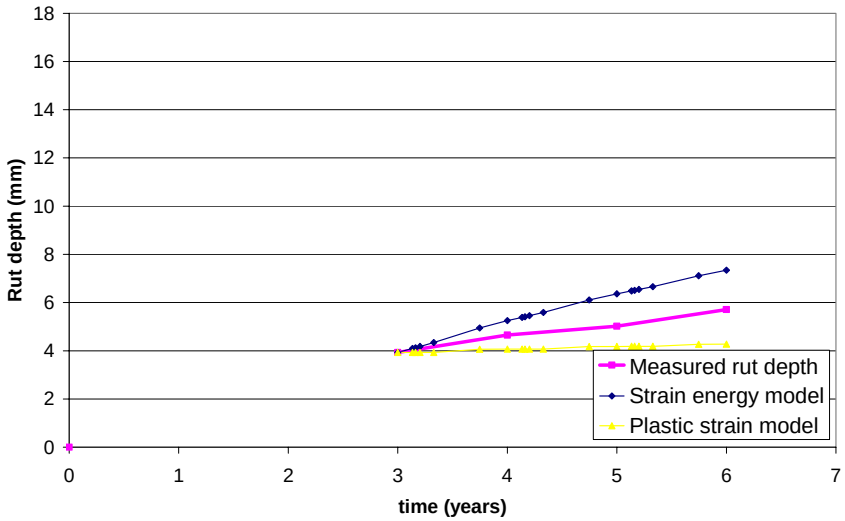

Figure 6.21 Measured and calculated rut depth at Eket when the rutting until the first rut depth measurement is not calculated

For both sections the energy model predicts faster rut depth development and overestimates the rutting for both sections. At least for the Hirtshals section, that can probably be explained by a difference between the assumed traffic and the real traffic. The plastic strain model is very close to the measured rut depths at the Hirtshals section but underestimates the rut depth development at Eket.

In the validation to theoretical sections, the energy model resulted in larger rut depth for the pavements with a lot of traffic. In the validation to real pavements it is shown that the parameters for that model result in too big rut depth for roads with much traffic. The α parameter shows the sensitivity to traffic load. It is possible that this parameter should be lower than the suggested 0.344. It is also possible that some of the model parameters should not be constant, but vary with either traffic or bearing capacity.

7 DISCUSSION AND CONCLUSIONS

As shown in Chapter 5, many different deterioration models have been developed during recent decades for different purposes. The most recently developed design procedures require deterioration models that are based on pavement response. That kind of design is often called analytical-empirical design. The deterioration used in future pavement design should also be iterative, and able to calculate the growth of deterioration and not only pavement service life. Unfortunately, most deterioration models cannot be used in such design procedures.

In this study, two iterative rut depth models are studied and compared. The energy model treats the pavement as a unit and uses three model parameters to describe rut depth. The plastic strain model calculates the deformation of each layer and uses two or three model parameters for each pavement layer.

The test sections used in this study are all flexible pavements, and the materials used are quite similar. There are, however, quite large differences in the thicknesses of the layers, and therefore also the strength of the pavements. The rut depth at the end of the tests varies from less than 5 mm to almost 25 mm.

Often when the results of rut depth models are compared, the number of loads to a certain rut depth is an important comparison parameter. Since the maximum rut depths for the test sections are so different from each other it is hard to make a fair comparison in that way with these data. That kind of comparison is also less important for modern deterioration models, since it is interesting if the models describe the deterioration during the whole service life, and not just the length of the service life.

The energy model uses fewer input parameters, and no time dependant material parameters are needed. The material testing for that model is therefore easier to perform.

The plastic strain model treats each material layer individually and could therefore probably be used in a wider range of different constructions. It is possible that the energy model is of more limited use. For the pavement sections used in this study, the energy model is at least as good as the plastic strain model.

Another advantage of the plastic strain model is that it can easily consider the lateral wander of the traffic. On narrow lanes all vehicles will drive almost in the same path, but on wider lanes there will be a greater distribution of the traffic. Such differences are not easily included in the energy model. Often

the lateral wander is considered with an empirical correction factor in the calculation of number of standard axles, but with the plastic strain model it is easy to use a more analytical approach to that problem.

7.1 Conclusions

7.1.1 Part 1 of the evaluation: the potential of the models

Both models can describe the rut depth development of all test sections, and it is not obvious that one gives better rut depth description than the other.

The model parameters vary a lot between the sections, so an average value of the parameters is probably not a good estimation of the true parameters.

7.1.2 Part 2 of the evaluation: the calibration of the models

The energy model gives reasonably accurate results for all sections. The RMS is less than 1 mm for three of the five sections. For one of the other two sections (Se02) the rut depth development is accurate, but at the wrong level.

The result from the energy model is closer to the measured value on 4 of the 5 sections.

The best fit of model parameters for the plastic strain model results in large deformation in the AC layer. By setting one of the AC parameters to a fixed value it is possible to get more reasonable results, even though the deformation of the subgrade is smaller than expected.

The small deformation of the subgrade with the plastic strain model indicates that the model parameters obtained from this study probably do not describe the real deformations. To obtain better model parameters, measurements of permanent deformations of different layers of the pavement are probably necessary.

7.1.3 Validation

The theoretical pavements designed with ATB Väg (SNRA, 2001) result in reasonable rut depths for both models. This indicates that probably no shift factor is needed to transform the laboratory results from this study to real pavements. With the model parameters used in this study, the energy model results in larger rut depth for sections with a lot of traffic. This indicates either that the value of the α parameter is too high or that the model parameters should vary with either traffic or bearing capacity.

Both models overestimate the rut depth at the two real pavements used for the evaluation. Especially for the M90 section, one reason can be that the traffic used for the calculations is not the real traffic. For the energy model, another reason can be the above mentioned possible error of the α parameter.

The model parameters were obtained from accelerated tests on relatively weak pavements, and the results from these tests could not be directly transformed to strong pavements under real traffic. Since there are two differences between the sections used to obtain the parameters and the validation sections, the reason for the difference can be found in two places. Either the main difference is the strength of the pavements, or the main difference is the dissimilar nature of accelerated tests and reality. The resting period between loads on real pavements can result in longer service life than in accelerated tests. Tests at the Danish Road Testing Machine show that the bearing capacity will increase during rest periods (Zhang et al., 1998).

7.2 Looking in the review mirror

The quality control of the measured response should have been more thorough, and maybe more data should have been rejected. For example, the stress measurements at the test site in Linköping almost certainly gave smaller stress than the real stress. Maybe these measurements should have been rejected instead of just adding a correction factor. With more data rejected, perhaps more sections should have been used from other test sites.

The measurements used for the study were not enough to get a good calibration of the plastic strain model. Measurements of permanent deformations of layers or parts of the pavement should have been used. Even if such measurements are not very common, they have been performed. Deformations of layers were, for example, measured with emu-coils at a temporary test site in Sunninge on the Swedish west coast, while constructing a major highway (Ekdahl, 2003). The pavements used for those tests were not normal flexible pavements, and could therefore not be used in this study. Similar measurements have probably been performed at other test sites that could have been used for the calibration.

When obtaining E-moduli from the response measurements, there were sometimes quite large variations between different measurements. Maybe the material parameters that were used for the deterioration calculations should have been taken from a regression analysis or some kind of average value (for example moving average).

Some more real pavement sections should have been used for the validation. Some weaker pavements could show if the difference between measured and

calculated rut depth was due to the strength of the pavement or to the difference between accelerated tests and real pavements. It is, however, not as easy to find low volume roads with as many trustworthy rut depth and FWD measurements as are necessary for this validation.

7.3 Recommendations and further research

The material parameters for a pavement are often obtained from FWD measurements. In accelerated tests, more information that can be used to obtain the material parameters is often known. For example, response somewhere in the pavement is often measured. In this study, the information from both response measurements and FWD measurements was used. It would be interesting to study what influence the new information might have on the calculated material parameters, and also if there is a better way to give the different measurements their weight in the analysis. Perhaps the number of functioning gauges should influence the weight, and not only the variation of the measured values.

The energy model seems to give reasonable results for the accelerated test sections. For normal flexible pavements, that model can probably be used with quite good accuracy. The model parameters obtained from this study are probably usable under conditions similar to the test roads. The most important model parameter (α) has almost the same value in three different studies, which indicates that that value is probably close to the best possible value. On the other hand, the validation to real roads gave an indication that perhaps the α parameter should be lower than the suggested value. For the other two parameters, this study differs from the other two, and calibration to more test sections can probably improve the parameter values.

The energy model is based on the assumption that the total rut depth depends on the strain energy at the top of the subgrade. From this study it seems that that can be a good assumption for normal flexible pavements, but it is not certain that that is a good assumption for other pavements. The plastic strain model has the advantage that it is easier to change the model when conditions change. For other types of pavements, such as full depth pavements or stabilized subgrade, that model is probably easier to adapt to new conditions.

Because of the small deformations in the subgrade from the plastic strain model, the parameters obtained in this study should not be used. To get more accurate parameters, a calibration to measured permanent deformation of the different layers should be made.

Especially for the evaluation of the energy model, a validation of the model parameters to low volume roads could be valuable. Such validation can

provide information for determining whether there should be a correction factor for the transformation between accelerated tests and reality, or if the parameters should vary with traffic or bearing capacity.

REFERENCES

AASHTO, 1981- "AASHTO Interim Guide for Design of Pavement Structures", American Association of State Highways and Transportation Officials, Washington DC, 1981

AASHTO, 1993- "AASHTO Guide for Design of Pavement Structures", American Association of State Highways and Transportation Officials, Washington DC, 1993

Agardh, 2002- Agardh S., "Calculating Pavement Response Using Elastic Material Models", Licentiate thesis, Bulletin 14, Department of Technology and Society, Lund University, Lund, 1999

Al-Omari & Darter, 1992- Al-Omari B., Darter M.I., "Relationship Between IRI and PSR", Report No. UILU-ENG-92-2013, Illinois Department of Transportation, Springfield, IL, 1992

AMADEUS, 2000- "Advanced Models for Analytical Design of European Pavement Structures", Final report RO-97-SC.2137, European Commission, 2000

Archilla & Madanat, 2001- Archilla R. and Madanat S., "Estimation of Rutting Models by Combining Data from Different Sources", ASCE Journal of Transportation Engineering, Vol. 127, No. 5, 2001.

Baltzer et al, 1998- Baltzer S., Zhang W., Macdonald R. & Ullidtz P., "Comparison of Some Structural Analysis Methods Used for the Test Pavement in the Danish Road Testing Machine", Proceedings of the Fifth International Conference on the Bearing Capacity of Roads and Airfields, Trondheim, 1998

Boussinesq, 1885- Boussinesq J., "Application des potentials á l'étude de l'équilibre et du movement des solides élastique, Gauthier-Villard, Paris, 1885

Burmister, 1943- Burmister D.M., "The Theory of Stresses and Displacements in Layered Systems and Applications to the Design of Airport Runways", Proceedings, Highway Research Board, Vol. 23, 1943

Burmister, 1945- Burmister D.M., "The General Theory of Stresses and Displacements in Layered Soil Systems", Journal of Applied Physics, Vol 16, 1945

Busch, 1991- Busch C., "Composite Polymer Grid Reinforced Asphalt Overlays on PCC Slab Pavements – Design and Performance Prediction", Institute of Roads, Transport & Town Planning, Technical University of Denmark, Report No. 64, 1991

Carey & Huckins, 1962- Carey W.N., Huckins H.C., "Slope Variance as a Measure of Roughness and the Chloe Profilometer", Highway Research Board Special Report Number 73, Highway Research Board, Washington DC, 1962

Carey & Irick, 1960- Carey W.N. & Irick P.E., "The Pavement Servicability Performance Concept", Bulletin 250, Highway Research Board, 1960

van Cauwelaert, 1977- van Cauwelaert F., "Coefficient of Deformation of an Anisotropic Body", Journal of the Engineering Mechanics Division, October 1977

van Cauwelaert, 1980- van Cauwelaert F., "Contraintes et déplacements dans un massif semi-infinte anisotrope à plan isotrope – Application au compactage", Annales de Travaux Publics de Belgique, Fascicule No 2, Avril 1980

Chatti et al, 1999- Chatti K., Baladi G. Y. & Schumann E. W., "Field Verification of the MICHBACK-MICHPAVE Pavement Response System", Post-Conference Presentations, International Conference on Accelerated Pavement Testing, Reno, Nevada, 1999

Claessen et al, 1977- Claessen A.I.M., Edwards J.M., Sommer P. & Uge P., "Asphalt Pavement Design – The Shell Method", Proceedings, 4th International Conference on the Structural Design of Asphalt Pavements, 1977

Collop & Cebon, 1995- Collop A.C. & Cebon D., "A Model of Whole-Life Flexible Pavement Performance", Journal of Mechanical Engineering Science, IMechE Vol 209, pp 389-407, 1995

COST 324, 1997- "COST 324 – Long Term Performance of Road Pavements", Final report EUR 17546, European Commission, Luxembourg, 1999

COST 333, 1999- "COST 333 - Development of New Bituminous Pavement Design Method", Final report EUR 18906, European Commission, Luxembourg, 1999

Cundall & Strack, 1979- Cundall P.A. & Strack O.D.L., "A Discrete Numerical Model for Granular Assemblies", Geothéchnique 29, No 1, pp 47-65, 1979

Darter et al, 1991- Darter M.I., Elliot R.P., Hall K.T., "Revision of AASHTO Pavement Overlay Design Procedures", Transportation Research Board, Washington DC, 1991

Ekdahl, 1997- Ekdahl P., "Mätprojekt Eket – En beskrivning av instrument och montering", Arbetsrapport 5 avd för Vägbyggnad, Lunds Tekniska Högskola, 1997

Ekdahl, 1998- Ekdahl P., "Mätprojekt Eket – Fallviktsmätningar på mätstation Eket - maj 1998" Lunds tekniska Högskola, 1998

Ekdahl, 1999- Ekdahl P., "A Sensitivity Test of Two Deterioration Models for Flexible Pavements", Licentiate thesis, Bulletin 9, Department of Technology and Society, Lund University, Lund, 1999

Ekdahl, 1999b- Ekdahl P., "Analysis of the Stresses and Strains Collected in COST 333 (The Swiss Contribution)", European Commission Directorate General Transport, Brussels, 1999

Ekdahl, 2003- Ekdahl P., "Test Plan – Test Site E6", Scandiaconsult Sverige AB, Malmö, 2003

Elkins et al, 2003- Elkins G. E., Schmalzer P., Thompson T., Simpson A., "Long Term Pavement Performance – Information Management System - Pavement Performance Database User Reference Guide" Report No FHWA-RD-03-088, Federal Highway Administration, 2003

Ferrez et al, 1996- Ferrez J.-A., Müller D. & Liebling T.M., "Parallel Implementation of Distinct Element Method for Granular Media Simulation on the Cray T3D", EPFL Supercomputing Review 8, 1996

Fredriksson et al, 1989- Fredriksson R., Lenngren A., Gustafsson K., "Dubbslitage på provvägar", Beläggningskonferens i Borlänge 1989

Frölich, 1934- Frölich ,"Druckverteilung in Baugrunde",Springer Verlag, Wien, 1934

George & Husain, 1986- George K.P. & Husain S., "Thickness Design for Flexible Pavement: A Probabilistic approach" Transport Research Record 1095, Transportation Research Board, Washington DC, 1986

Gillespie et al, 1980- Gillespie T.D., Sayers M.W., Segal L, "Calibration of Response-Type Road Roughness Measuring Systems", NCHRP Report Number 228, Transportation Research Board, Washington DC, 1980

Gillespie, 1992- Gillespie T. D., "Everything You Always Wanted to Know about the IRI, But Were Afraid to Ask!", Road Profile Users Group Meeting, Lincoln, Nebraska, September 22-24, 1992

Harr, 1977- Harr, M. E., "Mechanics of particulate Media", McGraw-Hill, 1977

Highway Research Board, 1962- Highway Research Board, The AASHO Road Test, Report 5: "Pavement Research", Special Reports No. 61E, National Academy of Sciences, National Research Council, Washington DC, 1962

Hildebrand & Bruun, 2004- Hildebrand G. & Bruun P.F., "Skærvemakadam er et godt alternative", Dansk Vejtidsskrift nr 4-2004

Hildebrand, 2002- Hildebrand G., "Verification of Flexible Pavement Response from a Field Test", VI report 121, Danish Road Institute, 2002

Hopman et al, 1997- Hopman P.C., Nilsson R.N. & Pronk A.C., "Theory, Validation and Application of the Visco-Elastic Multilayer Program VEROAD", Procedings of the eight International Conference on Asphalt Pavements, Seattle, 1997

Huang, 1967-Huang, Y.H., "Stresses and Displacements in Viscoelastic Layered Systems Under Circular Loaded Areas", 2nd International Conference on Structural Design of Asphalt Pavements, 1967

Huang, 1993-Huang, Y.H., "Pavement Analysis and Design", Prentice Hall, New Jersey, 1993

Hult, 1966- Hult J., "Hållfasthetslära", Almquist & Wicksell, Uppsala, 1966

Jacobsson et al, 1997- Jacobsson T., Wågberg L.G., "Utvecklning av prognosmodell för beläggningsslitage, slitageprofil och årskostnad", VTI-notat 21, Väg- och transportforskningsinstitutet, Linköping, 1997

Karan et al, 1979- Karan, M.A., D.H. Kobi, C.B. Bauman, R.C. Hass, "Subjective and Mechanical Estimations of Pavement Serviceability for Rural-Urban Road Networks" Transportation Research Record 715, Transportation Research Board, Washington DC, 1979

Kerkhoven & Dormon, 1953- Kerkhoven R.E. & Dormon G.M., "Some Considerations on the California Bearing Ratio for the Design of Flexible Pavement, Shell Bitumen Monograph No. 1, 1953

Krarup, 1994- Krarup J., Bearing Capacity and Water, Part II: Measured Response", Danish Road Institute, Note 249, 1994

MacDonald & Zhang, 1998- MacDonald R. A., Zhang W., "Accelerated Load Testing of the RTM2 Test Pavement in the Danish Road Testing Machine", Proceedings of the Fifth Iinternational Conference on the Bearing Capacity of Roads and Airfields, Trondheim, 1998

Madanat, 1997- Madanat S., "Predicting Pavement Deterioration", Institute of Transportation Studies Review, University of California, May 1997, Vol. 20, No. 3, 1997

Magnusson, 1987- Magnusson G., "Mätning av dynamisk hjullast", VTI-rapport 279, Väg och trafikinstitutet, Linköpng, 1987

Misra & Sen, 1975- Misra B., Sen B. R., "Stresses and Displacements in Granular Materials due to Surface Load", International journal of Engineering Science, Vol 13, pp 743-761, Pergamon Press, Great Britain, 1975

NCHRP, 2004- "Guide for Mechanistic-Empirical Design of new and rehabilitated pavement structures", National Cooperative Highway Research Program, 2004

Nilsson, 2001a- Nilson R., "Fatigue of Asphalt Mixtures- Continuum Damage Mechanics Applied to Data from Laboratory Tests", Bulletin 13, Department of Technology and Society, Lund University, 2001

Nilsson, 2001b- Nilsson R., "Viscoelastic Pavement Analysis using VEROAD", PhD thesis Departement of Infrastructure and Planning, Royal Institute if Technology, Stockholm, 2001

Nygårdhs, 2003- Nygårdhs S., "Aquaplaning – Development of a Risk Pond Model from Road Surface Measurements", Linköpings tekniska högskola, LiTH-ISY-EX-3409-2003, Linköping, 2003

Odemark, 1949- Odemark N., "Undersökning av elasticitetsegenskaperna hos olika jordarter samt teori för beräkning av beläggningar enligt elasticitetsteorin" Statens Väginstitut, meddelande 77, 1949

Odermatt, 1997- Odermatt N., "Road Deterioration Caused by Heavy Vehicles – A Literature Study", Royal Institute of Technology, Stockholm, 1997

Paterson, 1986- Paterson W.D.O., "International Roughness Index: Relationship to Other Measures of Roughness and Riding Quality", Transportation Research Record 1084. Transportation Research Board, National Research Council, Washington DC, 1986

Paterson, 1987- Paterson W.D.O., "Road Deterioration and Maintenance Effects: Models for Planning and Management", The Highway Design and Maintenance Series, The John Hopkins University Press, Baltimore, Maryland, 1987

Prozzi, 2001- Prozzi J.A., "Modeling Pavement Performance by Combining Field and Experimental Data", Doctoral dissertation, University of California, Berkeley, 2001

Queiroz, 1983- Queiroz C., "A Mechanistic Analysis of Asphalt Pavement Performance in Brazil", Proceedings of the Association of Asphalt Paving Technology, Vol. 52, 1983

Saal & Pell, 1960- Saal R.N.J. & Pell P.S., "Kolloid-Zeitschrift MI", Heft 1, 1960

Sayers & Karamihas, 1998- Sayers M.W. & Karamihas S.M., "The Little Book of Profiling – Basic Information about Measuring and Interpreting Road Profiles", University of Michigan, 1998

Shell, 1990- "Shell Bitumen Handbook", Shell Bitumen, 1990

Shook et al, 1982- Shook J.F., Finn F.N., Witczak M.W. & Monismith C.L., "Thickness Design of Asphalt Pavements – The Asphalt Institute Method", Proceedings, 5th International Conference on the Structural Design of Asphalt Pavements, 1982

SNRA, 1994- "VÄG 94", Vägverket publikation 1994:21, Vägverket, 1994

SNRA, 2000- "Bearbetning av deflektionsmätdata, erhållna vid provbelastning av väg med FWD-apparat" Metodbeskrivning 114:200, Vägverket, 2000

SNRA, 2001- "ATB Väg", Vägverket, 2001

Sparrow & Tory, 1966- Sparrow R.W. & Tory A.C., "Behavior of a Soil mass under Dynamic Loading", Journal of Soil Mechanics and Foundations Division, ASCE, 1966

Stiady, 1999- Stiady, J., "A Stochastic Model of Ground Subsidence in Granular Media", http://bridge.ecn.purdue.edu/~stiady/Research/subsidence.html, 2001-11-16

Turtschy & Perret, 1999- Turtschy J.-C. & Perret J., "Full-Scale Accelerated Loading Test at the Halle-Fosse (LAVOC-EPFL)"Swiss contribution to COST action 333: Development of New Pavement Design Methods". European Commission Directorate General Transport, Brussels, 1999

Ullidtz & Ekdahl, 1998- Ullidtz P., Ekdahl P., "Full-scale Testing of Pavement Response", Proceedings of the Fifth International Conference on the Bearing Capacity of Roads and Airfields, Trondheim, 1998

Ullidtz et al, 1999- Ullidtz P., Zhang W. & Baltzer S., "Validation of Pavement Response and Performance Models", International Conference on Accelerated Pavement Testing, Reno, Nevada, 1999

Ullidtz, 1978- Ullidtz P., "Computer Simulation of Pavement Performance", Report No 18, The Institute of Roads, Transport and Town Planning, The Technical University of Denmark, 1989

Ullidtz, 1979- Ullidtz P., "A Fundamental Method for Prediction of Roughness, Rutting and Cracking of Pavements", Proceedings, Associations of Asphalt Pavement Technologists, Vol 48, 1979

Ullidtz, 1987- Ullidtz P., "Pavement Analysis", Elsevier, Denmark, 1987

Ullidtz, 1998- Ullidtz P., "Modelling Flexible Pavement Response and Performance", polyteknisk Forlag, Denmark, 1998

Verhasselt & Choquet, 1993- Verhasselt A.F. & Choquet F.S., "Comparing field and laboratory ageing of bitumens on a kinetic basis", 72nd Annual Meeting of the Transportation Research Board, Washington DC, 1993.

Veverka, 1973- Veverka V., "Modules, contraintes et déformations des massifs et couches granulaires", Rapport de Recherche no 162, vv, Centre de rechereche Routières, Bruxelles

Way & Eisenberg, 1980- Way G.B. & J. Eisenberg, "Pavement Management System for Arizona - Phase II: Verification of Performance Prediction

Models and Development of Database", Arizona Department of Transportation, Phoenix, 1980

Wiman, 2001- Wiman L. G., "Accelerated Load Testing of Pavements – HVS-Nordic tests in Sweden 1999", VTI Rapport 477A-2001, 2001

Zhang & Macdonald, 2000- Zhang W. & Macdonald R.A., "Responses and Performance of a Test Pavement to one Freeze-Thaw Cycle", Danish Road Institute Report 102, 2000

Zhang et al, 1997- Zhang W., Ullidtz P. & Macdonald R.A., "Pavement Subgrade Performance Study – Data Analysis Report", Danish Road Institute, 1997

Zhang et al, 1998- Zhang W., Ullidtz P. & Macdonald R.A., "Pavement Subgrade Performance Study – Part II: Modeling Pavement Response and Predicting Pavement Performance", Danish Road Institute, 1997

APPENDIX A

Calculating pavement response with elastic material models

All equations below uses polar coordinate system according to figure below:

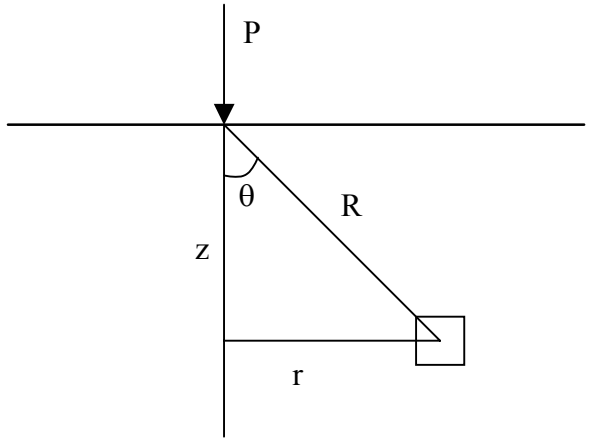

Linear elastic (Boussinesq)

Normal stresses:

$$\sigma_z = \frac{3P}{2\pi R^2}\cos^3\theta$$

$$\sigma_r = \frac{P}{2\pi R^2}\left(3\cos\theta\sin^2\theta - \frac{1-2\nu}{1+\cos\theta}\right)$$

$$\sigma_t = \frac{(1-2\nu)P}{2\pi R^2}\left(-\cos\theta + \frac{1}{1+\cos\theta}\right)$$

$$\sigma_1 = \frac{3P}{2\pi R^2}\cos\ \theta$$

$$\sigma_v = \frac{(1+\nu)P}{3\pi R^2}\cos\theta$$

Shear stresses:

$$\tau_{rz} = \frac{3P}{2\pi R^2}\cos^2\theta\sin\theta$$

$$\tau_{rt} = \tau_{rz} = 0$$

Strains:

$$\varepsilon_z = \frac{(1+\nu)P}{2\pi R^2 E}\left(3\cos^3\theta - 2\nu\cos\theta\right)$$

$$\varepsilon_r = \frac{(1+\nu)P}{2\pi R^2 E}\left(-3\cos^3\theta + (3-2\nu)\cos\theta - \frac{1-2\nu}{1+\cos\theta}\right)$$

$$\varepsilon_t = \frac{(1+\nu)P}{2\pi R^2 E}\left(-\cos\theta + \frac{1-2\nu}{1+\cos\theta}\right)$$

$$\varepsilon_v = \frac{(1+\nu)P}{\pi R^2 E}(1-2\nu)\cos\theta$$

Deflections:

$$d_z = \frac{(1+\nu)P}{2\pi RE}\left(2(1-\nu) + \cos^2\theta\right)$$

$$d_r = \frac{(1+\nu)P}{2\pi RE}\left(\cos\theta\sin\theta - \frac{(1-2\nu)\sin\theta}{1+\cos\theta}\right)$$

$$d_t = 0$$

For centreline under circular uniformly distributed load:

$$\sigma_z = \sigma_0\left(1 - \frac{1}{\left(\sqrt{1+\left(\frac{a}{z}\right)^2}\right)^3}\right)$$

$$\sigma_r = \sigma_t = \sigma_0\left(\frac{1+2\nu}{2} - \frac{1+\nu}{\sqrt{1+\left(\frac{a}{z}\right)^2}} - \frac{1}{2\left(\sqrt{1+\left(\frac{a}{z}\right)^2}\right)^3}\right)$$

$$\varepsilon_z = \frac{(1+\nu)\sigma_0}{E}\left(\frac{\frac{z}{a}}{\left(\sqrt{1+\left(\frac{z}{a}\right)^2}\right)^3} - (1-2\nu)\left(\frac{\frac{z}{a}}{\sqrt{1+\left(\frac{z}{a}\right)^2}} - 1\right)\right)$$

$$\varepsilon_r = \frac{(1+\nu)\sigma_0}{E}\left(\frac{-\frac{z}{a}}{\left(\sqrt{1+\left(\frac{z}{a}\right)^2}\right)^3} - (1-2\nu)\left(\frac{\frac{z}{a}}{\sqrt{1+\left(\frac{z}{a}\right)^2}} - 1\right)\right)$$

$$d_z = \frac{(1+\nu)\sigma_0 a}{E}\left(\frac{1}{\sqrt{1+\left(\frac{z}{a}\right)^2}} + (1-2\nu)\left(\sqrt{1+\left(\frac{z}{a}\right)^2} - \frac{z}{a}\right)\right)$$

Equations for a rigid plate can be found in (Ullidtz, 1998).

Stress concentration

$$\sigma_R = \sigma_1 = \frac{nP}{2\pi R^2}\cos^{n-2}\theta$$

$$\sigma_z = \frac{nP}{2\pi R^2}\cos^{n}\theta$$

$$\sigma_r = \frac{nP}{2\pi R^2}\cos^{n-2}\theta\sin^2\theta$$

$$\sigma_t = 0$$

$$p = \frac{\sigma_1}{3}$$

$$n = concentration\ factor$$

For a uniformly distributed load:

$$\sigma_z = \sigma_0 \left(1 - \frac{1}{\left(\sqrt{1 + \left(\frac{a}{z} \right)^2} \right)^n} \right)$$

The displacement in the direction of major principal stress (pointing towards load point) is calculated by:

$$u = KR^{\alpha} \cos\theta$$

$$\alpha = 1 - \frac{1}{\nu}$$

$$K = \frac{nP}{2\pi\alpha c}$$

$$c = \frac{E}{R^{\frac{1}{\nu}-2} \cos^{n-3}\theta}$$

The displacement perpendicular to that direction is calculated by:

$$v = \nu K R^{\alpha} \sin\theta$$

Anisotropy

The relation between stresses and strains in an cross-anisotropic body are described as

$$E\varepsilon_x = n\sigma_x - n\nu\sigma_y - \mu\sigma_z$$

$$E\varepsilon_y = -n\nu\sigma_x + n\sigma_y - \mu\sigma_z$$

$$E\varepsilon_z = -\mu\sigma_x - \mu\sigma_y - \sigma_z$$

where

$$E = E_z$$

$$n = \frac{E_z}{E_x}$$

μ, ν = poisson's ratio in different directions

(van Cauwelaert, 1977)

Assuming that $\nu=\mu$ and considering the centreline of the load where $\varepsilon_x=\varepsilon_y=\varepsilon_h$, and $\sigma_x=\sigma_y=\sigma_h$ this will give

$$E_v\varepsilon_v = -2\nu\sigma_h + \sigma_v$$
$$E_v\varepsilon_h = -n\nu\sigma_h + n\sigma_h - \nu\sigma_v$$

From the first line in the equation above it is possible to calculate the horizontal stress by

$$\sigma_h = \frac{\sigma_v - E_v\varepsilon_v}{2\nu}$$

and with that equation inserted in line two the horizontal strain can be calculated by

$$\varepsilon_h = (1-\nu)\frac{\sigma_h}{E_h} - \frac{\nu\sigma_v}{E_v}$$

Response under a point load:

$$\sigma_z = \frac{szP}{2\pi(1-s)}\left(\frac{1}{\left(\sqrt{s^2z^2+r^2}\right)^3} - \frac{1}{\left(\sqrt{z^2+r^2}\right)^3}\right)$$
$$\varepsilon_z = \frac{szP}{2\pi(1-s)E}\left(\frac{s^2(\rho+\nu)}{\left(\sqrt{s^2z^2+r^2}\right)^3} - \frac{1+\nu}{\left(\sqrt{z^2+r^2}\right)^3}\right)$$
$$d_z = \frac{sP}{2\pi(1-s)E}\left(\frac{\rho+\nu}{\left(\sqrt{s^2z^2+r^2}\right)^3} - \frac{1+\nu}{\left(\sqrt{z^2+r^2}\right)^3}\right)$$

where

$$E = E_v$$
$$\rho = \frac{E_v}{E_h}$$
$$s = \sqrt{\frac{\rho-\nu^2}{\rho^2-\nu^2}}$$

For the centreline under a uniformly distributed load the equations will be:

$$\sigma_z = \frac{\sigma_0}{1-s}\left(1 - s - sz\left(\frac{1}{\sqrt{s^2z^2 + r^2}} - \frac{1}{\sqrt{z^2 + r^2}}\right)\right)$$

$$\varepsilon_z = \frac{\sigma_0 s}{(1-s)E}\left((1+\nu)\left(\frac{z}{\sqrt{z^2 + a^2}} - 1\right) - s(\rho+\nu)\left(\frac{sz}{\sqrt{s^2z^2 + a^2}} - 1\right)\right)$$

$$d_z = \frac{\sigma_0 s}{(1-s)E}\left((\rho+\nu)\left(\sqrt{s^2z^2 + a^2} - sz\right) - (1+\nu)\left(\sqrt{z^2 + a^2} - z\right)\right)$$

Shear sensitivity

$$\sigma_z = \frac{P}{2\pi(\alpha-\beta)z^2}\left(\frac{1}{\left(\sqrt{\beta^2 + \left(\frac{r}{z}\right)^2}\right)^3} - \frac{1}{\left(\sqrt{\alpha^2 + \left(\frac{r}{z}\right)^2}\right)^3}\right)$$

$$\varepsilon_z = \frac{(1+\nu)zP}{2\pi(\alpha-\beta)E}\left(\frac{\alpha^2 A}{\left(\sqrt{\alpha^2z^2 + r^2}\right)^3} - \frac{\beta^2 B}{\left(\sqrt{\beta^2z^2 + r^2}\right)^3}\right)$$

$$d_z = \frac{(1+\nu)P}{2\pi(\alpha-\beta)E}\left(\frac{A}{\left(\sqrt{\alpha^2z^2 + r^2}\right)^3} - \frac{B}{\left(\sqrt{\beta^2z^2 + r^2}\right)^3}\right)$$

where α^2 and β^2 are the roots of the equation:

$$x^2 + (K' - 2)x + 1 = 0$$

where

$$K' = \frac{1-K}{1-\nu}$$

$$K = \frac{E}{1+\nu}\left(\frac{1}{G} - \frac{1+\nu}{E}\right)$$

$$A = \frac{K - \alpha^2}{\alpha^2 - 1}$$
$$B = \frac{K - \beta^2}{\beta^2 - 1}$$

For the centreline under a uniformly distributed load:

$$\sigma_z = \frac{\sigma_0}{\alpha - \beta}\left(\alpha - \beta + \frac{z}{\sqrt{\alpha^2 z^2 + a^2}} - \frac{z}{\sqrt{\beta^2 z^2 + a^2}}\right)$$
$$\varepsilon_z = \frac{(1+\nu)\sigma_0}{(\alpha - \beta)E}\left(\beta B\left(\frac{\beta z}{\sqrt{\beta^2 z^2 + a^2}} - 1\right) - \alpha A\left(\frac{\alpha z}{\sqrt{\alpha^2 z^2 + a^2}} - 1\right)\right)$$
$$d_z = \frac{(1+\nu)\sigma_0}{(\alpha - \beta)E}\left(A\left(\sqrt{\alpha^2 z^2 + a^2} - \alpha z\right) - B\left(\sqrt{\beta^2 z^2 + a^2} - \beta z\right)\right)$$

Probabilistic stress distribution

$$\sigma_z = \frac{P}{2\pi\mu z^2} e^{-\frac{r^2}{2\mu z^2}}$$
$$\sigma_r = \frac{r^2}{z^2}\sigma_z$$
$$\sigma_t = 0$$
$$\varepsilon_z = \frac{P}{2\pi\mu z^2}\left(1 - \frac{\nu r^2}{z^2}\right) e^{-\frac{r^2}{2\mu z^2}}$$

where

$$\mu = \frac{1}{\alpha z}$$
$$\alpha = \frac{\Delta z}{\Delta x^2}$$

For a uniformly distributed load:

$$\sigma_z = \sigma_0 \left(1 - e^{-\frac{a^2}{2\mu z^2}} \right)$$

$$\varepsilon_z = \frac{\sigma_0}{E} \left((1 - 2\nu\mu) \left(1 - e^{-\frac{a^2}{2\mu z^2}} \right) + \frac{\nu a^2}{z^2} e^{-\frac{a^2}{2\mu z^2}} \right)$$

Deflections are calculated by the sum (integral) of the strains.

APPENDIX B

Large amount of data has been used for this thesis, and it would take lots of pages to print everything. All data used can be acquired on a CD-ROM from the address on the title page. Below are some example tables from that CD-ROM.

Measured data from the Lausanne test site

Total passes	rut B	rut J	KYH2E01	KYH2E05	KYH2E08	KYH2S03	TRL2L01	TRL2L02
60242	0	0	-8,625	16,185	-27,885	-262,18	-28,9075	-29,5025
70532	1	0	66,475	58,73	21,245	-230,18	-24,135	-22,2
78228	1	1	62,34	65,245	11,93	-274,975	-23,3875	-21,0125
88524	0,5	0,5	48,88	54,11	9,65	-233,625	-23,0775	-20,1325
98298	1	0	105,455	106,225	77,075	-190,91	-24,4	-20,855
108370	1	2,5	63,705	65,73	25,59	-220,66	-23,9825	-20,24
118446	2	3	55,015	54,115	21,78	-233,58	-25,0575	-22,0675
128558	2	3	69,665	74,85	32,66	-214,715	-25,365	-21,3625
138674	1,5	3	51,205	59,54	5,66	-241,55	-24,5725	-21,74
148788	2	3	67,545	73,79	39,85	-210,375	-24,155	-19,625
158928	2	3	58,395	62,37	20,855	-219,23	-24,29	-19,625
169064	2	3,5	50,59	56,275	12,935	-218,805	-24,2	-19,495
179184	2	4	56,425	65,87	18,75	-225,62	-25,1025	-20,22
189284	2	4	64,76	66,715	27,08	-206,69	-24,5725	-19,5175
199430	2,5	4,5	53,34	58,11	11,805	-219,235	-24,8625	-20,925
209572	3	5	57,49	63,57	24,93	-214,745	-24,3775	-18,8325
219692			59,65	68,88	31,49	-212,59	-23,015	-19,67
229820	3	5,5	56,86	81,24	-15,4	-211,01	-26,1575	-19,0775
239958	3	5,5	58,945	68,035	-20,945	-215,615	-25,0575	-19,405

Measured rut depths at the Copenhagen test site, RTM2

load repetition	RD mm
1000	1.75
3000	2.331
10000	3.567
20000	4.167
30000	4.74
40000	4.896
50000	5.115
50000	5.393
51000	5.499
53000	5.649

load repetition	RD mm
60000	6.019
70000	6.335
80000	6.571
90000	6.844
100000	7.113
101000	7.178
103000	7.224
110000	7.772
120000	8.601
130000	9.086
140000	9.441
150000	9.783

Measured response

load repetition	50000	100000	150000
TZ0V270	1559,25	1901,5	2633,75
TY0V210	-522,222	-510,625	-638,264
TX0H210	-310,417	-332,056	-442,917
TX0V420	-241,736	-286,042	-349,028
TY0H420	-410,347	-409,306	-484,028
TZ0H600	2067,5	2258,75	2822,5
TZ2V180	1255,162	1595,949	1872,222
TZ2H360	786,285	1026,168	1307,64
TX0V630	-279,167	-317,222	-380,556
SZ1V150	83,75459	103,1173	150,6549
TZ1V299	1757,277	2047,634	2593,415
SY1H169	25,85508	25,54945	32,43933
TZ1H389	1616,514	1905,94	2323,395
SZ1H270	47,74134	67,31126	106,4924
TY1H449	-566,929	-719,783	-975,217
SX1H335	26,04379	29,91603	29,77041
TX1V419	-371,071	-428,915	-452,712
TZ1V539	2126,807	2376,576	2761,008
SY1V359	27,16078	32,56981	40,54428
TX1H629	-450,064	-538,355	-677,329
SZ1V480	63,25711	89,63415	89,63415
TZ1H690	2291,585	2477,094	2787,134
SX1H494	21,44078	23,43048	27,44616
SZ1H570	88,81064	107,1987	125,3912

Measured response at Linköping Se01

Total passes	208000		366546		510201		677360	
Side loc	0	-15	0	-15	0	-15	0	-15
ASG 1	-229,3	407,3333	-243,8	419,95				
ASG 3	-3,85	662,7333	670,6	712,8		705,9667		701,7
ASG 4	441,35	379,4667			407,8667	315,9667	316,2333	252,7667
ASG 5	-124,867	788,5667	670,2	839,4667				
ASG 7		639,6	246,95	696,4		680,2		661,1333
ASG 9		654,8		687,3667		681,6		706
ASG 12	162,1333	218,4667	177,7667	240,7	185,55	264,2667	203,1667	285,4333
ASG 13	179,0333	248,1	196,2	272,1333	207,2667	198,7667	224,4	222,6
ASG 14	140,6667	177,5667	157,5	193,9667	164,1667	207,7	173,4	230,3
ASG 15	-466,867	-540,467	-495,1	-574,733	-476,167	-548,033	-489,833	-558,4
SPC 16	15,8	14,3	16,7	15,06667	17,76667	16,1	19,13333	17,75
SPC 17	31,5	31,16667	36,36667	35,6	38,33333	37,36667	45,66667	44,75
SPC 18	18,2	16	20,8	17,76667	21,83333	18,83333	23,3	20
SPC 19	32,76667	33,15	34,66667	33,03333	36,7	35,55	39,53333	38,25
SPC 21	16,43333	14,4	17,4	15,5	18,46667	16,03333	19,93333	17,36667
SPC 22	30,36667	31,2	32,16667	32,13333	33,56667	32,7	37,83333	37,53333
SPC 37	74,43333	109,95	67,55	99,65	75	106,6	86,56667	124,5667
SPC 39	69,06667	118,9333	71,36667	122,9	80,13333	133,65	110,6667	173,9333
SPC 40	19,2	47,1	15,2	44,1	13,35	39,23333	21,33333	53,03333